UNIVERSITAT DE BARCELONA

Holographic duals of lower dimensional theories

David Pravos Fernández

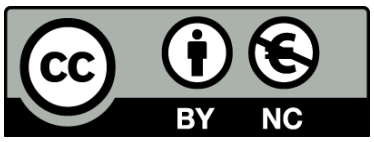

Aquesta tesi doctoral està subjecta a la llicència ***Reconeixement- NoComercial 4.0. Espanya de Creative Commons***.

Esta tesis doctoral está sujeta a la licencia ***Reconocimiento - NoComercial 4.0. España de Creative* Commons**.

This doctoral thesis is licensed under the ***Creative Commons Attribution-NonCommercial 4.0. Spain License***.

Tesis doctoral

Holographic duals of lower dimensional theories

Autor:
David Pravos Fernández

UNIVERSITAT DE
BARCELONA

Holographic duals of lower dimensional theories

Memoria presentada para optar al título de doctor por la

Universitat de Barcelona

Programa de doctorado en Física
Facultad de Física

Autor:
David Pravos Fernández

Directores:
David Mateos Solé y **Antón Fernández Faedo**

Tutor:
Domènec Espriu Climent

UNIVERSITAT DE
BARCELONA

A mis padres y a Anna.

Contents

Preface **ix**

Acknowledgements **xi**

1. The AdS/CFT correspondence **1**
1.1. Basic aspects of (super)string theory 1
1.2. Dp-branes 3
1.3. The large N_c limit 5
1.4. The AdS/CFT correspondence 6
1.5. Precise formulation of the duality 9
1.6. The duality for non-conformal branes 10

2. Duals of $\mathcal{N} = 1$ three-dimensional gapped non-confining theories **13**
2.1. Introduction 13
2.2. Preliminaries 17
2.3. Geometry of $\mathbb{CP}^3$ 19
2.4. Singular flows 22
2.4.1. $\mathbb{B}_8^+$ family 27
2.4.2. $\mathbb{B}_8^\infty$ solution 29
2.4.3. $\mathbb{B}_8^{\rm OP}$ solution 30
2.4.4. $\mathbb{B}_8$ solution 30
2.4.5. $\mathbb{B}_8^-$ family 31
2.4.6. $\mathbb{B}_8^{\rm conf}$ solution 31
2.5. Adding fractional branes 32
2.6. Regular flows 37
2.6.1. $\mathbb{B}_8^+$ family 39
2.6.2. $\mathbb{B}_8^\infty$ solution 40
2.6.3. $\mathbb{B}_8^{\rm OP}$ solution 41
2.6.4. $\mathbb{B}_8$ solution 42
2.6.5. $\mathbb{B}_8^-$ family 43

2.6.6. $\mathbb{B}_8^{\text{conf}}$ solution 43
2.6.7. Range of validity 44
2.7. Limiting dynamics 45
2.7.1. Quasi-confining dynamics 46
2.7.2. Quasi-conformal dynamics 47
2.8. Quark-antiquark potential 49
2.9. Discussion 53

3. Mass spectrum of gapped, non-confining theories with multi-scale dynamics 57
3.1. Introduction 57
3.2. Summary of known results 59
3.2.1. Type IIA/M-theory solutions and their field theory duals . . . 59
3.2.2. Four-dimensional description 61
3.2.3. Fluctuations 67
3.3. Mass spectrum 69
3.3.1. Tensor modes 70
3.3.2. Scalar modes 72
3.3.3. Hard-wall cutoff in the IR 75
3.4. Conclusions and Discussion 77

4. Two-dimensional gauge theories with unquenched flavour 79
4.1. Introduction 79
4.2. Internal geometries 81
4.2.1. Tri-Sasakian manifold 82
4.2.2. Sasaki-Einstein manifold 83
4.2.3. Weak-G_2 manifold 83
4.3. D1-branes on a tri-Sasakian manifold 85
4.4. $\mathcal{N} = (0, 3)$ theories with flavour 88
4.5. Theories with less supersymmetry 91
4.5.1. $\mathcal{N} = (0, 2)$ theories and Sasaki-Einstein manifolds 91
4.5.2. $\mathcal{N} = (0, 1)$ theories and weak-G_2 manifolds 93
4.6. Conclusions 95

5. Summary 97

6. Resumen en castellano 101

Appendix A. Hyperscaling violating toy model **107**

Appendix B. Conventions for the supersymmetric analysis **111**

Bibliography **113**

Preface

This thesis[1] gathers most of the research projects I participated in during my predoctoral studies, from 2015 to 2019, in the group of Gravity and Strings of Universitat de Barcelona under the supervision of David Mateos and Antón F. Faedo. These projects were always aimed to understand the theoretical description of strongly coupled quantum field theories using holographic techniques and they led up to a series of publications [1, 2, 3].

The content of this thesis is distributed as follows

- Chapter 1 consists on an introduction to the theoretical framework in which this work is developed, string theory and the AdS/CFT correspondence, advancing some concepts that will be recurrent during the following chapters.
- In chapter 2 we describe a family of supergravity solutions dual to three-dimensional quantum field theories that present multi-scale dynamics and mass gap without confinement. In chapter 3 we compute the mass spectrum of spin-0 and spin-2 modes in these solutions.
- In chapter 4 we study systems of D1-branes with special holonomy manifolds and obtain some solutions dual to quantum field theories in two dimensions.
- Finally, chapters 5 and 6 present a summary of the thesis in english and spanish, respectively.

[1] Cover image credits to Ben Felten.

Acknowledgements

First of all, I want to thank my thesis supervisor David Mateos. During my doctorate I have realised how a good scientist he is, but not only that. He has shown himself to be a great leader, patient and understanding, and always respectful. I have learnt from him a lot of physics but also insight, assertiveness and respect. Moreover, he has never hesitated to fund my travels to international workshops and schools, which have allowed me to expand my scientific and not scientific horizons.

I also need to express my gratitude to Antón. He started being a collaborator, but has ended up being my co-supervisor and a friend. He has spent hours and hours teaching me physics and reviewing my computations. But we have also shared very good moments talking about music, politics and many other things. He is a true physicist and a great mentor.

Thanks to my collaborators Javi and Daniel, who have done an amazing job carrying this project forward. It has been a pleasure working with them.

I cannot forget my office partners, specially Miquel, who is a good friend and has always been a helping hand. I also keep in mind Genis, Marina, Adriana,Vicente, Albert, Iván, Raimon, David, Marija and Mikel. Thanks to the department staff who always works to make our life easier.

Finalmente he de dar las gracias a mis seres queridos. A mis amigos que han hecho que estos años sean una aventura. A Anna, que ha luchado conmigo hasta el final. Y a mis padres, que lo han dado todo por mí, y todo aquello que consiga será gracias a ellos.

1. The AdS/CFT correspondence

The AdS/CFT correspondence, originally proposed in the late 1990's [4, 5, 6], is a very useful tool to understand the strongly coupled quantum field theories. This correspondence establishes a duality between superstring theories, which are gravitational theories, and gauge quantum field theories without gravity. The quantum field theory can be interpreted as living in the boundary of the gravitational theory, for this reason the correspondence is also referred as *holography*. A remarkable scientific implication of this is that we can study and understand the dynamics of strongly coupled theories through gravity, something that is not accesible by the usual perturbative methods in quantum field theory.

In this chapter we will review the correspondence, introducing its main statement and some of the important features that will be used in the next chapters. Everything stated here is quite standard and contained in several textbooks [7, 8] and reviews [9, 10], and is a common topic in lectures in graduate courses.

1.1. Basic aspects of (super)string theory

The AdS/CFT correspondence is formulated in the framework of superstring theory. For that reason, we should begin by introducing some fundamental concepts of this theory that will be useful for the development of the chapter.

The main difference between superstring theories and usual quantum field theories for particles is that it considers that the fundamental components of the universe are one-dimensional objects called *strings*, in contrast to the point-like particles. An important feature is the presence of a fundamental energy scale given by (the inverse of) the string length ℓ_s. Sometimes we may use the so called Regge slope, $\alpha' = \ell_s^2$ instead.

String theory can be defined perturbatively, first specifying the elements of the free theory and then introducing interactions via diagrams. To begin let us consider a single string, which can be either open or closed. Its state is defined by two parameters σ^α ($\alpha = 0, 1$) and its trajectory in the spacetime is given by an embedding $X^M(\sigma^\alpha)$ which

defines a Riemann surface called *worldsheet*.

In the same way that the action for a particle is given by the volume (length) of its spacetime trajectory, the action for a string is given by the volume (area) of its worldsheet. This is the Nambu-Goto action:

$$S_{\mathrm{NG}}\left[X^M\right] = \frac{1}{2\pi\ell_s^2}\int_\Sigma \mathrm{d}^2\sigma\ \sqrt{-\gamma}, \tag{1.1}$$

where γ is the determinant of the induced metric $\gamma_{\alpha\beta}$ in the worldsheet by the spacetime metric η_{MN},

$$\gamma_{\alpha\beta} = \partial_\alpha X^M \partial_\beta X^N \eta_{MN}, \tag{1.2}$$

and the coefficient in front of the action is there for units consistency and can be interpreted as the tension of the string. One can find that this highly non-linear action is equivalent to the Polyakov action,

$$S_{\mathrm{Poly}}\left[X^M, \gamma_{\alpha\beta}\right] = \frac{1}{4\pi\ell_s^2}\int_\Sigma \mathrm{d}^2\sigma\ \sqrt{-\gamma}\,\gamma^{\alpha\beta}\partial_\alpha X^M \partial_\beta X^N \eta_{MN}, \tag{1.3}$$

where γ_{ab} now has been promoted to be a dynamical degree of freedom.

Upon quantization we find the Hilbert space of the single-string states. These states are different vibrational modes of the string and correspond to different particles, with a given mass and spin, from the spacetime point of view. The final result is a tower of states spaced by $M_s \sim \ell_s^{-1}$. At energies below M_s we can keep the massless sector and ignore the rest.

The massless sector of the closed string contains a spin 2 state which can be decomposed into its traceless symmetric component (G_{MN}), anti-symmetric part (B_{MN}) and trace (Φ), called *dilaton* field. Then, even when we are starting with a flat spacetime with metric η_{MN}, the string theory itself includes a dynamical gravitational field so it is, in particular, a theory of gravitation.

In light-cone quantization, requiring Lorentz invariance after quantization of the string has a dramatic consequence. It fixes the dimension of the spacetime to a particular value, called *critical dimension*. For the bosonic string theory this value is $D = 26$, but for *superstring theory* (a theory that includes fermionic degrees of freedom in the worldsheet) this dimension is $D = 10$.

Interactions in string theory are introduced geometrically. For simplicity, consider the closed string. Any amplitude can be constructed considering any possible topology for the worldsheet in a genus expansion (fig. 1.1), weighted by the number of 3-point vertices that each diagram contains, contributing each one with a power of the string

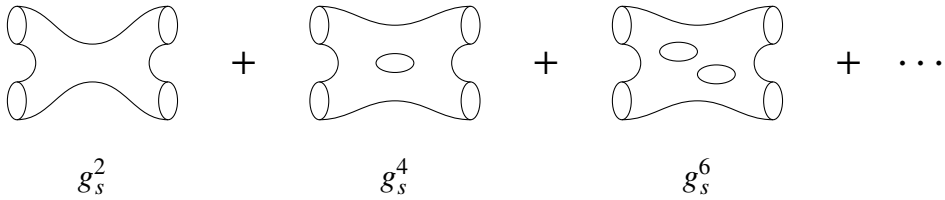

Figure 1.1.: Genus expansion of the 4-point scattering amplitude for closed strings.

coupling g_s. Thus an amplitude for a process of string scattering will be an infinite sum of the form

$$\mathcal{A} = \sum_{g=0}^{\infty} g_s^{2g-2} f_g(\ell_s), \tag{1.4}$$

where $f_g(\ell_s)$ is some function associated to the topology with genus g containing the details about the amplitude. The string coupling is not a free parameter of the theory, but it is dynamically determined because it is given by the asymptotic value of the dilaton field

$$g_s = e^{\Phi}\big|_{\partial\mathcal{M}}. \tag{1.5}$$

If we expand the superstring action at low energies $E \ll \ell_s^{-1}$, the leading term corresponds to a supergravity theory. Most of the computations in holography are done in this approximation.

The massless sector of superstring theories can also contain extra bosonic modes parametrised by forms F_p of different degrees p together with their fermionic superpartners.

1.2. Dp-branes

Superstring theory is not only a theory of strings. There are very important non-perturbative solution of superstring theory, called Dp-branes. These are $p+1$-dimensional hyperplanes where Dirichlet boundary conditions for open strings can be imposed. It is often said that open strings end in D-branes. In the low energy limit, the Dp-branes correspond to a supergravity solution called extremal black p-brane. The metric for the extremal black p-brane in flat space can be written as

$$\mathrm{d}s_{10}^2 = h^{-1/2}\left(-\mathrm{d}t^2 + \mathrm{d}x_p^2\right) + h^{1/2}\left(\mathrm{d}r^2 + r^2\mathrm{d}\Omega_{(8-p)}^2\right), \qquad h = 1 + \left(\frac{L}{r}\right)^{7-p}, \tag{1.6}$$

where $\mathrm{d}\Omega_d^2$ is the metric of a sphere of dimension d. The solution is accompanied with some matter fields, a scalar dilation Φ and a $(p+2)$-form given by

$$e^{\Phi} = g_s h^{\frac{3-p}{4}}, \qquad F_{(p+2)} = \mathrm{d}t \wedge \mathrm{d}x^1 \wedge \cdots \wedge \mathrm{d}x^p \wedge \mathrm{d}\left(h^{-1}\right) \tag{1.7}$$

Of paramount importance is the Dp-brane with $p = 3$. In that case, we see that asymptotically, when $r \gg L$, the space becomes flat. On the other hand, for $r \ll L$ the sphere factorises and the space becomes $\mathrm{AdS}_5 \times S^5$:

$$\mathrm{d}s_{10}^2 \sim \left(\frac{r}{L}\right)^2 \left(-\mathrm{d}t^2 + \mathrm{d}x_3^2\right) + \left(\frac{L}{r}\right)^2 \mathrm{d}r^2 + R^2 \mathrm{d}\Omega_5^2. \tag{1.8}$$

This observation is crucial in the derivation of the AdS/CFT duality.

The tension of a Dp-brane is

$$T_{\mathrm{D}p} = \frac{1}{(2\pi\ell_s)^p g_s \ell_s}. \tag{1.9}$$

The g_s^{-1} dependence shows the non-perturbative nature of the D-branes.

The length scale L associated to the brane is related to its tension through Newton's constant in ten dimensions $G_{10} \sim g_s^2 \ell_s^8$. The power of ℓ_s is given by the units and the power of g_s is fixed by comparing the gravitational term in the low energy action with the Einstein-Hilbert action. Then,

$$L^{7-p} \sim G_{10} T_{\mathrm{D}p} \sim \ell_s^{7-p} g_s. \tag{1.10}$$

If instead of only one brane we have N_c stacked branes the tension acquires a factor of N_c,

$$\left(\frac{L}{\ell_s}\right)^{7-p} \sim g_s N_c. \tag{1.11}$$

Thus, if $g_s N_c \ll 1$ then the strings see flat space in the directions transverse to the brane.

Strings attached to Dp-branes can also be quantized. The massless sector of open strings attached to a Dp-brane contains

- A gauge field A_μ ($\mu = 0, \ldots, p$) living in (coupled to) the worldvolume of the brane.
- $9 - p$ scalar fields X^m ($m = p+1, \ldots, 9$) transverse to the brane, corresponding to its embedding in the full spacetime.

The effective action for the brane at low energies is given by de Dirac-Born-Infeld (DBI) action

$$S_{\mathrm{DBI}} = T_{\mathrm{D}p} \int \mathrm{d}^{p+1}\sigma\, e^{-\Phi} \sqrt{\det\left(g_{\mu\nu} + 2\pi l_s^2 F_{\mu\nu}\right)}, \tag{1.12}$$

where $g_{\mu\nu} = \partial_\mu X^M \partial_\nu X^N G_{MN}$ is the induced metric on the brane and $F_{\mu\nu}$ is the field strength associated to A_μ. Notice that due to diff-invariance in the worldvolume of the brane we can choose the $(p+1)$ spacetime coordinates parallel to the brane to be $X^\mu = \sigma^\mu$ ($\mu = 0, \ldots, p$), and redefine the transverse coordinates as $X^i = 2\pi\ell_s^2\phi^i$ ($i = p+1, \ldots, 9$). In a background with $\Phi = 0$ and $G_{MN} = \eta_{MN}$, the DBI action can be expanded in powers of the derivatives of the fields, yielding

$$S_{\mathrm{DBI}} \sim T_{\mathrm{D}p} \int \mathrm{d}^{p+1}\sigma \left[\text{const.} - \frac{1}{4}F^2 - \sum_i \frac{1}{2}(\partial\phi^i)^2 + \cdots\right] \tag{1.13}$$

which is the action for a Maxwell-scalar theory. If instead of having a single brane we are dealing with a stack of N_c branes, then the gauge symmetry would get enhanced from U(1) to U(N_c) and the brane would contain a Yang-Mills sector with coupling

$$g_{\mathrm{YM}}^2 = 4\pi g_s (2\pi\ell_s)^{p-3}. \tag{1.14}$$

1.3. The large N_c limit

Quantum Chromodynamics (QCD) is an SU(3) non-abelian gauge theory. Due to dimensional transmutation it has no expansion parameter. In [11] 't Hooft proposes a generalisation of QCD considering a SU(N_c) theory and using as an expansion parameter $1/N_c$. This theory contains $N_c^2 - 1$ gluon degrees of freedom that we can approximate to N_c^2 in the regime where $N_c \gg 1$. Also there are N_c degrees of freedom corresponding to the quarks. In the large N_c limit we can ignore them and focus on the gluons only.

Consider the self-energy of the gluon (fig. 1.2). If we want to keep this diagram finite when $N_c \to \infty$ then we must ensure that the combination $\lambda \equiv g_{\mathrm{YM}}^2 N_c$ also stays finite. This quantity receives the name *'t Hooft coupling*.

Gluon diagrams are classified by their topology and number of loops. Each diagram can be associated to a Riemann surface with genus g and it will scale with N_c^{2-2g}. On the other hand, counting the number $n+1$ of loops of the diagram (for any topology) will give us the scaling with the 't Hooft coupling as λ^n. Any amplitude can be computed

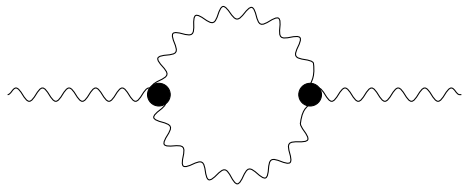

Figure 1.2.: Self-energy of the gluon.

as the following expansion

$$\mathcal{A} = \sum_{g=0}^{\infty} N_c^{2-2g} \sum_{n=0}^{\infty} c_{g,n} \lambda^n = \sum_{g=0}^{\infty} N_c^{2-2g} F_g(\lambda). \tag{1.15}$$

This means that in the $N_c \to \infty$ limit, the *planar diagrams* (those with $g = 0$) dominate in the expansion. Notice that this expansion has the same form than (1.4) if we associate $N_c^{-1} \sim g_s$. This similitude suggests a connection between the perturbative expansion of string theory and the large N_c limit of gauge theories.

1.4. The AdS/CFT correspondence

After this preamble we can dive into the most famous realisation of the AdS/CFT correspondence and formulate it. Consider a stack of N_c D3-branes and let us study its ground state. As we have said, the gravitational radius of the system is related to the string coupling and the number of branes by equation (1.10). There are to possible limits:

1. If $g_s N_c \ll 1$, then $L \ll \ell_s$. This means that the strings will see flat space and the branes are just an hypersurface where to impose boundary conditions for open strings. This is called the *open strings description*.

2. If $g_s N_c \gg 1$, then $L \gg \ell_s$. This is known as the decoupling limit. The spacetime curvature is noticeable, so we are perceiving the backreaction of the branes in the spacetime and the best description for the system is as a background geometry for closed strings. This is the *closed strings description*.

We now consider excitations in both cases. In the open strings picture the closed-closed and closed-open string interactions are controlled by the energy of the system (because gravity couples to energy). In the low energy limit, the closed strings decouple and become free. However, the open-open string interactions are controlled by $g^2_{\rm YM} \sim g_s$ so they remain finite when $E \ll \ell_s^{-1}$, thus resulting in a gauge theory. In particular, the theory is $\mathcal{N} = 4$ super Yang-Mills with gauge group SU(N_c). The global content of the system at low energies is $\mathcal{N} = 4$ SYM SU(N_c) plus free gravity in ten dimensional flat space.

In the closed strings picture there are not open strings. Closed strings far in the asymptotic region have a very big wavelenght that cannot resolve the throat of radius R of the background, and closed strings down the throat do not have enough energy to climb out of it, so both sets cannot interact with each other. The strings in the throat see the decoupling limit metric (1.8) $\mathrm{AdS}_5 \times S^5$, while the strings in the asymptotic region see flat space. Then, in this case the system is composed by closed strings in $\mathrm{AdS}_5 \times S^5$ plus free gravity in flat space.

The AdS/CFT correspondence states that, because we are just choosing two different descriptions of the same system (a stack of N_c D3-branes in string theory), physically they should actually be equivalent. Thus we can formulate:

$\mathcal{N} = 4$ SU(N_c) SYM in $D = 4$	$\equiv$	IIB superstrings in $\mathrm{AdS}_5 \times S^5$

This SYM gauge theory is conformal, that is why the duality receives the name of AdS/CFT correspondence. However there are also examples of non-AdS/non-CFT correspondence. For this reason this duality is also sometimes called gauge/gravity or gauge/string duality.

We can see how parameters in one side of the duality relate to the ones in the other. The gauge theory is characterised by the 't Hooft coupling λ and the number of colours N_c, while the superstrings theory is given by the string coupling constant g_s and the size of the AdS space L. By looking at the expansion of the DBI action we have already argued that $g^2_{\rm YM} \sim g_s$. So,

$$\left(\frac{L}{\ell_s}\right)^4 \sim g_s N_c \sim g^2_{\rm YM} N_c = \lambda. \tag{1.16}$$

Now, if we want to keep the low energy terms in the $1/\ell^s$ expansion, we must ask that $\ell_s \gg R$, which means $\lambda \gg 1$, that is, when the gauge theory is strongly coupled,

then the gravity side is dominated by the supergravity action and we can ignore stringy effects.

On the other hand, if we compare the size of the spacetime with the Planck length we have

$$\frac{L^4}{\ell_P^4} \sim \frac{L^4}{\sqrt{G_{10}}} \sim \frac{g_s N_c \ell_s^4}{g_s \ell_s} \sim N_c. \tag{1.17}$$

Thus if we want to keep quantum gravity effects suppressed, we must demand $N_c \gg 1$. This means that we can study strongly coupled gauge theories in the large N_c limit with classical supergavity.

A check of consistency of the duality is the comparison of symmetries in the gauge and gravity theories. On the gauge theory side we have:

- Conformal symmetry in 3 + 1 dimensions.
- R-symmetry group SU(4)
- 16 supercharges superpartners of the Poincaré translations.
- 16 supercharges superpartners of the special conformal symmetries.

While on the gravity side,

- SO(2, 4) invariance in AdS_5.
- SO(6) symmetry on the sphere.
- 32 Killing spinors, because the solution is maximally supersymmetric.

We can match these symmetries, since the conformal group in 3 + 1 dimensions is isomorphic to SO(2, 4) and SU(4) is isomorphic to SO(6).

Since $\mathcal{N} = 4$ SYM is a conformal theory, this means that it does not have an intrinsic energy scale. In the Poincaré patch of AdS_5, the directions where the brane lives (the Minkowski ones) are invariant under a rescaling $x^\mu \to \Lambda x^\mu$ as long as the coordinate r is also rescaled by $r \to r/\Lambda$. This means that short-distance physics in the gauge theory is associated to physics in the boundary of AdS_5 and r is identified with the renormalisation group scale. For this reason we say that the gauge theory lives in the boundary of AdS_5.

Instead of Dp-branes in flat space we can consider another background manifold. The result is that in the dual theory the gauge group or the amount of supersymmetry will be different. This technique will allow us to construct holographic duals to different quantum field theories along this thesis.

1.5. Precise formulation of the duality

We have argued that a classical supergravity is equivalent to a strongly coupled gauge theory in the large N regime. But how do we actually compute things? We should establish the dictionary between both sides: a map relating observables in both theories.

We know that the asymptotic value of the dilaton field gives the string coupling g_s, which regulates g_{YM} in the gauge theory. This suggests us a relation between the asymptotic values of fields in the gravity side and couplings in the gauge theory, that is, a scalar field $\Phi(r, x)$ acts as a source $\phi(x)$ for an operator $\mathcal{O}(x)$ as

$$\int \mathrm{d}^4 x\, \phi(x)\mathcal{O}(x), \tag{1.18}$$

where $\phi(x) = \Phi(x, r)|_{\partial \mathrm{AdS}}$.

We can postulate that the partition functions of both theories are equivalent, identifying the gravity fields in the boundary with couplings of the gauge theory:

$$Z_{\mathrm{gauge}}[\phi] = Z_{\mathrm{strings}}[\,\Phi|_{\partial \mathrm{AdS}}] \tag{1.19}$$

In the strong coupling, large N_c limit, the partition function for string theory is well approximated by the on-shell action of classical supergravity,

$$Z_{\mathrm{strings}} \approx e^{-S_{\mathrm{SUGRA}}}. \tag{1.20}$$

The direct consequence is that we can easily compute on supergravity any correlation function for a strongly coupled gauge theory.

As we said, the coupling ϕ of an scalar operator $\mathcal{O}$ in the gauge theory is given by the asymptotic behaviour of a scalar field Φ in supergravity. The dynamics of this scalar field is dictated by a second order differential equation, so near the boundary $r \to \infty$ we can write an expansion

$$\Phi(x, r) \sim \frac{\phi(x)}{r^\alpha} + \cdots + \frac{\tilde{\phi}(x)}{r^\beta} + \cdots \tag{1.21}$$

where $\beta < \alpha$. The expansion depends on two modes. The leading term $\phi(x)/r^\alpha$ is called *non-normalizable mode* and the sub-leading one $\tilde{\phi}(x)/r^\beta$ is called *normalizable mode*. If α is not zero, the field will not approach a finite quantity in the boundary, so the coupling dual to this field will actually be given by

$$\phi(x) = \lim_{r\to\infty} r^\alpha \Phi(x, r). \tag{1.22}$$

Under a scale transformation, ϕ transforms as a scalar density with mass dimension α, so, in order to keep the action (1.18) invariant, the operator $\mathcal{O}$ must have a mass dimension $\Delta \equiv 4 - \alpha$.

The coupling $\phi(x)$ acts as a *source* for the operator $\mathcal{O}$. The interpretation for the normalizable mode is that it acts as a *vacuum expectation value* (vev) for the operator. We can understand this as follows. In the supergavity action, integrating by parts and evaluating the scalar field on the boundary one can find a term were both modes are multiplied:

$$S_{\text{SUGRA}} \supset \int_{\text{AdS}} (\partial\Phi)^2 \sim \int_{\partial\text{AdS}} \Phi\, \partial\Phi \sim \phi^2 + \cdots + \phi\tilde{\phi} + \cdots \tag{1.23}$$

Then, when reading this as the partition function for the gauge theory, we can compute the 1-point function for $\mathcal{O}$ by varying with respect to the sources and setting them to zero:

$$\langle \mathcal{O}(x) \rangle \sim \frac{\delta}{\delta\phi(x)} \log Z_{\text{gauge}}\Big|_{\phi(x)=0} \sim \frac{\delta}{\delta\phi(x)} S_{\text{SUGRA}}\Big|_{\phi(x)=0} \sim \tilde{\phi}(x) + \cdots \tag{1.24}$$

In principle there are two independent solutions for Φ, but after imposing regularity in AdS, the normalizable mode is given in terms of the non-normalizable one. Speaking in gauge theory terminology, once we have selected a source, the vev is dynamically determined. We control the sources by imposing boundary conditions to Φ in the AdS boundary.

1.6. The duality for non-conformal branes

In section 1.4 we proposed the AdS/CFT conjecture by studying a stack of N_c D3-branes in flat and we found that the conformal field theory living in the branes is dual to string theory in an AdS background, thus the name AdS/CFT correspondence. But this duality goes beyond scale invariant theories. In [12] the correspondence is studied for other types of branes. We will review here the cases of D2-branes and D1-branes, that we will use in the forthcoming chapters.

Consider the case of N_c D2-branes. We can enunciate the duality as follows:

$\mathcal{N} = 8$ SU(N_c) SYM in $D = 3$	$\equiv$	D2-branes in IIA superstring theory

Unlike the D3-branes, the theory living in the D2-branes is not conformal, and the Yang-Mills coupling constant is not dimensionless, $g^2_{\rm YM} \sim \text{length}^{-1}$. Then, at a given energy scale U, the effective dimensionless coupling of the theory is $g^2_{\rm eff} \sim g^2_{\rm YM} N_c U^{-1}$. The system can be described perturbatively when $U \gg g^2_{\rm YM} N_c$.

If $U \ll g^2_{\rm YM} N_c$ then the system is well described by supergravity. Following equation (1.6), the solution for the D2-branes in flat space in the decoupling limit is

$$\mathrm{d}s^2_{10} = \left(\frac{r}{L}\right)^{\frac{5}{2}} \mathrm{d}x^2_{1,2} + \left(\frac{L}{r}\right)^{\frac{5}{2}} \left(\mathrm{d}r^2 + r^2 \mathrm{d}\Omega^2_6\right), \tag{1.25}$$

$$e^{\Phi} = g_s \left(\frac{L}{r}\right)^{5/4} \tag{1.26}$$

where $r = \alpha' U$ and $L^5 = 6\pi^2 N_c (\alpha')^3 g^2_{\rm YM}$. Notice that U should not be too small, because in that case the dilaton would blow up. We must impose $g^2_{\rm YM} N_c^{1/5} \ll U$.

In the region $U \ll g^2_{\rm YM} N_c^{1/5}$, the type IIA supergravity is not a valid description. This supergravity can be obtained by reducing eleven-dimensional supergravity in a circle. The radius of this circle is proportional to the dilaton, so the reduction is consistent while the dilaton is small. For large values of the dilaton we must use the eleven-dimensional supergravity description. This is the low energy limit of M-theory.

For D1-branes the analysis is similar. The duality now establishes

$\mathcal{N} = (8,8)$ SU(N_c) SYM in $D = 2$	$\equiv$	D1-branes in IIB superstring theory

The Yang-Mills coupling has dimensions of $g_{\rm YM} \sim \text{length}^{-2}$. The perturbative description is valid for energies $U \gg g_{\rm YM} \sqrt{N}$.

For $U \ll g_{\rm YM} \sqrt{N}$ the theory is well described by type IIB supergravity, with the background

$$\mathrm{d}s^2_{10} = \left(\frac{r}{L}\right)^{3} \mathrm{d}x^2_{1,1} + \left(\frac{L}{r}\right)^{3} \left(\mathrm{d}r^2 + r^2 \mathrm{d}\Omega^2_7\right), \tag{1.27}$$

$$e^{\Phi} = g_s \left(\frac{L}{r}\right)^{3} \tag{1.28}$$

where now $L^6 = 2^6 \pi^3 N_c (\alpha')^4 g^2_{\rm YM}$. Again this description is valid up to energies $U \sim g_{\rm YM} N^{1/6}$. In the region $U \ll g_{\rm YM} N^{1/6}$ the dilaton is large, and so it is the string coupling. We can use S-duality to find a suitable representation of the system, by switching $g_s \to g_s^{-1}$. Then the solution becomes a fundamental string.

2. Duals of $\mathcal{N} = 1$ three-dimensional gapped non-confining theories

2.1. Introduction

Holographic duals of gauge theories that possess a mass gap are also expected to exhibit confinement in the sense of an asymptotically linear potential between an external quark-antiquark pair. Geometrically, the reason is simple, as illustrated in fig. 2.1. The mass gap arises because the geometry ends smoothly at a non-zero value of the holographic coordinate. The linear potential comes from the fact that a string hanging from a well-separated quark-antiquark pair finds it energetically advantageous to place most of its length near the regular end of the geometry, where it attains a constant, minimum energy per unit length. A crucial ingredient in this argument is that the string configuration cannot consist of two disconnected pieces. The reason is charge conservation since, in a regular background, each piece would have no place to end. Put differently, an isolated quark or antiquark is not an allowed configuration.

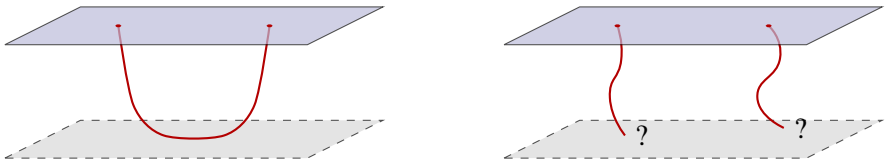

Figure 2.1.: (Left) Connected string configuration (thick red curve) in the calculation of the quark-antiquark potential in string theory. The top, continuous, black, horizontal line represents the boundary on which the gauge theory resides. The bottom, dashed, black, horizontal line is the place where the geometry ends smoothly. (Right) Disconnected configuration that is not allowed due to charge conservation, since the endpoints of the strings have no place to end.

The system that we present in this chapter is a counterexample to this expectation. The crucial point is that the gauge theories in question possess a regular supergravity description in eleven-dimensional M-theory but not in ten-dimensional string theory. Hence the existence of a mass gap or the presence of confinement can only be reliably

addressed in eleven dimensions. The eleven-dimensional geometries end smoothly at a non-zero value of the holographic coordinate, thus leading to a mass gap. However, no confinement arises. The reason is that, in M-theory, the quark-antiquark potential is calculated from the action of a membrane wrapped on the M-theory circle, which is just the uplift of the corresponding string calculation in ten dimensions. This is illustrated in fig. 2.2.

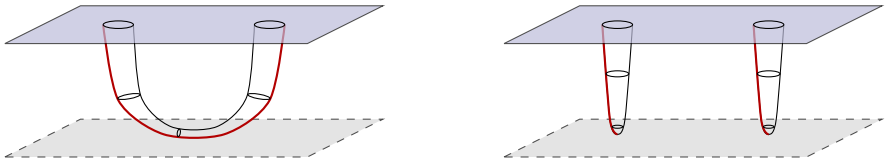

Figure 2.2.: (Left) Connected membrane configuration in the calculation of the quark-antiquark potential in M-theory. The projection of the membrane onto the non-compact directions is represented by the thick, red curve. The M-theory circle at each point is represented next to it by the black circles. The top, continuous, black, horizontal line represents the boundary on which the gauge theory resides. The bottom, dashed, black, horizontal line is the place where the geometry ends smoothly. (Right) Disconnected membrane configuration allowed by charge conservation, since the membrane closes off smoothly at the bottom of the geometry and hence it has a cigar-like topology with no boundary.

In the geometries in question this circle shrinks smoothly to zero size in the infrared, leading to a cigar-like topology. A membrane wrapped on this cigar has no boundary and is thus compatible with charge conservation. In other words, an isolated quark or antiquark is an allowed configuration. As a consequence, a configuration consisting of two cigar-like membranes hanging from the quark and the antiquark at the boundary competes with the connected configuration and is in fact energetically preferred for a sufficiently large separation. It follows that there is a phase transition from the connected to the disconnected configuration at a critical quark-antiquark separation that cuts-off the linear growth of the potential.

The geometries that realize the physics above consist of a one-parameter family of supergravity solutions dual to a one-parameter family of three-dimensional gauge theories. We emphasize that these supergravity solutions themselves are not new [13], but we present them in what we hope is a user-friendly, comprehensive treatment. Throughout the chapter we will find it useful to switch back and forth between the descriptions in ten and eleven dimensions. All solutions preserve two supercharges, corresponding to $\mathcal{N} = 1$ supersymmetry in three dimensions. Because of the small amount of supersymmetry it is difficult to determine the precise details of the dual gauge

theories. Nevertheless, they are presumably quiver-like, super Yang–Mills (SYM) gauge theories with a product gauge group of the form $\mathrm{U}(N+M)\times\mathrm{U}(N)$ and possible additional Chern-Simons-Matter terms (CSM) [14, 15]. For brevity, we will refer to these as SYM-CSM theories.

Each of the eleven-dimensional solutions is based on an eight-dimensional transverse geometry of Spin(7) holonomy,[1] as we will review in section 2.4. Given the transverse geometry, the two additional ingredients needed to obtain the corresponding eleven-dimensional solution are appropriate fluxes through the transverse geometry and a warp factor. If the ranks of the two gauge groups are the same, i.e. if $M = 0$, then the resulting warp factor is singular, and so is the eleven-dimensional solution, as we explain in section 2.4. In order to have $M \neq 0$ one must add fractional branes to the system, as we review in section 2.5, which results in additional fluxes. Under these circumstances it is then possible to construct completely regular eleven-dimensional solutions, as we show in section 2.6. This configuration is reminiscent of the Klebanov–Strassler solution [16] but with a three-dimensional gauge dual and a better behaved UV.

The set of solutions is pictorially summarized in fig. 2.3. Each curve or straight line running downwards represents an eleven-dimensional solution labelled by its corresponding eight-dimensional transverse geometry. The arrows indicate the direction of the Renormalization Group (RG) flow from the ultraviolet (UV) to the infrared (IR). In the UV all solutions[1] are dual to a SYM-CSM theory, as described above. Asymptotically, the corresponding ten-dimensional geometries are those of D2-branes placed at a cone over $\mathbb{CP}^3$, hence the label at the top vertex of the figure. These geometries are accompanied by two types of fluxes. First,[1] an ABJM-like [17] flux of the Ramond-Ramond (RR) two-form proportional to the Kähler form on $\mathbb{CP}^3$. As in ABJM, we expect this to indicate the presence of CSM interactions and to determine the CS level. Second, fluxes associated to the presence of fractional branes that render the IR metrics regular and shift the rank of one of the two gauge groups.

The family of supergravity solutions is parametrized by a constant that we call y_0 and that takes values between -1 and ∞. We expect this parameter to be related to the difference between the couplings of the two factors in the gauge group, as we will comment further in section 2.6. All the transverse eight-dimensional geometries can be foliated by squashed seven-spheres viewed as an S^1 fibration over an S^2 base that is itself fibered over an S^4. Thus one can also view these geometries as a squashed S^3 fibered over S^4, or as an S^1 fibered over a squashed $\mathbb{CP}^3$. Following the original

[1] Except for the one labelled $\mathbb{B}_8^{\mathrm{conf}}$, see below.

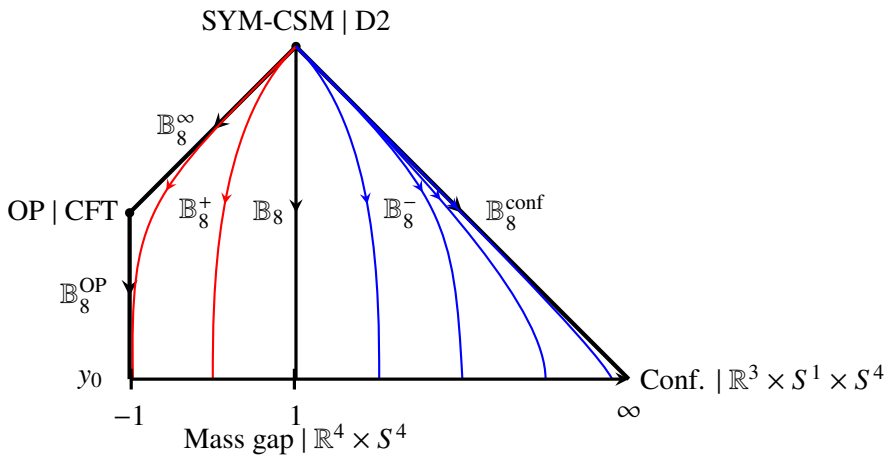

Figure 2.3.: Pictorial representation of the different solutions (see main text).

references, we refer to solutions with $y_0 \in (-1, 1)$ as the $\mathbb{B}_8^+$ family [13], to the solution with $y_0 = 1$ as $\mathbb{B}_8$ [18], and to solutions with $y_0 \in (1, \infty)$ as the $\mathbb{B}_8^-$ family [13]. Despite this technical distinction, the physics is continuous as a function of y_0 for $y_0 \in (-1, \infty)$. In this set of solutions the S^3 shrinks smoothly to zero size in the IR, whereas the size of the S^4 remains non-zero. The IR transverse geometry is thus $\mathbb{R}^4 \times S^4$. We will see that this leads to a mass gap but no confinement.

For $y_0 = -1$ the IR physics is radically different. The transverse geometry was found and dubbed $\mathbb{B}_8^{\infty}$ in [15]. In this case the entire S^7 shrinks to zero size in the IR, but once the warp factor is taken into account the resulting geometry is AdS_4 times a squashed seven-sphere of non-zero size. This fixed point is dual to the so-called Ooguri–Park (OP) conformal field theory (CFT) [19], which is an $\mathcal{N} = 1$ deformation of the ABJM theory [17]. Remarkably, the OP fixed point admits a relevant deformation that drives it to an IR theory with a mass gap but no confinement. The eleven-dimensional solution describing this flow is based on a transverse geometry found in [20, 21] that we call $\mathbb{B}_8^{\text{OP}}$. As we will explain in section 2.7.2, solutions with y_0 close to -1 describe RG flows that approach the concatenation of the $\mathbb{B}_8^{\infty}$ and the $\mathbb{B}_8^{\text{OP}}$ flows. These solutions exhibit "walking" or quasi-conformal behavior in a certain range of energies, as we will confirm in section 2.8 with a calculation of the potential between an external quark-antiquark pair.

If the RR two-form is set to zero, one obtains a solution based on an internal geometry

found in [20, 21] that we call $\mathbb{B}_8^{\text{conf}}$. The eleven-dimensional solution flows to an IR theory that exhibits both a mass gap and confinement. The geometric reason is that, in this case, the S^1 is trivially fibered over the rest of the geometry and it remains non-contractible along the entire flow; in particular, the IR transverse geometry is $\mathbb{R}^3 \times S^1 \times S^4$. This implies that a membrane wrapped on this S^1 cannot end anywhere in the bulk since it would have a cylinder-like geometry and hence a boundary, which is not allowed by charge conservation. On the gauge theory side, the existence of confinement seems to be a consequence of the absence of CSM interactions (we will come back to this point in section 2.9). We will confirm the presence of an asymptotic linear potential for an external quark-antiquark pair in section 2.8. We will also show in section 2.7.1 that the $\mathbb{B}_8^{\text{conf}}$ can be obtained as the $y_0 \to \infty$ limit of the $\mathbb{B}_8^-$ solutions.

2.2. Preliminaries

As explained in section 2.1, the type IIA solutions of interest in this chapter describe RG flows that start from a D2-brane-like asymptotic geometry in the UV. Some of these flows end at AdS_4 geometries in the IR. Moreover, throughout the chapter we will be switching between the type IIA description of these solutions in ten dimensions and their M-theory description in eleven dimensions. We therefore begin by reviewing a few facts about the simplest examples of these kinds of solutions.

The metric and dilaton of the type IIA solution describing N D2-branes at the tip of a manifold of G_2 holonomy take the form

$$\begin{aligned} \mathrm{d}s^2_{\text{st}} &= h^{-\frac{1}{2}}\, \mathrm{d}x^2_{1,2} + h^{\frac{1}{2}}\, \mathrm{d}s^2(\mathrm{M}_7), \\ e^{\Phi} &= h^{\frac{1}{4}}. \end{aligned} \tag{2.1}$$

The requirement of G_2 holonomy guwarantees that the solution preserves $\mathcal{N} = 1$ supersymmetry in three dimensions, i.e. two supercharges. If the transverse seven-dimensional space is a cone then the base must be a nearly-Kähler six-dimensional manifold (NK_6):

$$\mathrm{d}\mathrm{d}s^2(\mathcal{M}_7) = \mathrm{d}r^2 + r^2\, \mathrm{d}s^2\,(\mathrm{NK}_6)\,. \tag{2.2}$$

In terms of the radial coordinate on the cone, the warp factor in (2.1) behaves as

$$h \sim \frac{N}{r^5}. \tag{2.3}$$

In the particular case that the NK manifold is S^6 the supersymmetry is enhanced to $\mathcal{N} = 8$ (i.e. sixteen supercharges) and the gauge theory dual is maximally supersymmetric YM in three dimensions [12]. In the present work the NK manifold of interest is $\mathbb{CP}^3$, in which case the gauge theory dual is expected to be a quiver YM-type theory with gauge group U(N) × U(N) [14].

The uplift of the D2-brane solution to eleven dimensions is straightforwardly obtained via the usual ansatz

$$\mathrm{d}s_{11}^2 = e^{-\frac{2}{3}\Phi}\,\mathrm{d}s_{\mathrm{st}}^2 + e^{\frac{4}{3}\Phi}\,\ell_p^2\,(\mathrm{d}\psi + C_1)^2\,, \tag{2.4}$$

where ψ parameterizes the M-theory circle, ℓ_p is the eleven-dimensional Planck length and C_1 is the RR one-form potential of type IIA. Since the D2-brane solution has $C_1 = 0$, the result is the M2-brane-type metric

$$\mathrm{d}s_{11}^2 = H^{-2/3}\,\mathrm{d}x_{1,2}^2 + H^{1/3}\,\mathrm{d}s_8^2, \tag{2.5}$$

with

$$H = e^{\Phi}\,h^{3/4} = h, \qquad\qquad \mathrm{d}s_8^2 = \mathrm{d}r^2 + r^2\mathrm{d}s^2\,(\mathrm{NK}_6) + \ell_p^2\,\mathrm{d}\psi^2. \tag{2.6}$$

We see that the fact that in the D2-brane solution the RR two-form vanishes implies that the M-theory circle is trivially fibered over the rest of the directions, and that it has constant size in the eight-dimensional transverse metric.

Let us contrast this with the uplift of the $\mathrm{AdS}_4\times\mathbb{CP}^3$ solution of type IIA supergravity, whose gauge theory dual is the ABJM CSM theory [17]. In this case we view $\mathbb{CP}^3$ as a Kähler manifold instead of as a NK manifold (see below for more details on this distinction). The RR two-form is proportional to the Kähler form, the dilaton is constant and the warp factor scales as $h \sim r^{-4}$, which results in the uplift

$$H = h^{3/4} \sim r^{-3}, \qquad\qquad \mathrm{d}s_8^2 = \mathrm{d}r^2 + r^2\mathrm{d}s^2(\mathbb{CP}^3) + r^2\,(\mathrm{d}\psi + C_1)^2\,. \tag{2.7}$$

It can be checked that the metric in eleven dimensions contains again an AdS_4 factor. We see how the M-theory circle is non-trivially fibered over, and that its size grows as that of the other directions.

The solutions of interest in the rest of the chapter are based on the eight-dimensional Spin(7)-holonomy metrics of [13], which combine ingredients of the two cases above. On the one hand, the M-theory circle is non-trivially fibered over the rest of the coordinates. On the other hand, its size does not grow asymptotically with the other

directions but approaches a constant. In the type IIA description this means that the metric and the dilaton behave asymptotically as in the D2-brane solution (2.1) but, unlike in the pure D2-brane solution, the RR two-form does not vanish. For these reasons we expect the dual gauge theory in the UV to be a quiver SYM theory with gauge group U(N) × U(N) and additional CSM terms.

2.3. Geometry of $\mathbb{CP}^3$

Since this manifold will play a crucial role in our solutions, we will discuss some of its properties in this section. For our purposes, a useful way to describe $\mathbb{CP}^3$ is as the twistor space over the four sphere, or in other words, as an S^2 fibration over S^4:

$$\begin{array}{ccc} S^2 & \hookrightarrow & \mathbb{CP}^3 = \mathrm{Tw}\left(S^4\right) \\ & & \downarrow \\ & & S^4 \end{array} \tag{2.8}$$

This non-trivial fibration allows us to consider deformations in which we squash the fiber with respect to the base. A convenient set of coordinates was introduced in [22], and we follow their notation with slight differences. In terms of the vielbeins E^i to be defined below, the metric can be written as

$$\mathrm{d}s_6^2 = \alpha^2 \left[\left(E^1\right)^2 + \left(E^2\right)^2\right] + \mathrm{d}\Omega_4^2, \tag{2.9}$$

where the metric in brackets is the metric on a round S^2 and E^1, E^2 describe the non-trivial fibration (i.e. they contain coordinates of S^4). We have included the squashing parameter α that controls the size of the fiber with respect to the base. There are two special values of this parameter for which the metric becomes Einstein: $\alpha^2 = 1$ and $\alpha^2 = 1/2$. If $\alpha^2 = 1$ we recover the unsquashed $\mathbb{CP}^3$ with the Fubini–Study metric, which is Kähler. This is the metric appearing in the ABJM construction [17]. If $\alpha^2 = 1/2$, the metric admits instead a nearly Kähler structure, as in (2.2). This is the metric that was used in the construction of [23], where unquenched flavour was added to three-dimensional SYM.

There is another special point, $\alpha^2 = 1/5$, for which the metric, despite it not being Einstein, supports a minimally supersymmetric AdS solution. Its uplift to M-theory corresponds to the squashed seven-sphere, and the dual gauge theory is an $\mathcal{N} = 1$ deformation of ABJM [19].

Two more important facts about this geometry are the following. First, the isometry group of the metric (2.9) is generically Sp(2) ~ SO(5), which is enhanced to SU(4) ~ SO(6) at the special point $\alpha^2 = 1$. This means that it will be convenient to describe $\mathbb{CP}^3$ as the coset Sp(2)/U(2), since we are interested in solutions preserving these isometries. Second, the non-vanishing Betti numbers are

$$b_0 = b_2 = b_4 = b_6 = 1, \tag{2.10}$$

meaning that $\mathbb{CP}^3$ possesses non-trivial two- and four-cycles.

In constructing the solutions, an important ingredient is the set of Sp(2)-left-invariant forms on the coset Sp$S\,p(2)$/U(2). We will be using the coordinate system in [22] to facilitate the comparison, although a coordinate system is not indispensable. Given the SU(2)-left-invariant forms ω^i, verifying

$$\mathrm{d}\omega^i = \frac{1}{2}\epsilon_{ijk}\omega^j \wedge \omega^k, \tag{2.11}$$

the metric of the four-sphere can be written as

$$\mathrm{d}\Omega_4^2 = \frac{4}{(1+\xi^2)^2}\left(\mathrm{d}\xi^2 + \frac{\xi^2}{4}\omega^i\omega^i\right), \tag{2.12}$$

with ξ a non-compact coordinate. If the S^2 fiber is parameterized by the usual angles θ and φ, then the non-trivial fibration is described by the vielbeins

$$\begin{aligned} E^1 &= \mathrm{d}\theta + \frac{\xi^2}{1+\xi^2}\left(\sin\varphi\,\omega^1 - \cos\varphi\,\omega^2\right), \\ E^2 &= \sin\theta\left(\mathrm{d}\varphi - \frac{\xi^2}{1+\xi^2}\omega^3\right) + \frac{\xi^2}{1+\xi^2}\cos\theta\left(\cos\varphi\,\omega^1 + \sin\varphi\,\omega^2\right). \end{aligned} \tag{2.13}$$

For our purposes, it is convenient to consider a rotated version of the vielbeins on the

four-sphere that read[2]

$$\begin{aligned}
\mathcal{S}^1 &= \frac{\xi}{1+\xi^2}\left[\sin\varphi\,\omega^1 - \cos\varphi\,\omega^2\right],\\
\mathcal{S}^2 &= \frac{\xi}{1+\xi^2}\left[\sin\theta\,\omega^3 - \cos\theta\left(\cos\varphi\,\omega^1 + \sin\varphi\,\omega^2\right)\right],\\
\mathcal{S}^3 &= \frac{\xi}{1+\xi^2}\left[\cos\theta\,\omega^3 + \sin\theta\left(\cos\varphi\,\omega^1 + \sin\varphi\,\omega^2\right)\right],\\
\mathcal{S}^4 &= \frac{2}{1+\xi^2}\,\mathrm{d}\xi.
\end{aligned} \tag{2.14}$$

Despite the fact that these forms depend on the S^2 angles, it is easily checked that

$$\mathcal{S}^n\mathcal{S}^n = \mathrm{d}\Omega_4^2. \tag{2.15}$$

In terms of these, the left-invariant two-forms on the coset are

$$X_2 = E^1 \wedge E^2, \qquad\qquad J_2 = \mathcal{S}^1 \wedge \mathcal{S}^2 + \mathcal{S}^3 \wedge \mathcal{S}^4. \tag{2.16}$$

Similarly, the globally defined, left-invariant three-forms are:

$$\begin{aligned}
X_3 =& E^1 \wedge \left(\mathcal{S}^1 \wedge \mathcal{S}^3 - \mathcal{S}^2 \wedge \mathcal{S}^4\right) - E^2 \wedge \left(\mathcal{S}^1 \wedge \mathcal{S}^4 + \mathcal{S}^2 \wedge \mathcal{S}^3\right),\\
J_3 =& - E^1 \wedge \left(\mathcal{S}^1 \wedge \mathcal{S}^4 + \mathcal{S}^2 \wedge \mathcal{S}^3\right) - E^2 \wedge \left(\mathcal{S}^1 \wedge \mathcal{S}^3 - \mathcal{S}^2 \wedge \mathcal{S}^4\right).
\end{aligned} \tag{2.17}$$

Finally, the invariant four-forms are the wedges of the two-forms

$$X_2 \wedge J_2, \qquad\qquad J_2 \wedge J_2 = 2\epsilon_{(4)}, \tag{2.18}$$

where $\epsilon_{(n)}$ denotes the volume-form of the n-sphere. Left-invariance ensures that this system of forms closes under exterior differentiation and Hodge duality. In particular we have

$$\mathrm{d}X_2 = \mathrm{d}J_2 = X_3, \qquad\qquad \mathrm{d}J_3 = 2\left(X_2 \wedge J_2 + J_2 \wedge J_2\right),$$

$$\star\, X_2 = \frac{1}{2\alpha^2} J_2 \wedge J_2, \qquad\qquad \star\, J_2 = \alpha^2 X_2 \wedge J_2, \tag{2.19}$$

$$\star\, X_3 = -J_3. \tag{2.20}$$

[2]With respect to [22], we are taking $\mathcal{S}^{\xi}_{\text{there}} = \mathcal{S}^4_{\text{here}}$ and $\mathcal{S}^3_{\text{there}} = -\mathcal{S}^3_{\text{here}}$.

From these forms it is easy to construct both the Kähler and the nearly Kähler structures on $\mathbb{CP}^3$. When the squashing in (2.9) is fixed to $\alpha^2 = 1$ the metric admits a Kähler structure, whose Kähler form is

$$J_{\mathrm{K}} = X_2 - J_2, \tag{2.21}$$

which is closed by virtue of (2.19). If instead the squashing is $\alpha^2 = 1/2$, the almost-complex structure associated to the NK structure reads

$$J_{\mathrm{NK}} = \frac{1}{2} X_2 + J_2. \tag{2.22}$$

This shows that the set of Sp(2)-invariant forms is general enough for our purposes. In the following we will use them to construct solutions of type IIA supergravity with $\mathbb{CP}^3$ as their internal geometry.

2.4. Singular flows

As explained in section 2.1, in this section we will construct type IIA solutions describing RG flows from a D2-brane-like asymptotic geometry in the UV to a singular geometry in the IR. The uplifts of these solutions to M-theory are also singular in the IR. In the following sections we will modify these solutions in such a way that their eleven-dimensional description is completely regular.

The transverse, seven-dimensional geometries that we will employ are the dimensional reduction of the eight-dimensional metrics found in [13], with which we will make contact below. Despite the fact that our UV asymptotic geometries are different from those in [22], which focused on AdS_4 solutions, the metrics that we are interested in fall within the ansatz studied in [22], which we therefore follow.

The ten-dimensional string-frame metric and dilaton take the form

$$\begin{aligned} \mathrm{d}s^2_{\mathrm{st}} &= h^{-\frac{1}{2}} \mathrm{d}x^2_{1,2} + h^{\frac{1}{2}} \mathrm{d}s^2_7, \\ e^{\Phi} &= h^{\frac{1}{4}} e^{\Lambda}, \end{aligned} \tag{2.23}$$

with the transverse geometry given by

$$\mathrm{d}s^2_7 = \mathrm{d}r^2 + e^{2f}\, \mathrm{d}\Omega^2_4 + e^{2g} \left[\left(E^1\right)^2 + \left(E^2\right)^2 \right]. \tag{2.24}$$

The warp factor h, the squashing functions f, g and the dilaton function Λ depend only on the radial coordinate r. Note that r, e^f and e^g have dimensions of length, whereas

h is dimensionless. The D2-brane solution (2.1), to which our more general solutions will asymptote, is recovered setting

$$h \sim \frac{N}{r^5}, \qquad e^{2f} = \frac{1}{2}r^2, \qquad e^{2g} = \frac{1}{4}r^2, \qquad e^{\Lambda} = 1. \tag{2.25}$$

The metric and dilaton (2.23) will be supported by the fluxes

$$F_2 = Q_k J_{\rm K}, \tag{2.26}$$

$$F_4 = \mathrm{d}^3 x \wedge \mathrm{d}\left(h^{-1} e^{-\Lambda}\right), \tag{2.27}$$

where we recall that $J_{\rm K}$ is the Kähler form of $\mathbb{CP}^3$ given in (2.21). The fact that F_4 does not involve any new functions beyond those appearing in the metric and the dilaton is a reflection of supersymmetry. Closure of F_2 implies that Q_k is a constant.

The first-order BPS equations ensuring $\mathcal{N} = 1$ supersymmetry follow from the results in [22] and read

$$\begin{aligned} \Lambda' &= 2Q_k\, e^{\Lambda-2f} - Q_k\, e^{\Lambda-2g}, \\ f' &= \frac{Q_k}{2}\, e^{\Lambda-2f} - \frac{Q_k}{2}\, e^{\Lambda-2g} + e^{-2f+g}, \\ g' &= Q_k\, e^{\Lambda-2f} + e^{-g} - e^{-2f+g}. \end{aligned} \tag{2.28}$$

The warp factor can be expressed in terms of the other functions as [22]

$$h = e^{-\Lambda}\left[h_0 - Q_c \int^r e^{2\Lambda(z)-4f(z)-2g(z)}\mathrm{d}z\right]. \tag{2.29}$$

The constant Q_c is related to the number of D2-branes, as we will see below, and has dimensions of (length)^5. The integrand has dimensions of (length)$^{-6}$ and h is dimensionless. The integration constant h_0 can be shifted by changing the lower limit of the integral, so we will henceforth set $h_0 = 0$ without loss of generality.

The usual quantization condition for the RR fluxes takes the form

$$\int_{\Sigma_{8-p}} F_{8-p} = 2\kappa_{10}^2 T_{\mathrm{D}p}\, N_p, \tag{2.30}$$

where Σ_{8-p} is an appropriate cycle. In the case $p = 6$ this cycle is a $\mathbb{CP}^1 \subset \mathbb{CP}^3$ given by constant coordinates on the S^4 and we get

$$Q_k = \frac{\ell_s g_s}{2} k. \tag{2.31}$$

As in [17, 19], we expect k to be the CS level of the dual gauge theory. This can be inferred from a D4-brane probe in our background extending in the gauge theory directions and wrapping the two-cycle in the internal geometry. The Wess–Zumino part of its action includes the term

$$\frac{T_{\rm D}4\,(2\pi\alpha')^2}{2}\int_{\mathbb{CP}^1\times\mathbb{R}^{1,2}} C_1\wedge F\wedge F = \frac{T_{\rm D4}\,(2\pi\alpha')^2}{2}\int_{\mathbb{CP}^1\times\mathbb{R}^{1,2}} F_2\wedge A\wedge F = \frac{k}{4\pi}\int_{\mathbb{R}^{1,2}} A\wedge F, \tag{2.32}$$

where A and F are the gauge field on the D4-brane and its field strength respectively. This is precisely a Chern–Simons interaction at level k in the gauge theory dual.

In the case $p = 2$ the cycle is the entire $\mathbb{CP}^3$ and we find

$$Q_c = 3\pi^2\ell_s^5\, g_s\, N, \tag{2.33}$$

where N is the number of D2-branes and the rank of the field theory gauge group.

In order to make contact with [13], let us uplift our ansatz to eleven dimensions. The Kähler form (2.21) can be written as $J_{\rm K} = {\rm d}C_1$ with the potential

$$C_1 = -\left(\cos\theta\,{\rm d}\varphi - \xi\,\mathcal{S}^3\right). \tag{2.34}$$

This means that in terms of the vielbein

$$E^3 = {\rm d}\psi - \cos\theta\,{\rm d}\varphi + \xi\mathcal{S}^3, \tag{2.35}$$

with $\psi \in \left[0, \frac{4\pi}{k}\right)$, the eleven-dimensional metric can be written in the M2-brane form (2.5) with

$${\rm d}s_8^2 = e^{-\Lambda}\left\{{\rm d}r^2 + e^{2f}{\rm d}\Omega_4^2 + e^{2g}\left[\left(E^1\right)^2 + \left(E^2\right)^2\right]\right\} + e^{\Lambda}Q_k^2\left(E^3\right)^2 \tag{2.36}$$

and

$$H = he^{\Lambda}. \tag{2.37}$$

Comparing with the ansatz in [13] we see that the functions a, b, c used there are related to ours through

$$a^2 = e^{2g-\Lambda}, \qquad b^2 = Q_k^2 e^{\Lambda}, \qquad c^2 = e^{2f-\Lambda}, \tag{2.38}$$

and that their equations for special holonomy are equivalent to the BPS system (2.28). To be precise, in order to recover the results of [13] we should set $Q_k = -1$. Presumably, the sign is a choice of radial coordinate, and absolute values different from one

correspond to orbifolds of the construction in [13]. In most of this chapter we will focus on the case with negative Q_k. We conclude that all the solutions of [13] are also solutions of our equations and that we have directly constructed their ten-dimensional description.

Before we describe the family of metrics that will be our main interest, let us point out two particularly simple solutions that are dual to superconformal theories. If $Q_k > 0$ there is the ABJM fixed point [17] described by

$$e^{2f} = r^2, \qquad e^{2g} = r^2, \qquad e^{\Lambda} = \frac{r}{Q_k}. \tag{2.39}$$

The supersymmetry of this solution is enhanced generically to $\mathcal{N} = 6$. If $Q_k < 0$ there is the OP fixed point [19] at

$$e^{2f} = \frac{9}{5} r^2, \qquad e^{2g} = \frac{9}{25} r^2, \qquad e^{\Lambda} = \frac{3r}{5|Q_k|}. \tag{2.40}$$

The theory dual to the OP fixed point is an $\mathcal{N} = 1$ deformation of the ABJM model. It is easy to show that in both cases the coefficients of the three vielbeins E^i in the uplift coincide and that altogether they parameterize a round three-sphere fibered over S^4. Thus in the ABJM case the eleven-dimensional geometry is AdS_4 times a round S^7 (orbifolded by Z_k), whereas in the OP case the sphere is not round but squashed. For this reason, upon reduction to ten dimensions the internal metric involves the unsquashed $\mathbb{CP}^3$ in the ABJM case, corresponding to $\alpha^2 = 1$ in (2.9), whereas for OP it involves the squashed $\mathbb{CP}^3$ with $\alpha^2 = 1/5$.

We now proceed to describe the family of metrics that will be our main interest. The general solution to our BPS system can be found using the tricks developed in [13, 18]. First we define the master function

$$P(r) = e^{2f-\Lambda}, \tag{2.41}$$

which verifies the third-order equation

$$(P' - Q_k)\, T = P T', \tag{2.42}$$

where

$$T = 2PW' + (P' + 3Q_k)\, W, \qquad W = P' + Q_k. \tag{2.43}$$

Note that P has dimensions of (length)^2. We now change to a radial coordinate ϱ and a function $\gamma(\varrho)$ defined by the conditions

$$P' = \varrho, \qquad\qquad P'' = -\frac{\gamma}{P}. \tag{2.44}$$

With this we reduce the system to the first-order equation

$$\gamma\left(2\frac{\mathrm{d}\gamma}{\mathrm{d}\varrho} - 6Q_k\right) = (\varrho + 3Q_k)\left(\varrho^2 - Q_k^2\right). \tag{2.45}$$

The final change of variables to a new radial coordinate y and a new function $v(y)$ defined through

$$y = \frac{2\left(Q_k^2 - \gamma + Q_k\varrho\right)}{(Q_k + \varrho)^2}, \qquad\qquad \varrho = -Q_k\,(v+1)\,, \tag{2.46}$$

linearizes the equation to

$$2\left(1 - y^2\right)\frac{\mathrm{d}v}{\mathrm{d}y} = yv + 2. \tag{2.47}$$

Note that y and v are both dimensionless. This equation can be solved in terms of generalized hypergeometric functions, as we will explain below. Going back to (2.44), we see that the master function satisfies the equation

$$\frac{1}{P}\frac{\mathrm{d}P}{\mathrm{d}y} = \frac{v+1}{v\,(1-y^2)}. \tag{2.48}$$

The rest of the functions are determined in terms of P as

$$e^g = \frac{2P\,(2-v)}{Q_k\,(1+y)\,v^2}, \qquad\qquad e^\Lambda = \frac{4P\,(v-2)}{Q_k^2 v^3\,(1+y)}. \tag{2.49}$$

Following the chain of definitions, we see that the r and y coordinates are related through

$$\mathrm{d}r = -\frac{P}{Q_k v\,(1-y^2)}\mathrm{d}y, \tag{2.50}$$

and hence that the eight-dimensional, Spin(7)-holonomy metric takes the form

$$\mathrm{d}s_8^2 = \frac{v\,P\,(1+y)\,\mathrm{d}y^2}{4\,(v-2)\,(1-y^2)^2} + P\,\mathrm{d}\Omega_4^2 + \frac{P\,(v-2)}{v\,(1+y)}\left[\left(E^1\right)^2 + \left(E^2\right)^2\right] + \frac{4P\,(v-2)}{v^3\,(1+y)}\left(E^3\right)^2. \tag{2.51}$$

The general solution of (2.47) splits into several families depending on the initial conditions for the "flow" $v(y)$. We are particularly interested in the families denoted $\mathbb{B}_8^+$ and $\mathbb{B}_8^-$ in [13, 18]. Both are characterized by the fact that there is a value of the radial coordinate, $y = y_0$, such that

$$v(y_0) = 2. \tag{2.52}$$

At this point the three-sphere parametrized by E^i in (2.51) shrinks smoothly to zero size, whereas the size of the four-sphere remains finite. We will see that, in both families, the IR region lies at $y \to y_0$ and the UV at $y \to 1$. Since the allowed values of y_0 are different in each case, we will consider each family separately.

Let us finally mention that, aside from the solutions of $\mathbb{B}_8$-type that we are discussing in this thesis, the only other solution to the system (2.28) that provides a physically acceptable metric is the one dubbed $\mathbb{A}_8$ in [13]. This geometry, which exists for $Q_k > 0$, describes a flow that starts at the same UV theory as the $\mathbb{B}_8$ metrics, but that in the IR flows to the ABJM fixed point. The rest of the solutions of (2.28) are either singular and/or produce signature changes in the metric.

2.4.1. $\mathbb{B}_8^+$ family

In this case the range of the radial coordinate is

$$-1 \leq y_0 \leq y <, \tag{2.53}$$

and the solutions of (2.47) and (2.48) are

$$v = v^+(y) = \frac{1}{(1-y^2)^{1/4}}\left(v_0^+ + y\ {}_2F_1\left[\frac{1}{2}, \frac{3}{4}; \frac{3}{2}; y^2\right]\right), \tag{2.54}$$

$$P = P^+(y) = P_0^+ \frac{(1+y)^{3/4}}{(1-y)^{1/4}} v^+(y), \tag{2.55}$$

where v_0^+ is a dimensionless integration constant and P_0^+ is an integration constant with dimensions of (length)^2. Although P_0^+ sets the scale of the entire internal metric (2.51), we will show below that it can be completely eliminated from the full, eleven-dimensional metric once the warp factor is included. Nevertheless, we will need to fix the precise value of P_0^+ in order to ensure the same value of the dual gauge coupling for all solutions. We will come back to this at the end of section 2.6.1.

Given y_0, the condition (2.52) fixes v_0^+ and vice versa. Hence we will think of y_0 as the parameter labelling the different solutions in the $\mathbb{B}_8^+$ family. The presence of $1 - y^2$ in the denominators of the expressions above indicates that regular solutions correspond to $y_0 \in [-1, 1)$ or equivalently to $v_0^+ \in (-v_c, v_c]$, where

$$v_c = \frac{\Gamma[1/4]^2}{\sqrt{8\pi}} \tag{2.56}$$

is the value of v_0^+ that can be read off from (2.54) by setting $v = 2$ and taking the limit $y^2 \to 1$. Looking at (2.55) and (2.49), and noting that $v \geq 2$, we see that in order for P and e^g to be positive we must have $P_0^+ > 0$ and $k < 0$. As we will see, the negative sign of k is consistent with the fact that the $\mathbb{B}_8^+$ family contains a flow to the OP solution (2.40).

As we mentioned above, the UV corresponds to the region $y \to 1$, in which the behavior of the metric is universal for the entire family. In this region we can integrate the change of coordinates (2.50) to leading order to obtain

$$Q_k (1 - y)^{1/4} r = 2^{7/4} P_0^+. \tag{2.57}$$

With this result we can write the transverse metric (2.51) at leading order as

$$\mathrm{d}s_8^2 \propto \mathrm{d}r^2 + \frac{1}{2} r^2 \left\{ \mathrm{d}\Omega_4^2 + \frac{1}{2} \left[\left(E^1\right)^2 + \left(E^2\right)^2 \right] \right\} + \left(\frac{4P_0^+}{Q_k \left(v_0^+ + v_c\right)} \right)^2 (E_3)^2 . \tag{2.58}$$

Since the size of the E_3 circle becomes constant, we recognize this as the uplift of the D2-brane metric whose internal space in ten dimensions, given above between square brackets, is precisely the squashed $\mathbb{CP}^3$ at the NK point, corresponding to $\alpha^2 = 1/2$ in (2.9). Given our parametrization of the dilaton in (2.23), in order for the solution to asymptote to the D2-brane solution (2.1) with the correct normalization of the gauge coupling we must impose the boundary condition $e^\Lambda \to 1$. This fixes the dimensionful constant P_0^+ to the value

$$P_0^+ = \frac{Q_k^2 \left(v_0^+ + v_c\right)}{4}, \tag{2.59}$$

which, in particular, depends on y_0 through v_0^+. Since ψ has period $4\pi/|k|$, this is equivalent to normalizing the asymptotic radius of the M-theory circle in the eight-dimensional transverse metric to the usual result

$$R_{(11)} = \frac{2Q_k}{k} = g_s \ell_s. \tag{2.60}$$

Note that $e^{\Lambda} \to 1$ actually implies that we are setting $g_s = 1$. Nevertheless, we will keep explicit factors of g_s in our formulas in order to facilitate comparison with the literature.

For the $\mathbb{B}_8^+$ family we have $v_0^+ \neq v_c$ and so the IR is located at $y \to y_0$, where the geometry ends. In a suitable radial coordinate ρ defined through

$$4P_0^+ (y - y_0) = (1 - y_0)^{5/4} (1 + y_0)^{1/4} \rho^2, \tag{2.61}$$

the transverse metric at small ρ approaches

$$\mathrm{d}s_8^2 = \mathrm{d}\rho^2 + \frac{1}{4}\rho^2 \left[\left(E^1\right)^2 + \left(E^2\right)^2 + \left(E^3\right)^2 \right] + \frac{2P_0^+ (1 + y_0)}{\left(1 - y_0^2\right)^{1/4}} \mathrm{d}\Omega_4^2. \tag{2.62}$$

Since the E^i describe a three-sphere fibration over S^4, we find that in the IR the metric approaches locally $\mathbb{R}^4 \times S^4$, where the four-sphere has a finite radius squared proportional to P_0^+. However, solving for the warp factor with this transverse space we find an IR singularity, since near y_0 we have that

$$H = \frac{Q_c |Q_k| (1 - y_0)^{7/4}}{4 \left(P_0^+\right)^3 (1 + y_0)^{5/4}} \left[\frac{1}{y - y_0} + \frac{1}{8\left(1 - y_0^2\right)} \log (y - y_0) + O(y - y_0)^0 \right], \tag{2.63}$$

which diverges as $y \to y_0$. A singularity in the warp factor is also present for the rest of the solutions that we will discuss in this section. We will see in subsequent sections that this singularity can be removed by turning on appropriate additional components of F_4 corresponding to fractional M2-branes [24].

2.4.2. $\mathbb{B}_8^\infty$ solution

In the particular case $v_0^+ = v_c$, corresponding to $y_0 = -1$, after changing variables through

$$P_0^+ (1 + y)^{3/4} = \frac{9}{2^{11/4} \times 5} \rho^2, \tag{2.64}$$

one discovers that the transverse space in the IR corresponds to the OP solution

$$\mathrm{d}s_8^2 = \mathrm{d}\rho^2 + \frac{9}{20}\rho^2 \left\{ \mathrm{d}\Omega_4^2 + \frac{1}{5} \left[\left(E^1\right)^2 + \left(E^2\right)^2 + \left(E^3\right)^2 \right] \right\}, \tag{2.65}$$

since one can recognize the metric inside the square brackets as the squashed seven-sphere. The full geometry was denoted $\mathbb{B}_8^\infty$ in [15] and its significance had been

overlooked in studies prior to this reference. It interpolates between the theory on the D2-branes on the squashed $\mathbb{CP}^3$ and the OP fixed point, so it can be seen as an irrelevant deformation of the OP CFT whose UV completion is a SYM-CSM theory.

2.4.3. $\mathbb{B}_8^{\rm OP}$ solution

Remarkably, the OP fixed point also admits a relevant deformation that can be solved for analytically. In our variables, the metric functions and dilaton are

$$e^{2f} = \frac{9}{5}r^2\left[1-\left(\frac{r_0}{r}\right)^{5/3}\right], \quad e^{2g} = \frac{9}{25}r^2\left[1-\left(\frac{r_0}{r}\right)^{5/3}\right]^2, \quad e^{\Lambda} = \frac{3r}{5|Q_k|}\left[1-\left(\frac{r_0}{r}\right)^{5/3}\right], \tag{2.66}$$

with the radial direction ending at $r = r_0$, which plays a role analogous to that of P_0^+ in the $\mathbb{B}_8^+$ family. Changing coordinates from r to ϱ through

$$20|Q_k|r = 3\varrho^2 \tag{2.67}$$

we see that this solution corresponds to the original Spin(7) manifold of [20, 21], whose metric is

$$\mathrm{d}s_8^2 = \frac{\mathrm{d}\varrho^2}{\left[1-\left(\frac{\varrho_0}{\varrho}\right)^{10/3}\right]} + \frac{9}{20}\varrho^2\mathrm{d}\Omega_4^2 + \frac{9}{100}\varrho^2\left[1-\left(\frac{\varrho_0}{\varrho}\right)^{10/3}\right]\left[\left(E^1\right)^2+\left(E^2\right)^2+\left(E^3\right)^2\right]. \tag{2.68}$$

The UV of this flow is of course the OP fixed point while the IR, which lies at $\varrho = \varrho_0$, is precisely of the form (2.62), with the four-sphere radius proportional to ϱ_0.

2.4.4. $\mathbb{B}_8$ solution

At the other end of the allowed values for v_0^+, i.e. when $v_0^+ \to -v_c$, corresponding to $y_0 \to 1$, the coordinate y ceases to be appropriate to describe the geometry. Instead, in the original radial coordinate r the solution takes the simple form

$$e^{2f} = \frac{1}{2}\frac{r^2\,(r-2r_0)}{(r-r_0)}, \qquad e^{2g} = \frac{1}{4}\frac{r^2\,(r-2r_0)^2}{(r-r_0)^2}, \qquad e^{\Lambda} = \frac{r_0}{2|Q_k|}\frac{r\,(r-2r_0)}{(r-r_0)^2}, \tag{2.69}$$

where one has to assume again that $k < 0$ and

$$r_0 = 2|Q_k|, \tag{2.70}$$

so that $e^{\Lambda} \to 1$ asymptotically. Note that the space ends at $r = 2\,r_0$. Again, r_0 plays a role analogous to that of P_0^+ in the $\mathbb{B}_8^+$. Uplifting to eleven dimensions we get the transverse space

$$\mathrm{d}s_8^2 = \frac{(r-r_0)^2\,\mathrm{d}r^2}{r\,(r-2r_0)} + \frac{r}{2}\,(r-r_0)\,\mathrm{d}\Omega_4^2 + \frac{r}{4}\,(r-2r_0)\left[\left(E^1\right)^2 + \left(E^2\right)^2\right] + \frac{r_0^2}{4}\frac{r\,(r-2r_0)}{(r-r_0)^2}\left(E^3\right)^2. \tag{2.71}$$

This metric was dubbed $\mathbb{B}_8$ in [13, 18]. The geometry ends smoothly at $r = 2r_0$ and has the same asymptotic behavior as the $\mathbb{B}_8^+$ family.

2.4.5. $\mathbb{B}_8^-$ family

Pushing further the values of y_0 one arrives to the $\mathbb{B}_8^-$ family of metrics, as described in [13, 18]. In our radial coordinate, they are defined in the range

$$1 < y \leq y_0 < \infty, \tag{2.72}$$

where again $v(y_0) = 2$. The functions in the solution can be written as

$$v = v^- = \frac{1}{(y^2-1)^{1/4}}\left(v_0^- + \frac{2}{\sqrt{y}}\;{}_2F_1\left[\frac{1}{4},\frac{3}{4};\frac{5}{4};\frac{1}{y^2}\right]\right),$$

$$P = P^- = P_0^-\frac{(y+1)^{3/4}}{(y-1)^{1/4}}v^-, \tag{2.73}$$

where $v_0^- \in \left(-\sqrt{2}\,v_c, \infty\right)$ is a dimensionless integration constant and P_0^- is an integration constant with dimensions of (length)^2 that sets the scale of the entire internal metric (2.51). To fix the correct asymptotics, $e^{\Lambda} \to 1$, we must choose

$$P_0^- = \frac{Q_k^2\left(v_0^- + \sqrt{2}\,v_c\right)}{4}. \tag{2.74}$$

Both the UV and IR behavior of the $\mathbb{B}_8^-$ metrics, located respectively at $y \to 1$ and $y \to y_0$, coincide with those of the $\mathbb{B}_8^+$ family.

2.4.6. $\mathbb{B}_8^{\mathrm{conf}}$ solution

In all the solutions above we assumed that $k < 0$. We close this section with the case $k = 0$. Changing coordinates through

$$\mathrm{d}r = \left(1 - \frac{\rho_0^4}{\rho^4}\right)^{-1/2}\mathrm{d}\rho \tag{2.75}$$

the BPS solution takes the form

$$e^{\Lambda} = 1, \qquad e^{2f} = \frac{1}{2}\rho^2, \qquad e^{2g} = \frac{1}{4}\rho^2\left(1 - \frac{\rho_0^4}{\rho^4}\right). \tag{2.76}$$

Since $k = 0$ the RR two-form vanishes. This translates into the fact that the M-theory circle is trivially fibered and hence the eight-dimensional transverse metric in eleven dimensions is a direct product of the form $\mathcal{M}_7 \times S^1$, where $\mathcal{M}_7$ is the G_2-manifold found in [20, 21]. The UV corresponds again to D2-branes on the NK $\mathbb{CP}^3$. It can be seen that in the IR, located at $\rho \to \rho_0$, the local geometry approaches $\mathbb{R}^3 \times S^4$, with a finite radius for the S^4. Again there is a singularity in the warp factor that can be cured with additional fluxes corresponding to fractional D2-branes [25], as we describe in the following sections.

The uplift of this metric is very simple and its transverse part reads

$$\mathrm{d}s_8^2 = \frac{\mathrm{d}\rho^2}{\left(1 - \frac{\rho_0^4}{\rho^4}\right)} + \frac{1}{2}\rho^2\,\mathrm{d}\Omega_4^2 + \frac{1}{4}\rho^2\left(1 - \frac{\rho_0^4}{\rho^4}\right)\left[\left(E^1\right)^2 + \left(E^2\right)^2\right] + \ell_p^2\mathrm{d}\psi^2. \tag{2.77}$$

The IR limit corresponds now to $\mathbb{R}^3 \times S^1 \times S^4$, since the circle that before was fibered over S^2 to form the three-sphere in $\mathbb{R}^4$ is now trivial and remains of finite size in the IR. As we will see, this change in topology has dramatic consequences in the dual field theory.

2.5. Adding fractional branes

The transverse geometries presented in the previous section are suitable to support D2-brane solutions in ten dimensions or M2-brane solutions in eleven dimensions preserving $\mathcal{N} = 1$ supersymmetry in three dimensions. However, the corresponding warp factors diverge in the IR, thus rendering the full metrics singular. Fortunately, these singularities can be removed by the standard procedure of adding new fluxes to the system. This mechanism was dubbed “transgression" in [25]. As usual in this type of constructions, the new fluxes can be interpreted as resulting from the addition of fractional branes and can be chosen so that supersymmetry is preserved.

We start by reviewing the transgression mechanism as used for instance in [25]. Imagine that one starts with the solution for a D2-brane preserving $\mathcal{N} = 1$ supersymmetry, that is, a solution of the form (2.1) where the transverse space is a (non-compact)

G_2-holonomy manifold. Since manifolds with special holonomy are Ricci-flat the only equation that needs to be solved is that for the warp factor,

$$\Box h = 0, \tag{2.78}$$

with $\Box$ the Laplacian of the seven-dimensional transverse metric. Now suppose that we modify the ansatz for the four-form to include a new piece

$$F_4 = \mathrm{d}^3 x \wedge \mathrm{d}\left(h^{-1}\right) + G_4, \tag{2.79}$$

where G_4 is a closed four-form on the transverse seven-dimensional space. The equation of motion for the NSNS three-form is then solved provided we also turn on

$$H_3 = \star_7 G_4, \tag{2.80}$$

where the Hodge dual is taken with respect to the transverse metric. Closure of H_3 then implies that G_4 is harmonic with respect to the G_2-holonomy metric. With this ansatz, all the equations of motion and Bianchi identities are satisfied as long as the warp factor obeys the inhomogeneous equation

$$\Box h = -\frac{1}{24} G_4^2. \tag{2.81}$$

The key point of this construction is that the transverse geometry is not modified.

The solutions that we are interested in include a non-zero RR two-form, since they correspond to deformation of the field theory by the addition of CS terms. This means that the transgression mechanism above must be generalized as follows.

Suppose that we have a solution of type IIA supergravity preserving at least $\mathcal{N} = 1$ supersymmetry with metric and dilaton given by (2.23), with a four-form given by (2.27), and with a non-zero F_2 with components only along the compact directions. We also assume that the dilaton depends only on the non-compact coordinates in $\mathrm{d}s_7^2$. These conditions are satisfied by the solutions that we discussed in section 2.4 and by all the solutions of [14, 17, 19, 22, 23]. Under these assumptions the only non-trivial equations to solve are those that determine the dilaton and the warp factor or, equivalently, Λ and h, and the equation of motion for h can be derived from that for F_4.

Now we would like to turn on additional fluxes with the purpose of resolving potential singularities as those that we encountered in the warp factor in section 2.4 or, more generally, in order to add fractional branes to the system. Consider therefore the

following modification of the fluxes

$$\begin{aligned} H_3 &= \mathrm{d}B_2, \\ F_4 &= \mathrm{d}^3x \wedge \mathrm{d}\left(h^{-1}\, e^{-\Lambda}\right) + (G_4 + B_2 \wedge F_2)\,, \end{aligned} \tag{2.82}$$

where G_4 is closed and the following duality condition on the transverse space is satisfied

$$e^{\Lambda}\,(G_4 + B_2 \wedge F_2) = \star_7\, H_3. \tag{2.83}$$

Under these circumstances the metric $\mathrm{d}s_7^2$ and the function Λ are left unchanged by the addition of the new fluxes. The only modified equation is that for the warp factor h. This can be derived from the equation for F_4 and becomes inhomogeneous because it is sourced by the new fluxes. We emphasize that the only assumptions about F_2 are that it does not contain components along non-compact directions and that it verifies its Bianchi identity. We will now implement this generalized transgression for the solutions of section 2.4.

The first task is to construct closed forms G_4 and H_3 on the metric (2.24) satisfying the duality condition (2.83). We start from the most general left-invariant ansatz using the forms defined on the coset:

$$\begin{aligned} B_2 &= b_X X_2 + b_J J_2, \\ H_3 &= \mathrm{d}B_2, \\ G_4 &= \mathrm{d}\,(a_X X_3 + a_J J_3) + q_c\,(J_2 \wedge J_2 - X_2 \wedge J_2)\,. \end{aligned} \tag{2.84}$$

Note that H_3 must be exact because it must be closed and $\mathbb{CP}^3$ has no non-trivial three-cycles —see (2.10). In contrast, G_4, which is also closed, can contain a non-exact piece along the non-trivial four-cycle of $\mathbb{CP}^3$. This non-trivial flux is a constant with dimensions of (length)^3 that we have called q_c and that, as we will see, is related to the number of fractional branes. The rest of the coefficients b_X, b_J, a_X, a_J are functions of the radial coordinate that we will determine below.

The duality condition (2.83) leads to the following set of equations

$$\begin{aligned} a_X' &= 0, \\ a_J' &= e^{-\Lambda}\,(b_X + b_J)\,, \\ b_X' &= 2e^{-4f+2g+\Lambda}\,(q_c + 2a_J - Q_k b_J)\,, \\ b_J' &= e^{-2g+\Lambda}\,[Q_k\,(b_J - b_X) + 2\,a_J - q_c]\,. \end{aligned} \tag{2.85}$$

Given the first equation and the closure of X_3, we see that the term $a_X X_3$ does not contribute to G_4, and therefore we will henceforth set $a_X = 0$. In addition, the requirement that G_4 be normalizable in the UV implies the relation

$$a_J = \frac{e^{2g}\left(Q_k b_J - q_c\right) - 2e^{2f+g-\Lambda}\left(b_J + b_X\right) + e^{2f}\left[q_c + Q_k\left(b_X - b_J\right)\right]}{2\left(e^{2f} + e^{2g}\right)}. \tag{2.86}$$

Moreover, the equation that is obtained by differentiating (2.86) is automatically satisfied by virtue of the equations for b_J, b_X in (2.85). We thus conclude that the system (2.85) can be reduced to two equations for the two functions b_J and b_X.

Finally, as anticipated, the equation for the warp factor acquires additional terms due to the flux sources and reads

$$H' = \left(e^{\Lambda} h\right)' = -e^{2\Lambda-4f-2g}\left[Q_c + Q_k\, b_J\left(b_J - 2b_X\right) + 2q_c\left(b_X - b_J\right) + 4a_J\left(b_X + b_J\right)\right], \tag{2.87}$$

where we recall that the eleven- and the ten-dimensional warp factors are related through (2.37). Remember that the equations (2.28) for the background are not modified by the new sources. This will allow us in the next section to solve the system sequentially: First we will solve for the background functions (2.28), then we will use that solution in (2.85) and we will solve for the fluxes, and finally we will integrate the warp factor (2.87). As we will see, in some cases we will be able to find fully explicit analytic solutions.

Again there is a correspondence between our functions and the ones used in [13] (see also [15]) to construct a self-dual four-form in the eight-dimensional Spin(7) space. Specifically, the functions u_i used in [13] are given by[3]

$$\begin{aligned} u_1 &= 4e^{2\Lambda-4f}\left(2a_J - Q_k\, b_J + Q_k^2\, q_c\right), \\ u_2 &= 2Q_k e^{2\Lambda-2f-2g}\left[Q_k\left(b_X - b_J\right) - 2a_J + q_c\right], \\ u_3 &= -\frac{2e^{\Lambda-2f-g}}{Q_k}\left(b_X + b_J\right). \end{aligned} \tag{2.88}$$

In order to interpret the additional fluxes as fractional branes we need to properly quantize them. From the different notions of charge that may be defined in supergravity [26], the one that is quantized and conserved and counts the number of branes is the Page charge. We begin with the D2-brane charge. Following [15] we compute the

[3] As explained below (2.38) we must set $Q_k = -1$ in order to reproduce [13] exactly.

number of D2-branes, which sets the rank of the dual gauge group, as

$$N = \frac{1}{2\kappa_{10}^2 T_{\rm D2}} \int_{\mathbb{CP}^3} \left(- \star F_4 - B_2 \wedge F_4 + \frac{1}{2} B_2 \wedge B_2 \wedge F_2 \right). \tag{2.89}$$

Note that in the presence of the additional fluxes this equation replaces (2.30), since it is not just $*F_4$ but the full integrand above that is a closed form. Nevertheless, the result is the same relation (2.33) between Q_c and N, thus confirming that the new fluxes have not modified the number of non-fractional D2-branes.

In the case of the D6-brane charge measured by the flux of F_2 through the $\mathbb{CP}^1$, equation (2.30) with $p = 6$ is unmodified by the new fluxes, since F_2 is closed. Hence the relation (2.31) between Q_k and k is also unmodified.

Finally, the new fluxes induce D4-brane charge that is interpreted as M fractional D2-branes. The quantization condition reads

$$\bar{M} = \frac{1}{2\kappa_{10}^2 T_{\rm D4}} \int_{\mathbb{CP}^2} (F_4 - B_2 \wedge F_2) = \frac{1}{2\kappa_{10}^2 T_{\rm D4}} \int_{\mathbb{CP}^2} G_4, \tag{2.90}$$

where

$$\bar{M} = M - \frac{k}{2}. \tag{2.91}$$

In the coordinates introduced in (2.13) the $\mathbb{CP}^2$ four-cycle is characterized by $\theta = \varphi = \pi/2$, so we get the relation

$$q_c = \frac{3\pi \ell_s^3 g_s}{4} \bar{M}. \tag{2.92}$$

Here M represents the shift in the gauge group due to the fractional branes, while the $k/2$ shift was argued in [27] to be needed to account for the Freed–Witten anomaly. We thus expect the gauge group of the dual quiver to be $\mathrm{U}(N)_k \times \mathrm{U}(N+M)_{-k}$, where the subindices indicate the CS levels. In the next section we will construct the regular backgrounds that are dual to this theory.

For completeness, we also quote here the value of the D4 and D2 Maxwell charges [26]:

$$Q_4^{\rm Max} = -\frac{1}{3} \left(\bar{M}^2 + 2|k|N \right)^{1/2} (\mathcal{B}_X + 2\mathcal{B}_J), \tag{2.93}$$

$$Q_2^{\rm Max} = -\frac{\left(\bar{M}^2 + 2|k|N \right)}{6|k|} \left[\mathcal{B}_J^2 + 2\mathcal{B}_X \mathcal{B}_J + 12 \mathcal{A}_J (\mathcal{B}_J - \mathcal{B}_X) - 3 \right], \tag{2.94}$$

where $\mathcal{B}_X, \mathcal{B}_J$ and $\mathcal{A}_J$ are the fluxes once the brane charges have been factorized, as defined in the next section (see (2.97)). The Maxwell charges run with the radial coordinate or, equivalently, with the energy scale. The differences between their UV and IR values are

$$\Delta Q_4^{\text{Max}} = \left(\bar{M}^2 + 2|k|N\right)^{1/2}(1 - b_0), \tag{2.95}$$

$$\Delta Q_2^{\text{Max}} = \left(N + \frac{\bar{M}^2}{2|k|}\right)(1 - b_0^2), \tag{2.96}$$

where the parameter b_0 controls the asymptotic value of the fluxes in the UV and again will be defined in the next section (see (2.102)). We will come back to these differences in section 2.6.1, once we have determined the dependence of b_0 with y_0.

2.6. Regular flows

We will now solve the equations that we introduced in the previous section in order to obtain regular geometries. Recall that we must solve for two fluxes b_J, b_X in (2.85) and for the warp factor H in (2.87). The dependence on the different charges can be factored out of the equations by writing them in terms of four dimensionless functions $\mathcal{B}_J, \mathcal{B}_X, \mathcal{A}_J$ and $\mathcal{H}$ defined through

$$\begin{aligned}
b_J &= -\frac{2q_c}{3|Q_k|} - \frac{\left(4q_c^2 + 3Q_c|Q_k|\right)^{1/2}}{3|Q_k|}\,\mathcal{B}_J,\\
b_X &= \frac{2q_c}{3|Q_k|} + \frac{\left(4q_c^2 + 3Q_c|Q_k|\right)^{1/2}}{3|Q_k|}\,\mathcal{B}_X,\\
a_J &= -\frac{q_c}{6} + \left(4q_c^2 + 3Q_c|Q_k|\right)^{1/2}\,\mathcal{A}_J,\\
H &= \frac{\left(4q_c^2 + 3Q_c|Q_k|\right)}{P_0^3}\,\mathcal{H}.
\end{aligned} \tag{2.97}$$

Note that, although the constant terms in b_J and b_X combine to give a closed form that does not contribute to H_3, they do contribute to B_2. In the expression for the warp factor, by P_0 we mean $P_0^{\pm}$ for the $\mathbb{B}_8^{\pm}$ family and the corresponding analogous scale for the other metrics discussed in section 2.4. At this point we can already see why these scales of the internal metric could be eliminated from the full, eleven-dimensional

solution. Indeed, we see from (2.97) that $H \sim P_0^{-3}$ and from (2.51) that $\mathrm{d}s_8^2 \sim P_0$. As a consequence, P_0 cancels out in the $H^{1/3}\mathrm{d}s_8^2$ term of the eleven-dimensional metric (2.5), and its contribution to the first term can be eliminated by rewriting the metric in terms of rescaled gauge theory coordinates defined through

$$\tilde{x}^\mu = \frac{P_0}{\left(4q_c^2 + 3Q_c|Q_k|\right)^{1/3}} x^\mu. \tag{2.98}$$

It follows that P_0 also cancels out in the ten-dimensional metric and dilaton, since these are directly read off from the eleven-dimensional metric. The RR-forms are also independent of P_0, since all the components (2.84) are manifestly P_0-independent, and the same rescaling (2.98) eliminates P_0 from the first term in F_4 in (2.82).

Substituting (2.97) in (2.85) we find that the dimensionless functions obey the equations

$$\begin{aligned}
\mathcal{B}_J' &= \frac{6\mathcal{A}_J + \mathcal{B}_J + \mathcal{B}_X}{(v-2)(y-1)}, \\
\mathcal{B}_X' &= \frac{2(v-2)(\mathcal{B}_J - 6\mathcal{A}_J)}{v^2(y-1)(1+y)^2}, \\
\mathcal{H}' &= \frac{\mathcal{B}_J(\mathcal{B}_J + 2\mathcal{B}_X) + 12\mathcal{A}_J(\mathcal{B}_J - \mathcal{B}_X) - 3}{36(1-y)^{1/4}(1+y)^{5/4}(v-2)^2},
\end{aligned} \tag{2.99}$$

where $\mathcal{A}_J$ is understood to be given by (2.86) as

$$\mathcal{A}_J = \frac{(1+y)v^2 - yv - 2}{6(y+2)v - 12}\mathcal{B}_J - \frac{v(1+y)(1+v)}{6(y+2)v - 12}\mathcal{B}_X. \tag{2.100}$$

$\mathcal{B}_J$, $\mathcal{B}_X$, $\mathcal{A}_J$ and $\mathcal{H}$ are functions only of y and a given solution is labelled only by the parameter y_0, since all the dependence on the charges has been factored out. This makes these functions ideally suited for numerical integration. In order to do so, we first solve (2.99) perturbatively around the IR and around the UV.

2.6.1. $\mathbb{B}_8^+$ family

In the IR, defined by the condition $v(y_0) = 2$, we find

$$\mathcal{B}_J = 1 - \frac{1}{2\left(1-y_0^2\right)}(y-y_0) + \frac{2-3y_0}{8\left(1-y_0^2\right)^2}(y-y_0)^2 + \mathcal{O}(y-y_0)^3\,, \tag{2.101}$$

$$\mathcal{B}_X = 1 - \frac{3}{4\left(1-y_0^2\right)^2}(y-y_0)^2 + \mathcal{O}(y-y_0)^3$$

$$\mathcal{H} = \mathcal{H}_{\rm IR} - \frac{7(y-y_0)}{48(1+y_0)^3\left(1-y_0^2\right)^{1/4}} - \frac{77(y_0-2)(y-y_0)^2}{576(1+y_0)^3\left(1-y_0^2\right)^{5/4}} + \mathcal{O}(y-y_0)^3\,,$$

where we have already imposed regularity of the warp factor, which fixes the integration constants in $\mathcal{B}_J$ and $\mathcal{B}_X$. The only undetermined constant in the IR expansion is $\mathcal{H}_{\rm IR}$, which will be fixed in the full numerical solution by requiring D2-brane asymptotics in the UV with the correct normalization.

In the UV, located at $y \to 1$, we find the expansions

$$\mathcal{B}_J = b_0\left[1 + \frac{2^{9/4}}{w_0^+}\Delta y^{1/4} + \frac{2^{7/2}}{\left(w_0^+\right)^2}\Delta y^{1/2} - \frac{2^{19/4}}{\left(w_0^+\right)^3}\Delta y^{3/4} + \frac{b_4}{\left(w_0^+\right)^4}\Delta y + \mathcal{O}(\Delta y)^{5/4}\right],$$

$$\mathcal{B}_X = b_0\left[1 + \frac{2^{9/4}}{w_0^+}\Delta y^{1/4} + \frac{3\times 2^{5/2}}{\left(w_0^+\right)^2}\Delta y^{1/2} + \frac{2^{23/4}}{\left(w_0^+\right)^3}\Delta y^{3/4} - \frac{\left(128+\frac{b_4}{2}\right)}{\left(w_0^+\right)^4}\Delta y + \mathcal{O}(\Delta y)^{5/4}\right],$$

$$\mathcal{H} = \mathcal{H}_{\rm UV} + \frac{\left(1-b_0^2\right)}{15\times 2^{3/4}\left(w_0^+\right)^2}\Delta y^{5/4} + \frac{2^{3/2}\left(1-2b_0^2\right)}{9\left(w_0^+\right)^3}\Delta y^{3/2} + \mathcal{O}(\Delta y)^{7/4}, \tag{2.102}$$

with $w_0^+ = \left(v_0^+ + v_c\right) \in (2v_c, 0)$ and $\Delta y \equiv 1 - y$. The undetermined constants in the UV are thus b_0, b_4 and $\mathcal{H}_{\rm UV}$. The latter must vanish in order to have the correct D2-brane asymptotics in the decoupling limit, i.e. in order for $H \to 0$ in the UV. Through the numerical integration, this requirement fixes the value of $\mathcal{H}_{\rm IR}$. Once this is done there is a unique solution for each value of y_0 and the UV constants b_0, b_4 can be simply read off from the solution. The result is displayed in Fig. 2.4, whereas Fig. 2.5 shows the IR value of the warp factor. The full solution is perfectly regular despite the fact that $\mathcal{H}_{\rm IR}$ diverges as $y_0 \to -1$.

We see from Fig. 2.4(left) that there is a one-to-one correspondence between y_0 and the values of b_0 in the interval $(0, 1)$. This is a nice consistency check of the fact that

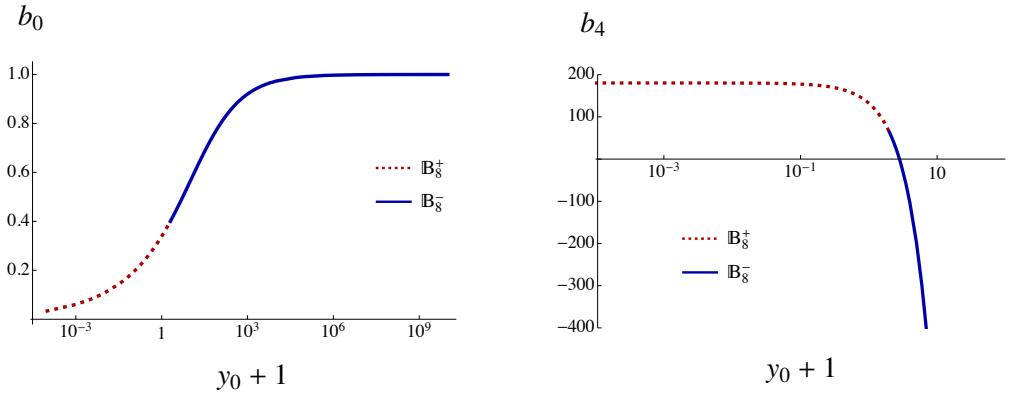

Figure 2.4.: Values of the UV parameters b_0 (left) and b_4 (right) from the numerical integration.

y_0 is related to the difference between the gauge couplings of the two gauge groups. The reason is that varying b_0 corresponds to varying the UV asymptotic flux of the NSNS two-form through the $\mathbb{CP}^1 \subset \mathbb{CP}^3$. Since this asymptotic flux is expected to specify the difference between the gauge theory couplings [15], the fact that b_0 can be mapped to y_0 in a one-to-one manner supports the idea that the family of theories under consideration are indeed parametrized by the difference between the gauge couplings.

Moreover, we now see that this information is partially encoded in the constant P_0 introduced in section 2.4, since this is determined by y_0 and the CS level through e.g. Eq. (2.59). Finally, we note that the dependence of b_0 on y_0 displayed in Fig. 2.4(left) immediately determines the differences between the UV and the IR values Maxwell charges (2.95).

Presumably, b_4 is related to the vacuum expectation value of some operator in the gauge theory.

2.6.2. $\mathbb{B}_8^\infty$ solution

When $y_0 \to -1$ the IR expansions above are not well defined, reflecting the dramatic change in the IR, which in this case is a fixed point instead of a gapped phase. Indeed, we have that the fluxes are constant

$$b_J = -\frac{2q_c}{3|Q_k|}, \qquad b_X = \frac{2q_c}{3|Q_k|}, \qquad a_J = -\frac{q_c}{6}. \tag{2.103}$$

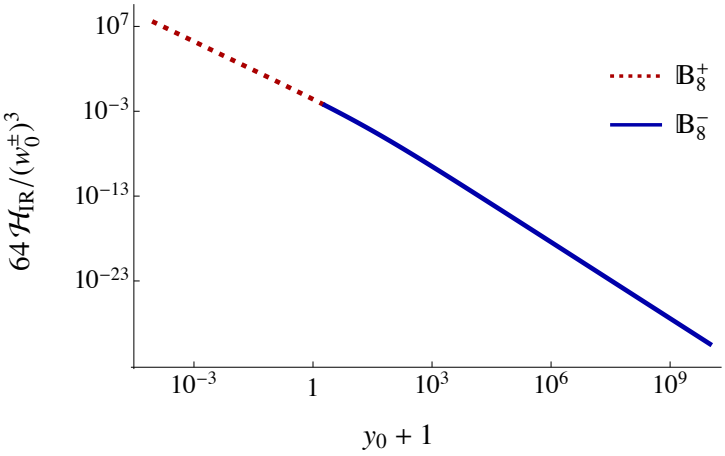

Figure 2.5.: Values of the parameter $\mathcal{H}_{\rm IR}$ from the numerical integration.

Using this, it is easy to find the expansions for the warp factor. In the IR, around $y = -1$, we get

$$\mathcal{H} = \mathcal{H}_{\rm IR} + (y+1)^{-9/4}\,\frac{5}{9\times 2^{5/4}}\left[\frac{5}{3} - \frac{13}{8}\,(y+1) + \frac{815}{1664}\,(y+1)^2 + \mathcal{O}\,(y+1)^3\right]. \tag{2.104}$$

Notice that the constant term $\mathcal{H}_{\rm IR}$ is not the leading term in this case and this causes the metric to be AdS. On the other hand, the UV expansion gives again D2-brane asymptotics, as can be obtained from the general expansion of the $\mathbb{B}_8^+$ family, specifying to $w_0^+ = 2v_c$ and $b_0 = 0$.

The only parameter to be found from the numerics is $\mathcal{H}_{\rm IR}$ such that the warp factor has no constant piece in the UV. From our results we find $\mathcal{H}_{\rm IR} \simeq -0.0087$.

2.6.3. $\mathbb{B}_8^{\rm OP}$ solution

The RG flow that connects the OP fixed point to the gapped phase can also be solved for analytically. In terms of a dimensionless coordinate

$$\rho = \frac{r}{r_0} \tag{2.105}$$

the fluxes are simply

$$\mathcal{B}_J = \frac{1}{\rho^{1/3}}, \qquad \mathcal{B}_X = \frac{6\rho^{5/3} - 1}{5\rho^2}, \tag{2.106}$$

and the regular warp factor is

$$\mathcal{H} = \frac{5}{243}\left[\frac{1}{\rho^2} - \frac{9}{\rho^{1/3}} - 3\,\frac{\rho^{4/3} - \rho^{1/3}}{\rho^{5/3} - 1}\right] + \\ + \frac{4\sqrt{2}}{81}\left(\sqrt{5 + \sqrt{5}}\arctan\left[\frac{\sqrt{10 + 2\sqrt{5}}}{4\rho^{1/3} + 1 - \sqrt{5}}\right] + \sqrt{5 - \sqrt{5}}\arctan\left[\frac{\sqrt{10 - 2\sqrt{5}}}{4\rho^{1/3} + 1 + \sqrt{5}}\right]\right). \tag{2.107}$$

2.6.4. $\mathbb{B}_8$ solution

In this case a complete analytic solution can be found. In terms of a dimensionless coordinate

$$\rho = \frac{r}{r_0}, \tag{2.108}$$

with r_0 given by (2.70), the fluxes take the form

$$\mathcal{B}_J = \frac{2\left(\rho^4 + \rho^3 - 4\rho + 4\right)}{5\rho^3\left(\rho - 1\right)}, \qquad \mathcal{B}_X = \frac{2\left(\rho^5 - 10\rho + 8\right)}{5\rho^3\left(\rho - 1\right)^2}, \tag{2.109}$$

where one integration constant was fixed to have D2-brane asymptotics in the UV while the other two were fixed by regularity. The M2-brane warp factor can be found again in closed form and is simply

$$\mathcal{H} = \frac{\left(1323\rho^6 + 924\rho^5 + 963\rho^4 + 510\rho^3 - 1340\rho^2 - 4340\rho + 2800\right)}{47250\,\rho^9\left(\rho - 1\right)^2}, \tag{2.110}$$

which is perfectly regular at $\rho = 2$. Notice that the boundary conditions have fixed all the integration constants, the only parameters being the quantized charges.

2.6.5. $\mathbb{B}_8^-$ family

For $y_0 > 1$ the equations admit expansions similar to those of the $\mathbb{B}_8^+$ family. Around the end of the geometry, imposing regularity, we find

$$\begin{aligned}
\mathcal{B}_J &= 1 + \frac{1}{2\left(y_0^2-1\right)}(y-y_0) + \frac{2-3y_0}{8\left(y_0^2-1\right)^2}(y-y_0)^2 + O(y-y_0)^3\,,\\
\mathcal{B}_X &= 1 - \frac{3}{4\left(y_0^2-1\right)^2}(y-y_0)^2 + O(y-y_0)^3\,,\\
\mathcal{H} &= \mathcal{H}_{\rm IR} + \frac{7(y-y_0)}{48\,(y_0+1)^3\left(y_0^2-1\right)^{1/4}} - \frac{77(y_0-2)(y-y_0)^2}{576\,(y_0+1)^3\left(y_0^2-1\right)^{5/4}} + O(y-y_0)^3\,.
\end{aligned} \tag{2.111}$$

Again, we have $\mathcal{H}_{\rm IR}$ as the only undetermined constant in the IR, which will be fixed in the numerics by the UV conditions. Similarly, for $y \to 1$ we have expansions identical to those in (2.102) with the replacements $(1-y) \to (y-1)$ and $w_0^+ \to w_0^- = \left(v_0^- + \sqrt{2}\,v_c\right) \in (0,\infty)$. The equations are solved using these expansions, with $\mathcal{H}_{\rm UV} = 0$ for D2-brane asymptotics, as boundary conditions.

2.6.6. $\mathbb{B}_8^{\rm conf}$ solution

In this case it is convenient to change from the ρ coordinate in (2.77) to a dimensionless coordinate

$$z = \frac{\rho}{\rho_0}. \tag{2.112}$$

The fluxes regularizing the solution are

$$\begin{aligned}
b_J &= \frac{Q_c}{4q_c} + \frac{2q_c}{3\rho_0}\left[\frac{z\sqrt{z^4-1} - \left(3z^4-1\right)U(z)}{z^4-1}\right],\\
b_X &= -\frac{Q_c}{4q_c} - \frac{2q_c}{3\rho_0}\left[\frac{z\sqrt{z^4-1} - \left(3z^4-1\right)U(z)}{z^4}\right],
\end{aligned} \tag{2.113}$$

where the dimensionless function U is defined as

$$U(z) = \int_1^z \left(\sigma^4-1\right)^{-1/2} \mathrm{d}\sigma. \tag{2.114}$$

The warp factor, both in ten and eleven dimensions, is given by

$$h = H = \frac{128 q_c^2}{9\rho_0^6}\int_z^\infty \left[\frac{2-3\sigma^4}{\sigma^3\left(\sigma^4-1\right)^2} + \frac{\left(4-9\sigma^4+9\sigma^8\right)U(\sigma)}{\sigma^4\left(\sigma^4-1\right)^{5/2}} + \frac{2\left(1-3\sigma^4\right)U(\sigma)^2}{\sigma^5\left(\sigma^4-1\right)^3}\right]\mathrm{d}\sigma. \tag{2.115}$$

2.6.7. Range of validity

We now turn to the determination of the range of validity of the supergravity solutions above. Since in the UV the dilaton goes to zero, the correct description is the ten-dimensional one. This one extends up to the UV scale at which the curvature ceases to be small in string units. The Ricci scalar of the ten-dimensional solutions grows in the UV as

$$\ell_s^2 R \sim \ell_s^2\left(\frac{|Q_k|}{4q_c^2+3Q_c|Q_k|}\frac{r}{\left(1-b_0^2\right)}\right)^{1/2}. \tag{2.116}$$

Requiring this to be small and translating to a gauge theory energy scale U via the usual relation $U = r/\ell_s^2$ [12] we find the condition

$$U \ll \lambda\left(1+\frac{\bar{M}^2}{2N|k|}\right)\left(1-b_0^2\right), \tag{2.117}$$

where we recall that λ is the 't Hooft coupling with dimensions of energy. We observe that the usual result $U \ll \lambda$ for the D2-branes gets modified due to the presence of the fractional branes. We have included the dependence on y_0 through the coefficient $1-b_0^2$, which vanishes as $y_0^{-1/2}$ when $y_0 \to \infty$. This is a manifestation of the fact that, in the limit $y_0 \to \infty$, Q_k must scale as $Q_k \sim k \sim y_0^{-1/2}$ in order to obtain a valid supergravity description. The origin of this scaling together with more details will be given in the next section.

In the IR the ten-dimensional metrics are singular, so the correct description is given in terms of the eleven-dimensional solutions, in which the IR value of the Ricci scalar in units of the eleven-dimensional Planck length $\ell_p = g_s^{2/3}\ell_s$ is finite and scales as

$$\ell_p^2 R \sim \left(\frac{\bar{M}^2}{2}+N|k|\right)^{-1/3}. \tag{2.118}$$

In order for this to be small we simply need to require that the combination

$$\frac{\bar{M}^2}{2}+N|k| \gg 1. \tag{2.119}$$

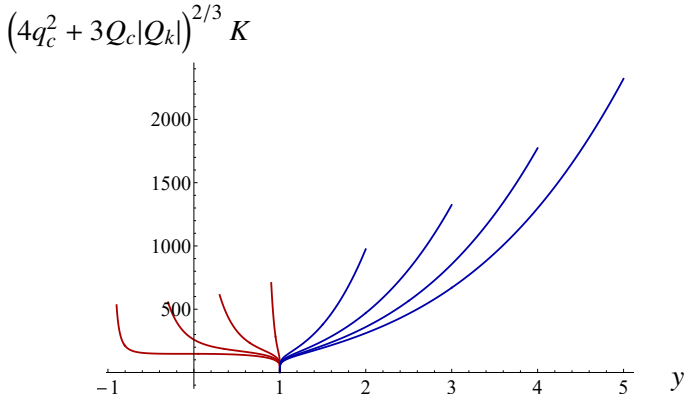

Figure 2.6.: Kretschmann scalar $K = R_{\mu\nu\rho\sigma}R^{\mu\nu\rho\sigma}$ as a function of y for $\mathbb{B}_8^+$ solutions (left, red curves) with $y_0 = -0.9, -0.3, 0.3, 0.9$ from left to right, and for $\mathbb{B}_8^-$ solutions (right, blue curves) with $y_0 = 2, 3, 4, 5$ from left to right. We see that at $y = 1$ all curves approach the same value since they all share the same UV asymptotics, whereas the curvature at the IR endpoint ($y = y_0$) diverges as y_0^2 as $y_0 \to \infty$.

For large y_0, however, the IR value of the Kretschmann scalar, $K = R_{\mu\nu\rho\sigma}R^{\mu\nu\rho\sigma}$, shown in fig. 2.6, grows as

$$\ell_p^4 K \sim \left(\frac{\bar{M}^2}{2} + N|k|\right)^{-2/3} y_0^2. \tag{2.120}$$

Thus in the limit $y_0 \to \infty$ we must impose the additional condition that

$$|k|^6 \left(\frac{\bar{M}^2}{2} + N|k|\right) \gg 1, \tag{2.121}$$

where again we have assumed that $k \sim y_0^{-1/2}$.

2.7. Limiting dynamics

In this section we will study the limits of the above metrics as $y_0 \to \infty$ and as $y_0 \to -1$. In the first case the solution approaches $\mathbb{B}_8^{\text{conf}}$ everywhere except in the deep IR. In the second case the solution approaches the combination of the $\mathbb{B}_8^{\infty}$ flow followed by the $\mathbb{B}_8^{\text{OP}}$ flow. In this sense the solutions with generic y_0 continuously interpolate between

quasi-confining and quasi-conformal dynamics. We will verify this with an explicit calculation of the quark-antiquark potential in section 2.8.

2.7.1. Quasi-confining dynamics

Consider the limit $y_0 \to \infty$ of the $\mathbb{B}_8^-$ solutions. Expanding the functions of the internal metric for large y_0 we find

$$e^{2f} = \frac{4\left(P_0^-\right)^2}{|Q_k|^2}\left(\frac{y+1}{y-1}\right)^{1/2}\left[1 - \frac{\left(y^2-1\right)^{1/4}}{\sqrt{y_0}} + O\left(y_0^{-1}\right)\right],$$
$$e^{2g} = \frac{4\left(P_0^-\right)^2}{|Q_k|^2}\frac{1}{\left(y^2-1\right)^{1/2}}\left[1 - \frac{2\left(y^2-1\right)^{1/4}}{\sqrt{y_0}} + O\left(y_0^{-1}\right)\right]. \tag{2.122}$$

Performing the change of variables

$$y = \frac{\rho^4 + \rho_0^4}{\rho^4 - \rho_0^4} \tag{2.123}$$

we see that, to leading order, we recover the confining metric (2.77) with an internal scale given by

$$\rho_0^2 = \frac{8\left(P_0^-\right)^2}{|Q_k|^2}. \tag{2.124}$$

Given that P_0^- was fixed by the UV condition $e^\Lambda \to 1$ as in (2.74), to leading order in y_0 we have

$$\rho_0^2 = 2\,|Q_k|^2\, y_0. \tag{2.125}$$

Note that, since $y_0 \to \infty$, ρ_0 seems to grow without bound. We may think of the limit in two (equivalent) ways. One is simply to keep all charges fixed as we take $y_0 \to \infty$ but to rescale the gauge theory coordinates as in (2.98) with P_0 replaced by ρ_0, since this cancels all the dependence of the solution on ρ_0. The other is to keep the gauge theory coordinates fixed but to scale $Q_k \sim y_0^{-1/2}$ as we take $y_0 \to \infty$. This is intuitive since we know that the $\mathbb{B}_8^{\text{conf}}$ solution has $k = 0$. By comparing with the analytic confining solution (2.77) it is possible to deduce how the parameters b_0, b_4 and $\mathcal{H}_{\text{IR}}$ must scale for large y_0, with the result

$$\left(1 - b_0^2\right) \sim \frac{6K(-1)}{\sqrt{2}}\, y_0^{-1/2}, \quad b_4 \sim -2^{7/2}\, K(-1)\, y_0^{3/2}, \quad \mathcal{H}_{\text{IR}} \sim \frac{h_{\text{conf}}}{256}\, y_0^{-3/2}, \tag{2.126}$$

where $K(m)$ is the complete elliptic integral of the first kind and $h_{\rm conf}$ is the IR value of the warp factor for the confining solution given by Eq. (2.115) with $z = 1$. We have verified these scalings with our numerical solutions. One way to see that both ways of taking the limit are equivalent is to note that in both cases the y_0-dependent coefficient in front of the $\mathrm{d}x_{1,2}^2$ term in (2.23) attains a finite limit as $y_0 \to \infty$.

In terms of the ρ coordinate, the first correction in (2.122) (the second term inside the square brackets) takes the form

$$\frac{\rho_0}{\rho}\frac{1}{\sqrt{y_0}\left(1-\frac{\rho_0^4}{\rho^4}\right)^{1/2}}. \tag{2.127}$$

We see that, no matter how large y_0 is, this first correction competes with the leading term (the 1 in (2.122)) sufficiently close to ρ_0. This was expected because we know that, sufficiently deep in the IR, the $\mathbb{B}_8^-$ and the $\mathbb{B}_8^{\rm conf}$ metric differ dramatically from one another: in $\mathbb{B}_8^-$ the M-theory circle shrinks to zero size whereas in $\mathbb{B}_8^{\rm conf}$ it does not. The intuitive picture is therefore that, by taking y_0 large enough, one can make the $\mathbb{B}_8^-$ and the $\mathbb{B}_8^{\rm conf}$ metrics arbitrarily close to one another on an energy range that extends form the UV down to an IR scale arbitrarily close to the mass gap. Throughout this range the S^1 of the internal metric has a constant and identical size in both metrics. Sufficiently close to the mass gap, however, the $\mathbb{B}_8^-$ metric abruptly deviates from the $\mathbb{B}_8^{\rm conf}$ metric and the internal S^1 closes off. Presumably this fast change of the size of the circle is related to the fact that the curvature in the deep IR diverges as $y_0 \to \infty$, as shown in fig. 2.6.

2.7.2. Quasi-conformal dynamics

The $\mathbb{B}_8^\infty$ and the $\mathbb{B}_8^{\rm OP}$ solutions arise as two different limits of the $\mathbb{B}_8^+$ metrics. If the limit $y_0 = -1$ of the $\mathbb{B}_8^+$ is taken at fixed y then the result is the $\mathbb{B}_8^\infty$ solution, as we saw in section 2.4.2.

Instead, if we first focus on the IR of $\mathbb{B}_8^+$ by expanding around $y - y_0$, so that we see the $\mathbb{R}^4 \times S^4$ region, and afterwards take the $y_0 \to -1$ limit, then the $\mathbb{B}_8^{\rm OP}$ metric is reproduced. Indeed, for the size of the four-sphere in the eight-dimensional transverse space we have in the strict IR

$$e^{2f-\Lambda} = 2^{3/4}\, P_0\, (y_0+1)^{3/4} + O\,(y_0+1)^{7/4}\,. \tag{2.128}$$

Comparing with the IR expansion for $\mathbb{B}_8^{\rm OP}$ suggests the relation

$$r_0 = \frac{2^{3/4} P_0}{3|Q_k|} (y_0+1)^{3/4} \,. \tag{2.129}$$

As in the previous subsection, we may take the limit in two ways, either by rescaling the gauge theory directions or by rescaling Q_k. In the latter case, in order for r_0 to be finite, we must scale Q_k as $(y_0+1)^{-3/4}$ when $y_0 \to -1$. Moreover, using this identification of parameters and integrating the change of coordinates (2.50) in the IR and around y_0+1 we get

$$\begin{aligned} y - y_0 = &\left[\frac{4\,(r-r_0)}{3r_0} + \frac{2\,(r-r_0)^2}{9r_0^2} + O\,(r-r_0)^3\right](y_0+1) - \\ &- \left[\frac{5\,(r-r_0)}{6r_0} + \frac{5\,(r-r_0)^2}{6r_0^2} + O\,(r-r_0)^3\right](y_0+1)^2 + O\,(y_0+1)^3 \,. \end{aligned} \tag{2.130}$$

Finally, substituting this expansion together with (2.129) for the metric functions in the IR of the $\mathbb{B}_8^+$ family and taking the $y_0 \to -1$ limit we arrive at

$$\begin{aligned} e^{2f} &= 3r_0\,(r-r_0) + 2\,(r-r_0)^2 - \frac{(r-r_0)^3}{9r_0} + O\,(r-r_0)^4 \,, \\ e^{2g} &= (r-r_0)^2 - \frac{2\,(r-r_0)^3}{3r_0} + O\,(r-r_0)^4 \,, \end{aligned} \tag{2.131}$$

which coincides, to this order, with the corresponding expansions for $\mathbb{B}_8^{\rm OP}$.

The intuitive picture is therefore that $\mathbb{B}_8^+$ solutions with $y_0 \gtrsim -1$ flow very close to the OP fixed point but eventually deviate from it and develop a mass gap. The mass scale M_* at which the deviation occurs can be estimated from the behavior of the dilaton, which is plotted in fig. 2.7. The mass scale M on the horizontal axis is the mass of a membrane stretched from the bottom of the geometry until the position y at which the dilaton is evaluated (see section 2.8). The normalization factor is

$$M_0 = \frac{|Q_k|}{2\pi \ell_s^2} = \frac{\lambda\,|k|}{4\pi\,N}. \tag{2.132}$$

We define M_* as the position of the maximum of each curve. We see that curves with $y_0 \to -1$ tend to the $\mathbb{B}_8^\infty$ curve but eventually deviate from it around the scale M_* and approach zero at the end of the geometry, instead of approaching the OP value as $\mathbb{B}_8^\infty$ does.

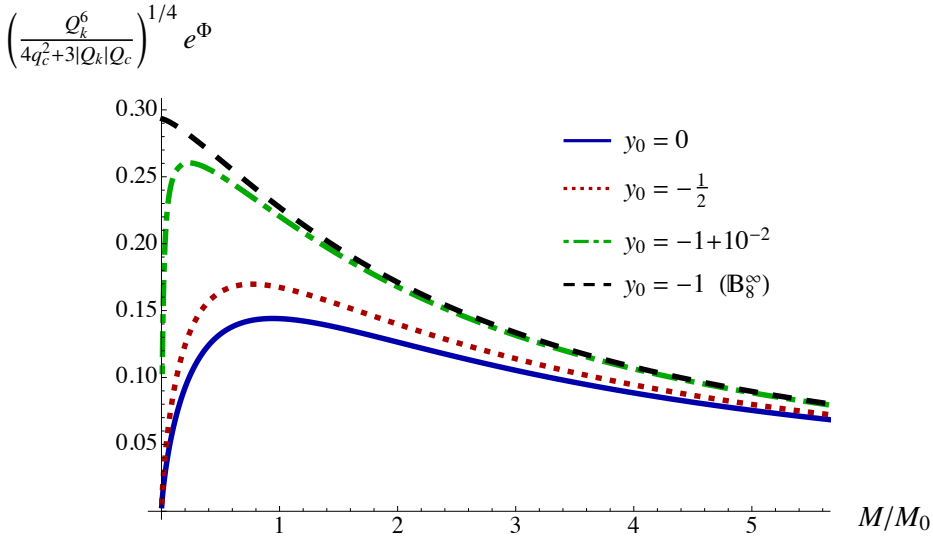

Figure 2.7.: Dilaton as a function of the energy scale for several $\mathbb{B}_8^+$ solutions.

2.8. Quark-antiquark potential

We will now present a computation of the potential between an external quark and an external antiquark separated by a distance L in the gauge theory directions. In the string description this would be extracted from the action of a string hanging from the quark and the antiquark. Instead, in M-theory we must consider a hanging membrane. Although the membrane is asymptotically wrapped on the M-theory circle, namely on the S^1 fiber of the internal geometry, as the membrane penetrates into the bulk geometry the circle wrapped by the membrane may vary. In particular, since the S^1 fiber is contractible inside the S^7, the circle wrapped by the membrane may shrink to zero size at some value of the holographic coordinate, even if at that point the entire S^7 has finite size. All in all this means that, in order to find the membrane with the minimum energy, strictly speaking we would need to solve a problem involving partial differential equations (PDEs) for the membrane embedding as a function of two worldspace intrinsic coordinates. Since this calculation is beyond the scope of this thesis, we will perform a simpler one that nevertheless is expected to capture the qualitative physics. We will therefore assume that the circle wrapped by the membrane is the S^1 fiber at all values of the holographic coordinate. This reduces the problem to

that of solving ordinary differential equations. We will come back to this simplification in section 2.9.

An important point in the calculation is that, generically, the membrane action is UV divergent. We will renormalize away this divergence by subtracting the action of two disconnected membranes extending from the UV all the way to the IR end of the geometry. For all metrics except for $\mathbb{B}_8^{\text{conf}}$ this is in itself a physically acceptable configuration that competes with the connected configuration. In the case of $\mathbb{B}_8^{\text{conf}}$ the disconnected configuration is not a physically acceptable configuration to which the connected one can transition, but it can still be used as a mathematical well defined quantity that can be used to regularize the membrane action.

The results for the quark-antiquark potential V as a function of the separation L for the $\mathbb{B}_8^+$ and $\mathbb{B}_8^-$ solutions are shown in Figs. 2.8(left) and 2.8(right), respectively, where M_0 is given by (2.132) and

$$L_0 = \frac{\left(4q_c^2 + 3Q_c|Q_k|\right)^{1/2}}{|Q_k|^2} = \frac{6\pi N\sqrt{\bar{M}^2 + 2|k|N}}{\lambda\,|k|^2}. \tag{2.133}$$

The behavior of these curves can be understood as follows. In the UV, i.e. in the limit $L \to 0$, the behavior is the same for all curves, since it is dictated by their common D2-brane asymptotics, which implies $VL \sim -L^{1/3}$. Thus, as L begins to increase from zero, the curves first go down (VL becomes more negative) until they reach a turning point and start going up.

This happens at the energy scale at which the Yang–Mills interaction ceases to dominate the dynamics and the CS interactions take over. This scale can be estimated from the radial position at which the first correction to the D2-brane metric is of the same order as the leading term, which yields

$$\lambda\frac{|k|}{N}\left(\frac{2b_0^2 - 1}{1 - b_0^2}\right). \tag{2.134}$$

This is the usual result dressed with a function of the dimensionless parameter y_0 through the dependence on b_0. After this point all curves except for the one corresponding to $\mathbb{B}_8^\infty$ reach $V = 0$ and cross the horizontal axis at a separation that we call L_*. When this happens the disconnected configuration becomes energetically preferred. In the case of $\mathbb{B}_8^\infty$ the product VL asymptotically approaches a negative constant corresponding to the OP fixed point, as expected form the fact that this is the endpoint of the $\mathbb{B}_8^\infty$ flow. In this case the preferred configuration is always the connected one. We

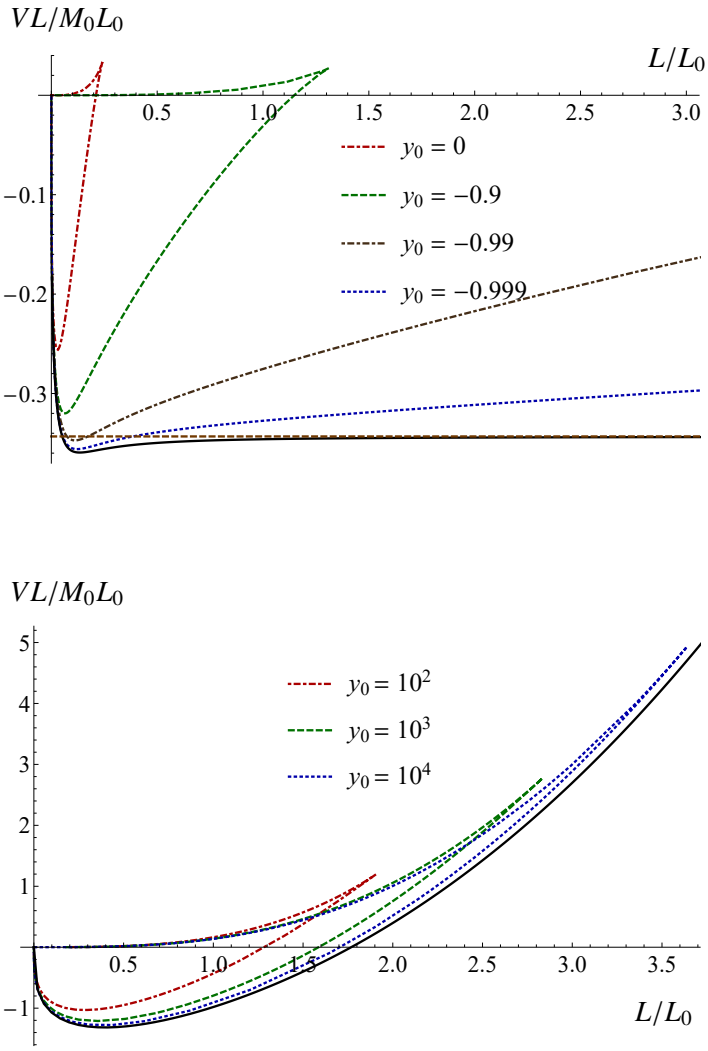

Figure 2.8.: (Up) Quark-antiquark potential for several $\mathbb{B}_8^+$ solutions and for the $\mathbb{B}_8^\infty$ solution, shown as a continuous black curve. M_0 and L_0 are given in (2.132) and (2.133), respectively. The red, dashed horizontal line at the bottom of the plot corresponds to the value of VL for the OP fixed point. (Down) Quark-antiquark potential for several $\mathbb{B}_8^-$ solutions with Q_k scaled as $Q_k^2 = \rho_0^2/2y_0$, as dictated by (2.125), where ρ_0 is the scale of the $\mathbb{B}_8^{\text{conf}}$ solution, whose quark-antiquark potential is shown as a continuous black curve.

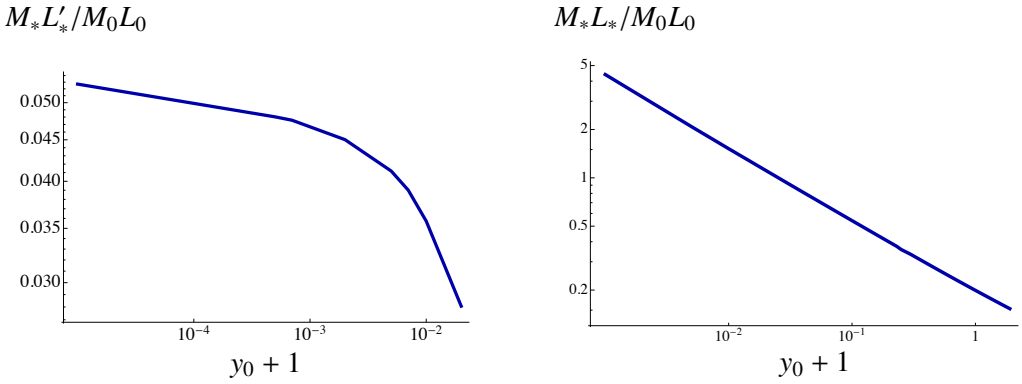

Figure 2.9.: Comparison of the emergent IR scales extracted from the behavior of the dilaton and of the quark-antiquark potential.

see from Fig. 2.8(left) that curves with y_0 closer and closer to -1 become flatter and flatter and cross the horizontal axis at a larger and larger L_*. These curves cross the OP horizontal line at a smaller value $L'_* < L_*$. In this way we see that two IR mass scales emerge for flows that come close to the OP fixed point:

$$M_L = 1/L_*, \qquad M'_L = 1/L'_*. \tag{2.135}$$

In fig. 2.9 we compare these scales to the scale M_* that we determined in fig. 2.7 from the behavior of the dilaton. Although it is difficult to push the numerics to arbitrarily small values of $y_0 + 1$, the plots in the figure suggest that, in the limit $y_0 \to -1$, M'_L is of the same order as M_* (at least over a large range of values of y_0), whereas M_L/M_* goes to zero. In other words, the theory first deviates from the quasi-conformal behavior at the scale $M_* \sim M'_L$ but the membrane becomes disconnected at a lower scale $M_L < M_*$.

In the opposite limit, as $y_0 \to \infty$, we see from fig. 2.8(right) that the curves approach that of the $\mathbb{B}_8^{\text{conf}}$ solution, as expected from the discussion in section 2.7.1. This suggests that these theories exhibit quasi-confining dynamics. We will come back to this point in section 2.9.

At distances L slightly larger than L_* all curves but $\mathbb{B}_8^{\text{conf}}$ reach a cusp and "turn back", thus making the plots multivalued. The reason for the cusp is that, as the penetration depth of the hanging membrane inside the bulk increases beyond the point corresponding to the cusp, L begins to decrease. This kind of behavior also appears

in e.g. calculations of the quark-antiquark potential in solutions with horizons, i.e. in gauge theories at non-zero temperature. As in those cases, the part of the curve beyond the cusp is always energetically disfavored.

2.9. Discussion

The solutions that we have presented here provide a counterexample to the expectation that holographic duals of gauge theories with a mass gap also exhibit confinement. The key point is that, geometrically, this intuition is based on thinking of the quark-antiquark potential in string theory, where it is computed by a hanging string. In this case the smooth capping off of the geometry associated to the mass gap, together with charge conservation, which prevents the string from becoming disconnected, lead to a linear quark-antiquark potential at large distances, as illustrated in fig. 2.1. In our examples, however, the ten-dimensional description is singular and one must resort to eleven-dimensional M-theory in order to have a regular description. In this context the potential is computed from a hanging membrane which is allowed to become disconnected because the M-theory circle on which it is wrapped shrinks to zero size in the IR, as shown in fig. 2.2. This cuts off the linear growth of the potential at long distances. A necessary condition for the consistency of these arguments is that the ten- and eleven-dimensional solutions are not simultaneously reliable in the IR, since otherwise they would have led to contradictory conclusions regarding the presence of confinement.

As we explained in section 2.8, a priori the quark-antiquark potential that we computed was a simplification because we did not allow the circle wrapped by the membrane to vary inside the S^7. However, the two key qualitative conclusions that we reached do not rely on this simplification. Indeed:

1. The exact calculation of the minimum-energy configuration of the membrane, involving PDEs, would exhibit no confinement except for the $\mathbb{B}_8^{\text{conf}}$ solution. This follows simply from the topology of the solutions in eleven dimensions, which allow for an isolated membrane with no boundary in all cases except $\mathbb{B}_8^{\text{conf}}$.

2. The exact calculation of the minimum-energy configuration of the membrane, involving PDEs, would yield a quark-antiquark potential that exhibits quasi-conformal and quasi-confining behaviour in the limits $y_0 \to -1$ and $y_0 \to \infty$, respectively. The reason for this is that, as we showed in section 2.7, in these

limits the entire eleven-dimensional metrics on which the calculation would performed approach $\mathbb{B}_8^{\infty}$ and $\mathbb{B}_8^{\text{conf}}$, respectively.

In summary, the conclusions that our family of solutions exhibit (1) a mass gap but no confinement (except for $\mathbb{B}_8^{\text{conf}}$), and (2) quasi-conformal and quasi-confining behaviour in the appropriate limits, are independent of the simplification that we used to compute the quark-antiquark potential.

We have seen that the presence of confinement in the $\mathbb{B}_8^{\text{conf}}$ solution seems to be associated with the absence of CSM terms in the dual gauge theory. Confinement in a theory with CS terms has been previously considered in [28, 29] in the case of a single gauge group, as opposed to the product gauge group of our model. Despite this difference, our results are compatible with those of [28, 29]. Both of these references distinguish between the bare CS level occurring in the microscopic Lagrangian and the effective IR CS level, and both of them claim that confinement appears only when the latter is zero, i.e. when no CS terms are present in the IR theory. This suggests that, in our model, we should think of k as the effective IR CS level, which is consistent with our identification of this parameter based on the analogy with the ABJM IR fixed point.

Both the arguments of section 2.7 and the quark-antiquark potential of section 2.8 suggest that the solutions we have discussed exhibit quasi-conformal and quasi-confining behavior in the appropriate limits. The latter deserves some further discussion. Indeed, looking at fig. 2.8(right) we see that the curves corresponding to solutions with $y_0 \to \infty$ approach the curve for the $\mathbb{B}_8^{\text{conf}}$ metric. The latter shows the expected linear behavior $V \sim L$ at asymptotically large distances, which appears as a parabola in the figure since we are plotting $VL \sim L^2$. Although the curves with large y_0 reproduce this behavior, we must remember that the connected configuration ceases to be preferred once the curves cross the horizontal axis at $L = L_*$. Therefore, strictly speaking, the potential becomes constant at distances beyond this crossing point. However, the transition from the connected to the disconnected configuration is a semiclassical one, since it requires a fluctuation of the membrane in such a way that the circle transitions from non-zero to zero size. We expect that these fluctuations are exponentially suppressed provided the size of the circle is large in Planck units. For $\mathbb{B}_8^{-}$ solutions this can be achieved up to arbitrarily long distance scales by taking y_0 and the appropriate charges to be large enough. For these solutions connected configurations with $VL > 0$ can be arbitrarily long lived, thus leading to an effective confining potential up to distance scales longer than L_*.

Interestingly, some of the features discussed above are shared by four-dimensional

Quantum Chromodynamics (QCD) if we think of the quark masses as adjustable parameters. Indeed, if all quarks are massive then QCD exhibits a mass gap but no confinement, since the growth of the potential between an external quark-antiquark pair is cut off by the breaking of the flux tube caused by the nucleation of a dynamical quark-antiquark pair. However, if the mass of the quarks is much larger than the QCD scale, then these nucleation is exponentially suppressed and the potential is effectively confining over a large range of distances.

It would be interesting to explore the analogies between the solutions that we have described and QCD further. For this purpose it would be useful to construct a four-dimensional analogue of our solutions. We leave these issues for future work.

3. Mass spectrum of gapped, non-confining theories with multi-scale dynamics

3.1. Introduction

Strongly coupled field theories in which more than one characteristic energy scale is dynamically generated allow for a rich set of phenomena due to observables developing dependences on ratios of such scales. Within the framework of gauge-gravity duality [4, 5, 6], there exists a number of examples constructed in string theory that exhibit non-trivial renormalization group (RG) flows leading to multi-scale dynamics [30, 31, 32, 33]. The reformulation of strongly coupled gauge theories in terms of classical higher-dimensional gravity provides a powerful tool with which analytical progress can be made.

A particularly interesting class of theories with multi-scale dynamics is that in which the RG flows come close to an infrared (IR) fixed point. As we will see, in the cases that we will consider this leads to quasi-conformal behaviour over a range of energies. Moreover, this IR fixed point corresponds to a supersymmetric conformal field theory (CFT) with a moduli space. The existence of an exact moduli space raises the possibility of the spontaneous breaking of scale invariance, suggesting the possible presence of a light dilaton in the spectrum, as emphasized in e.g. [34].

Using gauge-gravity duality, the spectra of composite states in the field theory can be found by studying fluctuations around backgrounds in the dual supergravity description. When the supergravity admits a consistent truncation to a sigma model composed of a number of scalar fields coupled to gravity in $d+1$ dimensions (where d is the number of field theory dimensions), there exists a powerful gauge-invariant formalism to treat the fluctuations in the bulk developed in [35, 36, 37, 38, 39], allowing for the calculation of spin-0 and spin-2 glueball spectra. This has been used to compute spectra for a number of backgrounds with quasi-conformal dynamics obtained as deformations of the Maldacena-Nunez [40, 41] and Klebanov-Strassler [16] backgrounds, leading to

the identification of a light state when there is an operator that acquires a VEV that is parametrically larger than the scale of confinement [42, 43, 44, 45, 46]. Quasi-conformal dynamics has also been explored holographically in a top-down context in [47, 48, 49].

In chapter 2 we studied a class of three-dimensional gauge theories that are dual to a one-parameter family of solutions in M-theory [13, 18]. In terms of ten-dimensional type-IIA supergravity, the asymptotic UV behaviour of the solutions corresponds to placing a stack of D2-branes at a cone over $\mathbb{CP}^3$ and turning on additional fluxes. The dual is expected to be a quiver-type Chern–Simons Matter (CSM) gauge theory with gauge group $\mathrm{U}(N)_k \times \mathrm{U}(N+M)_{-k}$, with k the Chern–Simons level. From the eleven-dimensional point of view, the solutions are all regular in the IR with an end-of-space leading to a mass gap. Despite this, the geometries describe non-confining field theories [1]. In this chapter, we compute the spectrum of spin-0 and spin-2 glueballs in those theories.

The parameter τ_*, related to the previously defined y_0 through equation (3.1), labelling the backgrounds controls, in the gauge dual, the difference between the microscopic couplings of each of the two factors in the gauge group [15]. By varying its value, it is possible to construct RG flows that come arbitrarily close to the IR fixed point given by the supersymmetric Ooguri–Park (OP) CFT [19], hence exhibiting quasi-conformal dynamics over a range of energies.

The moduli space of the OP theory is the same as that of the ABJM theory [17], namely $\mathbb{C}^4/\mathbb{Z}_k$. In the opposite limit, the solutions are quasi-confining, coming close to a confining solution [25] denoted as $\mathbb{B}_8^{\mathrm{conf}}$. Moreover, the system admits a consistent truncation to a sigma model composed of six scalar fields coupled to gravity in four dimensions, allowing us to make use of the aforementioned gauge-invariant formalism to compute the spectrum as a function of τ_*.

In order to gain insight into the physics underlying the various features of the spectrum, we also perform a study in which we introduce a hard-wall cutoff in the IR. Varying the energy scale at which the geometry is thus cut off, we are able to interpolate between the results obtained from a hard-wall IR cutoff and a smooth end of the geometry. We find that there are different regions of parameter space for which there is a light dilaton in the spectrum, and that, in the case of the geometry ending smoothly, the mass of such state is lifted by deep-IR effects. We will show that this result can be understood from the fact that the explicit and the spontaneous breakings of scale invariance that trigger the RG flow that starts directly at the OP fixed point and ends smoothly in the IR are of comparable magnitude and cannot be parametrically

separated.

In section 3.2, we summarize the type-IIA supergravity and M-theory solutions and their description in terms of a four-dimensional sigma model, as well as review the gauge-invariant formalism for the computation of spectra. Section 3.3 contains the numerical computation of the spin-0 and spin-2 glueball spectra. Finally, we conclude with a discussion of our results in section 3.4.

3.2. Summary of known results

3.2.1. Type IIA/M-theory solutions and their field theory duals

In this section we review some basic features of the ten and eleven-dimensional supergravity solutions that we described in chapter 2 in order to set a starting point and redefine some notation more suitable for the numerical computations. The starting point is a stack of N D2-branes at the tip of a cone over $\mathbb{CP}^3$, supported by a Ramond–Ramond (RR) four-form flux proportional to N.[1] In the decoupling limit, this solution is expected to be dual to a three-dimensional quiver-type Yang–Mills theory with gauge group $\mathrm{U}(N) \times \mathrm{U}(N)$ preserving minimal supersymmetry [14].

The backgrounds considered asymptote to this metric in the UV.[2] The internal manifold, $\mathbb{CP}^3$, can be seen as an S^2 fibration over S^4, so the D2-brane solution can be generalized by allowing the relative size of the fiber and the base to change with the radial coordinate and consequently along the RG flow of the dual theory. In particular, solutions exist in which the size of S^4 inside $\mathbb{CP}^3$ remains finite at the end of the geometry, that is, the deep IR, providing an additional scale in the gauge theory and pointing towards a mass gap. However, the ten-dimensional metric is singular in the IR. To be able to interpret these geometries as duals for gauge theories we need to regularize them.

The first step is to include additional two- and four-form RR fluxes as well as turning on the NS three-form. The two-form is proportional to the Kähler form of $\mathbb{CP}^3$, as in ABJM [17], so it will induce Chern–Simons (CS) interactions in the gauge theory dual. The new three- and four-form components can be seen to be sourced by fractional D2-branes [15], so similarly to [16] we expect a shift in the rank of one of the gauge groups proportional to the number M of such fractional branes. Thus, the

[1] This $\mathbb{CP}^3$ is not endowed with the usual Fubini–Study metric, but with a different Einstein metric admitting a Nearly Kähler structure.

[2] With the exception of what we call $\mathbb{B}_8^{\mathrm{OP}}$, which is AdS in the UV.

conjectured dual would be an $\mathcal{N} = 1$ quiver-type Yang–Mills theory with gauge group $\mathrm{U}(N)_k \times \mathrm{U}(N+M)_{-k}$, with k the level of the supplementary CS interactions.

The solutions with all these features are still singular in ten dimensions, so a further uplift to eleven-dimensional supergravity is needed. The non-vanishing type-IIA two-form induces a non-trivial fibering of the M-theory circle that combines with the S^2 to produce a (squashed) three-sphere. At the same time, this S^3 is fibered over the remaining internal four-sphere to give a (squashed) seven-sphere. The eleven-dimensional geometry obtained in this way corresponds to M2-branes in the Spin(7) holonomy manifolds $\mathbb{B}_8^{\pm}$, first found in [13, 18], and is perfectly regular. These special holonomy manifolds appear in a one-parameter family. We denote this parameter by y_0. As argued in [15, 1], we expect it to control the difference between the microscopic couplings of each of the two factors in the gauge group.

In figure 2.3 we represent pictorially the set of solutions as a function of such parameter, which ranges from -1 to $+\infty$, together with the dual interpretation. The gauge theories exhibit different physics varying continuously with y_0. This can be understood in terms of the geometry of the supergravity solutions. For the values $y_0 \in (-1, +\infty)$, describing the solutions $\mathbb{B}_8^{\pm}$ (and the special case $\mathbb{B}_8$ for which $y_0 = 1$), the S^3 shrinks to zero size smoothly in the IR, whereas the size of the S^4 remains finite. The IR transverse geometry is thus $\mathbb{R}^4 \times S^4$. In the dual theories, this implies the existence of a mass gap without confinement. The argument for this is that a quark-antiquark pair is represented by a couple of membranes wrapped around the M-theory circle. This $S^1 \subset S^3$ shrinks smoothly in the IR, so that each independent membrane can extend from the boundary to the bottom of the geometry ending in a cigar-like shape, as depicted to the right in figure 2.2. As the separation between the quark-antiquark pair is made large, this configuration is preferred over the connected one to the left in Figure 2.2.

When the parameter takes the value $y_0 = -1$, the physics is completely different. The whole S^7 shrinks to zero size in the IR (solution $\mathbb{B}_8^{\infty}$), but when taking the warp factor into account, the IR geometry becomes AdS_4 times a squashed seven-sphere of finite size. This fixed point is dual to the OP CFT [19]. The OP fixed point admits a relevant deformation ($\mathbb{B}_8^{\mathrm{OP}}$) that drives it to an IR with the transverse geometry $\mathbb{R}^4 \times S^4$ as in the previous case, leading again to a mass gap but no confinement. Solutions with y_0 close to -1 describe RG flows that approach the concatenation of the $\mathbb{B}_8^{\infty}$ and the $\mathbb{B}_8^{\mathrm{OP}}$ flows. These solutions exhibit quasi-conformal dynamics, remaining close to the OP fixed point over a tuneable range of energies.

In the case of vanishing RR two-form, one obtains a solution based on an internal

geometry found in [20, 21] that we call $\mathbb{B}_8^{\text{conf}}$. The eleven-dimensional solution flows to an IR theory that exhibits both a mass gap and confinement. The geometric reason is that, in this case, the M-theory circle is trivially fibered over the rest of the geometry and it remains non-contractible along the entire flow; in particular, the IR transverse geometry is $\mathbb{R}^3 \times S^1 \times S^4$. This implies that a membrane wrapped on this S^1 cannot end anywhere in the bulk since it would have a cylinder-like geometry and hence a boundary, which is not allowed by charge conservation. The disconnected, deconfined configuration is thus not admissible. On the gauge theory side, the existence of confinement appears to be a consequence of the absence of CSM interactions [1]. This solution can also be recovered as a limit of the $\mathbb{B}_8^-$ solutions when $y_0 \to +\infty$, implying that for large values of y_0 the solutions exhibit quasi-confining behavior.

Finally, it will be convenient to work with the redefined parameter

$$\tau_* = \frac{1}{2}\log(1 + y_0)\,, \tag{3.1}$$

whose range is $\tau_* \in (-\infty, \infty)$. The physical results in the next sections are presented in terms of it.

3.2.2. Four-dimensional description

Holographic spectra are conveniently computed using the gauge-invariant formalism discussed in [36, 39]. This requires the existence of a lower-dimensional sigma model containing at least all the modes that are excited in the background solutions. Moreover, it must be a consistent truncation of ten or eleven-dimensional supergravity in order to ensure that the set of fields that one retains is closed, that is, they do not source additional modes outside the truncation.

Fortunately, all the backgrounds of interest can be obtained as a solution to a four-dimensional supergravity. The details of the full reduction from ten dimensions can be found in [50], from which we will keep only the scalars and follow the notation of [1]. The resulting sigma model contains gravity plus six scalars, three of which, $\{\Phi, U, V\}$, come from the metric together with the dilaton, while the rest, $\{a_J, b_J, b_X\}$, descend from the forms. The four-dimensional action is given by

$$\mathcal{S}_4 = \int \mathrm{d}\rho\, \mathrm{d}^3x\, \sqrt{-g}\left(\frac{R}{4} - \frac{1}{2}G_{ab}(\Phi^a)g^{MN}\partial_M\Phi^a\partial_N\Phi^b - \mathcal{V}(\Phi^a)\right), \tag{3.2}$$

where g_{MN} is the four-dimensional metric ($M, N = 0, 1, 2, 3$), G_{ab} is the sigma-model

metric ($a, b = 1, \cdots, 6$), whose explicit form is given by

$$\begin{aligned} G_{ab}\partial_M\Phi^a\partial_N\Phi^b = &\frac{1}{4}\partial_M\Phi\partial_N\Phi + 2\partial_M U\partial_N U + 6\partial_M V\partial_N V + 4\partial_M U\partial_N V \\ &+ 16e^{-2U-4V+\frac{\Phi}{2}}\partial_M a_J\partial_N a_J + 2e^{-4V-\Phi}\left(\partial_M b_J\partial_N b_J + 2\partial_M b_X\partial_N b_X\right), \end{aligned} \tag{3.3}$$

and the potential $\mathcal{V}$ can be written in terms of a superpotential $\mathcal{W}$ as follows

$$\begin{aligned} \mathcal{V} &= \frac{1}{2}\mathcal{W}_a\mathcal{W}^a - \frac{3}{2}\mathcal{W}^2, \\ \mathcal{W} &= Q_k e^{-U-4V+\frac{3\Phi}{4}} - Q_k e^{-3U-2V+\frac{3\Phi}{4}} - 2e^{-2U-2V} - e^{-4V} \\ &\quad + 4e^{-3U-6V-\frac{\Phi}{4}}\left[4a_J\left(b_J + b_X\right) + 2q_c\left(b_X - b_J\right) + b_J Q_k\left(b_J - 2b_X\right) + Q_c\right], \end{aligned} \tag{3.4}$$

where

$$\mathcal{W}^a = G^{ab}\mathcal{W}_b = G^{ab}\frac{\partial\mathcal{W}}{\partial\Phi^b} \tag{3.5}$$

The constant parameters Q_k, Q_c and q_c appearing in the potential are two- and four-form charges. They are proportional respectively to the CS level k, the number of colours N and the shift in the rank of one of the gauge groups M due to the fractional branes.

All the solutions preserve Poincaré invariance in three dimensions, so we restrict ourselves to backgrounds that only depend on a radial coordinate ρ, for which the metric has the form of a domain wall

$$\mathrm{d}s_4^2 = \mathrm{d}\rho^2 + e^{2A(\rho)}\mathrm{d}x_{1,2}^2. \tag{3.6}$$

Moreover, they are $\mathcal{N} = 1$ supersymmetric, so as usual they can be obtained from a set of BPS equations that read

$$\Phi'^a = G^{ab}\frac{\partial\mathcal{W}}{\partial\Phi^b}, \qquad A' = -\mathcal{W}, \tag{3.7}$$

where prime denotes derivatives with respect to ρ. It can be seen that the equations for U, V, Φ and A found in this way decouple from the rest. It is convenient to write the scalars in terms of new functions $H(y)$, $P(y)$ and $v(y)$ as[3]

$$\begin{aligned} \Phi &= \frac{3}{4}\log\left(\frac{4H^{1/3}P(v-2)}{v^3(y+1)Q_k^2}\right), & U &= \frac{9}{16}\log\left(\frac{4H^{1/3}P(v-2)}{v^{11/9}(y+1)|Q_k|^{2/9}}\right), \\ V &= \frac{1}{16}\log\left(\frac{1024H^3P^9(v-2)}{v^3(y+1)Q_k^2}\right), & A &= \frac{3}{4}\log\left(\frac{2^{1/3}8H^{1/3}P^{7/3}(v-2)}{v^{5/3}(y+1)|Q_k|^{2/3}}\right), \end{aligned} \tag{3.8}$$

[3]Note that for all backgrounds in this section $Q_k < 0$.

and change the radial coordinate from ρ to y defined as

$$\mathrm{d}\rho = \mathrm{d}y\, \frac{2\sqrt{2}H^{3/4}P^{9/4}(v-2)^{1/4}}{|Q_k|^{1/2}v^{3/4}(1-y)(y+1)^{5/4}}. \tag{3.9}$$

As a consequence, the BPS equations for Φ, U, and V following from Eq. (3.7) are solved provided

$$\frac{\partial_y P}{P} = \frac{v+1}{v\,(1-y^2)}, \qquad \partial_y v = \frac{vy+2}{2\,(1-y^2)}. \tag{3.10}$$

After the shifts and rescalings of the fluxes

$$\begin{aligned} a_J &= -\frac{q_c}{6} + \sqrt{4q_c^2 - 3Q_cQ_k}\,\mathcal{A}_J, \qquad b_J = \frac{2q_c}{3Q_k} + \frac{\sqrt{4q_c^2 - 3Q_cQ_k}}{3Q_k}\mathcal{B}_J, \\ b_X &= -\frac{2q_c}{3Q_k} - \frac{\sqrt{4q_c^2 - 3Q_cQ_k}}{3Q_k}\mathcal{B}_X, \quad H = \frac{4q_c^2 - 3Q_cQ_k}{P_0^3}\mathcal{H}, \end{aligned} \tag{3.11}$$

where P_0 is a yet undetermined constant, the remaining BPS equations reduce to

$$\begin{aligned} \partial_y\mathcal{A}_J &= \frac{v^2\,(\mathcal{B}_J - \mathcal{B}_X)}{12(v-2)(y-1)}, \\ \partial_y\mathcal{B}_J &= \frac{(6\mathcal{A}_J + \mathcal{B}_J + \mathcal{B}_X)}{(v-2)(y-1)}, \\ \partial_y\mathcal{B}_X &= \frac{2(v-2)\,(\mathcal{B}_J - 6\mathcal{A}_J)}{v^2(y-1)(y+1)^2}, \\ \partial_y\mathcal{H} &= -\frac{P_0^3v^3(y+1)\,(12\mathcal{A}_J\,(\mathcal{B}_J - \mathcal{B}_X) + \mathcal{B}_J(\mathcal{B}_J + 2\mathcal{B}_X) - 3)}{36P^3(v-2)^2(y-1)}. \end{aligned} \tag{3.12}$$

Contrary to the previous ones, these cannot be solved analytically, so we will resort to numerical calculations. In the following, we also fix

$$\mathcal{A}_J = \frac{v^2 + (v-1)vy - 2}{6v(y+2) - 12}\mathcal{B}_J - \frac{v(v+1)(y+1)}{6v(y+2) - 12}\mathcal{B}_X, \tag{3.13}$$

which automatically solves Eq. (3.12) for $\mathcal{A}_J$.

Depending on the range of the radial coordinate y, the backgrounds that we will study fall into two families, $\mathbb{B}_8^{\pm}$, parameterized by y_0. For the $\mathbb{B}_8^{+}$ family, the range of y

is given by $-1 < y_0 \leq y < 1$ with the IR located at $y = y_0$ and the UV at $y = 1$. These backgrounds have

$$v = \frac{1}{(1-y^2)^{1/4}}\left(v_0^+ + {}_2F_1\left[\frac{1}{2},\frac{3}{4};\frac{3}{2};y^2\right]y\right), \qquad P = P_0\frac{(1+y)^{3/4}}{(1-y)^{1/4}}v, \tag{3.14}$$

where $P_0 = \frac{Q_k^2(v_0^+ + v_c)}{4}$, $v_c \equiv \frac{\Gamma[1/4]^2}{\sqrt{8\pi}}$, and v_0^+ is fixed by the requirement that $v(y_0) = 2$.

For the $\mathbb{B}_8^-$ family, the range of y is given by $1 < y \leq y_0 < \infty$ (as before the IR is located at $y = y_0$ and the UV at $y = 1$), and the backgrounds have

$$v = \frac{1}{(y^2-1)^{1/4}}\left(v_0^- + \frac{2}{\sqrt{y}}\,{}_2F_1\left[\frac{1}{4},\frac{3}{4};\frac{5}{4};\frac{1}{y^2}\right]\right), \quad P = P_0\frac{(y+1)^{3/4}}{(y-1)^{1/4}}v, \tag{3.15}$$

where $P_0 = \frac{Q_k^2(v_0^- + \sqrt{2}\,v_c)}{4}$ and v_0^- is again fixed by the requirement that $v(y_0) = 2$.

In order to construct the backgrounds numerically, we set up the boundary conditions in the IR and evolve Eq. (3.12) towards the UV, checking that we obtain the correct D2-brane asymptotics. It is convenient to work in the radial coordinate τ defined by

$$y = \frac{1+y_0}{2} + \frac{1-y_0}{2}\tanh(\tau), \tag{3.16}$$

in terms of which the IR (UV) is located at $\tau = -\infty$ ($\tau = +\infty$) for both $\mathbb{B}_8^\pm$ families. We define $\alpha \equiv e^{2\tau_*} \equiv 1 + y_0$, such that $-\infty < \tau_* < +\infty$. The IR expansions are given by

$$\begin{aligned}
\mathcal{B}_J &= 1 - \frac{1}{2\alpha}e^{2\tau} + \frac{\alpha+5}{8\alpha^2}e^{4\tau} - \frac{\alpha(5\alpha+22)+75}{80\alpha^3}e^{6\tau} + \mathcal{O}(e^{8\tau}),\\
\mathcal{B}_X &= 1 - \frac{3}{4\alpha^2}e^{4\tau} + \frac{\alpha+19}{8\alpha^3}e^{6\tau} - \frac{\alpha(3\alpha+34)+387}{64\alpha^4}e^{8\tau} + \mathcal{O}(e^{10\tau}),\\
\mathcal{H} &= \mathcal{H}_{IR} - \frac{7|2-\alpha|^{3/4}}{48\alpha^{13/4}}e^{2\tau} + \frac{7(|2-\alpha|^{3/4}(\alpha+33)}{576\alpha^{17/4}}e^{4\tau} + \mathcal{O}(e^{6\tau}).
\end{aligned} \tag{3.17}$$

We determine the integration constant $\mathcal{H}_{IR}$ by requiring that $\mathcal{H} = 0$ in the UV, corresponding to the decoupling limit of the D2-branes. All in all, once the charges Q_c, Q_k and q_c are fixed, the backgrounds are labelled by a single parameter τ_*. This means that once we select the gauge theory dual, with given gauge group and CS level, this parameter characterises completely the solution. As we already mentioned, it controls the difference between the microscopic couplings of each of the two factors in the gauge group.

Finally, let us consider the solutions far in the UV, where the asymptotic expansions are given by ($z \equiv e^{-\tau/2}$)

$$\begin{aligned}
\mathcal{B}_J &= b_0\left(1+\frac{4z}{\beta}+\frac{8z^2}{\beta^2}-\frac{16z^3}{\beta^3}+\tilde{b}_4 z^4\right)+O(z^5),\\
\mathcal{B}_X &= b_0\left(1+\frac{4z}{\beta}+\frac{12z^2}{\beta^2}+\frac{32z^3}{\beta^3}-\left(\frac{\tilde{b}_4}{2}+\frac{64}{\beta^4}\right)z^4\right)+O(z^5),\\
\mathcal{H} &= -\frac{2\left(\beta\left(b_0^2-1\right)P_0^3\right)z^5}{15\gamma^3}+\frac{8\left(1-2b_0^2\right)P_0^3 z^6}{9\gamma^3}+\frac{32\left(9-28b_0^2\right)P_0^3 z^7}{63\beta\gamma^3}+O(z^8).
\end{aligned}$$

For $\mathbb{B}_8^+$ backgrounds,

$$\beta=\frac{v_0^+ + v_c}{(4-2\alpha)^{1/4}},\qquad \gamma=\frac{2P_0(v_0^+ + v_c)}{(4-2\alpha)^{1/2}}, \tag{3.18}$$

while for $\mathbb{B}_8^-$ backgrounds,

$$\beta=\frac{v_0^- + \sqrt{2}v_c}{(2\alpha-4)^{1/4}},\qquad \gamma=\frac{2P_0(v_0^+ + \sqrt{2}v_c)}{(2\alpha-4)^{1/2}}. \tag{3.19}$$

The constants b_0 and $\tilde{b}_4$ are both determined in terms of τ_*. Note that in the UV limit the four-dimensional metric becomes proportional to

$$\mathrm{d}s_4^2 \sim \frac{4(1-b_0^2)(4q_c^2-3Q_cQ_k)\beta}{15z^{5/2}}\mathrm{d}z^2+\frac{\gamma^2}{z^{7/2}}\mathrm{d}x_{1,2}^2\,, \tag{3.20}$$

which under a rescaling $x\to\lambda x, z\to\lambda^{2/3}z$ exhibits hyperscaling violation $\mathrm{d}s_4^2\to\lambda^\theta\mathrm{d}s_4^2$ with hyperscaling violation coefficient $\theta=-1/3$.

.

Figure 3.1 shows the background functions for a few values of τ_*. For large τ_* (corresponding to large y_0) the backgrounds approach that of the confining solution $\mathbb{B}_8^{\mathrm{conf}}$ described in section 2.6.6. For small τ_* (corresponding to y_0 approaching -1), the solutions flow close to the OP fixed point. Notice from the bottom-right panel that, for these solutions, $\partial_\rho A$ becomes nearly constant over a range of the radial coordinate, indicating that the backgrounds indeed are close to AdS in this region. A relevant deformation of the OP CFT makes these solutions exit the AdS region and develop a mass gap in the deep IR. This part of the RG flow is well approximated by the metric

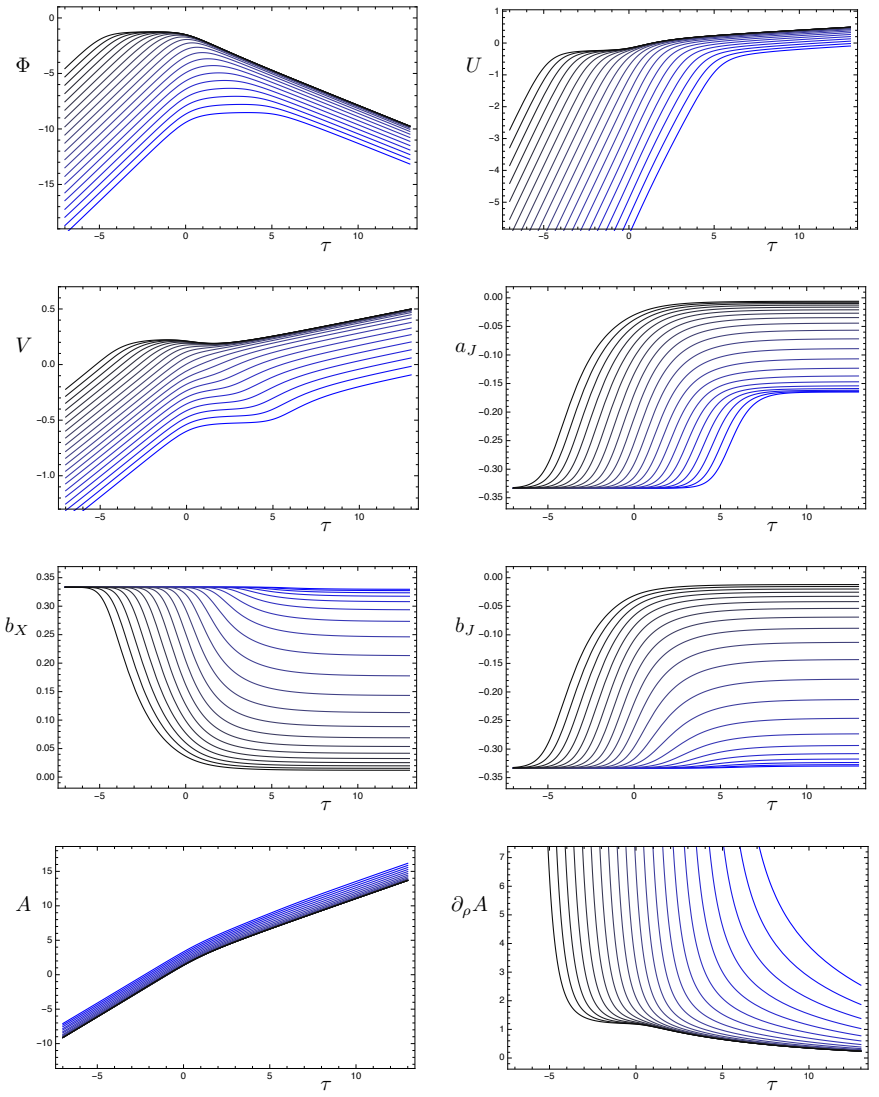

Figure 3.1.: Background functions for $\tau_* = -4.5, -4, \ldots, 5.5$. Lower (higher) values of τ_* correspond to black (blue). We have put $Q_c = 1/3$, $Q_k = -1$, $q_c = 0$ (the reason for this choice is explained in Section 3.3).

$\mathbb{B}_8^{\text{OP}}$ [20, 21]. From the explicit form of the $\mathbb{B}_8^{\text{OP}}$ solution given in section 2.6.3, it can be seen that the source for the relevant deformation is of the same order as any of the VEVs present.[4] This will be important for the physical interpretation of our results regarding the spectrum of composite states.

3.2.3. Fluctuations

In this section, we summarize the gauge-invariant formalism that we will use to compute the spin-0 and spin-2 glueball spectra of the dual theory. We follow closely [36, 39] to which the reader is referred for further details.

Spectra are obtained by studying small fluctuations of the scalar fields and the metric around a given background. The fluctuations are taken to depend on both the radial coordinate ρ as well the boundary coordinates x^μ. After going to momentum-space (defining $m^2 = -q^\mu q^\nu \eta_{\mu\nu}$ where q^μ is the three-momentum and $\eta_{\mu\nu} = \text{diag}(-1, 1, 1)$ is the boundary metric), one expands the equations of motion to linear order in the fluctuations and imposes the appropriate boundary conditions in the IR and UV. The spectrum is then given by those values of m^2 for which solutions exist.

More precisely, we expand in fluctuations $\{\varphi^a, v, v^\mu, \mathfrak{e}^\mu{}_\nu, h, H, \epsilon^\mu\}$ as

$$\begin{aligned} \Phi^a &= \bar{\Phi}^a + \varphi^a, \\ \mathrm{d}s_4^2 &= (1 + 2v + v_\sigma v^\sigma)\mathrm{d}\rho^2 + 2v_\mu \mathrm{d}x^\mu \mathrm{d}\rho + e^{2A}(\eta_{\mu\nu} + h_{\mu\nu})\mathrm{d}x^\mu \mathrm{d}x^\nu, \\ h^\mu{}_\nu &= \mathfrak{e}^\mu{}_\nu + iq^\mu \epsilon_\nu + iq_\nu \epsilon^\mu + \frac{q^\mu q_\nu}{q^2} H + \frac{1}{2}\delta^\mu{}_\nu h, \end{aligned} \tag{3.21}$$

where $\mathfrak{e}^\mu{}_\nu$ is transverse and traceless, ϵ^μ is transverse, and the three-dimensional indices μ, ν are raised and lowered by the boundary metric η.

The spin-2 fluctuation $\mathfrak{e}^\mu{}_\nu$ satisfies the linearized equation of motion

$$\left[\partial_\rho^2 + 3A'\partial_\rho + e^{-2A} m^2\right] \mathfrak{e}^\mu{}_\nu = 0. \tag{3.22}$$

After forming the gauge-invariant combination [36, 38]

$$\mathfrak{a}^a = \varphi^a - \frac{\bar{\Phi}'^a}{4A'} h, \tag{3.23}$$

[4] The mode proportional to $\tilde{r}^{-1/3}$ in $\mathcal{B}_J$ and $\mathcal{B}_X$ corresponds to turning on a source for an operator of dimension $8/3$. The spectrum of scalars around the OP fixed point together with the dimension of the dual operators can be found in Table 1 of [1].

the linearized equation of motion for the spin-0 fluctuations can be written as

$$\left[\mathcal{D}_\rho^2+3A'\mathcal{D}_\rho+e^{-2A}m^2\right]\mathfrak{a}^a-\left[\mathcal{V}^a_{\ |c}-\mathcal{R}^a_{\ bcd}\bar{\Phi}'^b\bar{\Phi}'^d+\frac{2(\bar{\Phi}'^a\mathcal{V}_c+\mathcal{V}^a\bar{\Phi}'_c)}{A'}+\frac{4\mathcal{V}\bar{\Phi}'^a\bar{\Phi}'_c}{A'^2}\right]\mathfrak{a}^c=0. \tag{3.24}$$

The different quantities involved in this expression are

$$\begin{aligned}
&\mathcal{G}_{abc}=\frac{1}{2}\left(\partial_b G_{ca}+\partial_c G_{ab}-\partial_a G_{bc}\right), && \bar{\Phi}'_a=G_{ab}\partial_\rho\bar{\Phi}^b,\\
&\mathcal{R}^a_{\ bcd}=\partial_c\mathcal{G}^a_{\ bd}-\partial_d\mathcal{G}^a_{\ bc}+\mathcal{G}^a_{\ ce}\mathcal{G}^e_{\ bd}-\mathcal{G}^a_{\ de}\mathcal{G}^e_{\ bc}, && \mathcal{V}^a_{\ |b}=\frac{\partial\mathcal{V}^a}{\partial\Phi^b}+\mathcal{G}^a_{\ bc}\mathcal{V}^c,
\end{aligned} \tag{3.25}$$

that is, $\mathcal{R}^a_{\ bcd}$ is the Riemann tensor corresponding to the sigma model metric. On the other hand, the background covariant derivative is defined as $\mathcal{D}_\rho\mathfrak{a}^a=\partial_\rho\mathfrak{a}^a+\mathcal{G}^a_{\ bc}\bar{\Phi}'^b\mathfrak{a}^c$.

In order to obtain the spectrum, we first introduce IR (UV) cutoffs at ρ_I (ρ_U). For backgrounds with an end-of-space in the IR located at $\rho=\rho_o$, the physical spectrum is obtained in the limit of $\rho_I\to\rho_o$, while similarly taking the limit of ρ_U towards the location of the UV boundary. The boundary conditions at ρ_I and ρ_U are obtained by requiring that the variational problem be well-defined. This necessitates adding localized boundary actions in the IR and UV, which up to quadratic order in the fluctuations are determined by symmetry and consistency, except for a term quadratic in the scalar fluctuations. Taking the limit of this term corresponding to adding infinite boundary-localized mass terms for the scalar fluctuations, we obtain the boundary condition

$$\varphi^a|_{\rho_{I,U}}=0, \tag{3.26}$$

which in terms of the gauge-invariant variable $\mathfrak{a}^a$ becomes

$$-\frac{e^{2A}}{m^2}\frac{\bar{\Phi}'^a}{A'}\left[\bar{\Phi}'_b\mathcal{D}_\rho-\frac{2\mathcal{V}\bar{\Phi}'_b}{A'}-\mathcal{V}_b\right]\mathfrak{a}^b\Big|_{\rho_i}=\mathfrak{a}^a\Big|_{\rho_{I,U}}. \tag{3.27}$$

Similarly, the boundary condition for the tensor fluctuations becomes

$$\partial_\rho\mathfrak{e}^\mu_{\ \nu}|_{\rho_{I,U}}=0. \tag{3.28}$$

These boundary conditions assure that subleading modes are selected in the limit of taking ρ_I towards the end-of-space and ρ_U towards the UV boundary, in accordance with standard gauge-gravity duality prescriptions.

Finally, we note that after a general change of radial coordinate from ρ to τ, Eq. (3.24) can be conveniently written as

$$\left[\delta^a_{\ b}\partial_\tau^2+S^a_{\ b}\partial_\tau+T^a_{\ b}+(\partial_\tau\rho)^2e^{-2A}m^2\delta^a_{\ b}\right]\mathfrak{a}^b=0, \tag{3.29}$$

where the matrices $S^a{}_b$ and $T^a{}_b$ are defined by

$$S^a{}_b = 2\mathcal{G}^a{}_{bc}\partial_\tau\bar{\Phi}^c + [3\partial_\tau A - \partial_\tau \log(\partial_\tau\rho)]\,\delta^a{}_b\,,$$
$$T^a{}_b = \partial_b\mathcal{G}^a{}_{cd}\partial_\tau\bar{\Phi}^c\partial_\tau\bar{\Phi}^d - (\partial_\tau\rho)^2\left[\left(\frac{2(\mathcal{V}^a\partial_\tau\bar{\Phi}^c + \mathcal{V}^c\partial_\tau\bar{\Phi}^a)}{\partial_\tau A} + \frac{4\mathcal{V}\partial_\tau\bar{\Phi}^a\partial_\tau\bar{\Phi}^c}{(\partial_\tau A)^2}\right)G_{cb} + \partial_b\mathcal{V}^a\right]. \tag{3.30}$$

3.3. Mass spectrum

In this section, we numerically compute the spectrum of spin-0 and spin-2 glueballs in the theories dual to the backgrounds of Section 3.2.2. We start by making a number of points common to both the spin-0 and spin-2 calculations.

The sigma-model action $\mathcal{S}_4$ defined by Eq. (3.2), Eq. (3.3), and Eq. (3.4) depends explicitly on the charges Q_c, Q_k, and q_c. However, after the redefinitions

$$\begin{aligned}
\Phi &= \tilde{\Phi} + \frac{1}{2}\log(X|Q_k|^{-3}), \qquad A = \tilde{A} + \frac{1}{2}\log(X^3|Q_k|^{-1}) \\
U &= \tilde{U} + \frac{1}{8}\log(X^3|Q_k|^{-1}), \quad V = \tilde{V} + \frac{1}{8}\log(X^3|Q_k|^{-1}), \\
d\rho &= \sqrt{X^3|Q_k|^{-1}}\,d\tilde{\rho}, \qquad\qquad X \equiv \sqrt{4q_c^2 - 3Q_cQ_k},
\end{aligned} \tag{3.31}$$

together with the analogous ones for a_J, b_J, and b_X in Eq. (3.11), $\mathcal{S}_4$ factorizes into a functional of the fields and an overall factor that only depends on the charges. Since we are only interested in ratios of masses, we can therefore put in the numerical computations $Q_c = 1/3$, $Q_k = -1$ and $q_c = 0$ without loss of generality.

The second point concerns the boundary conditions used for the fluctuations. Following Section 3.2.3, we will impose Eq. (3.27) and Eq. (3.28) for the spin-0 and spin-2 modes, respectively, at an IR cutoff $\tau = \tau_I$, and make sure that the calculation of the spectrum converges to the physical result in the limit $\tau_I \to -\infty$. In principle, one should follow the analogous procedure in the UV, introducing a UV cutoff at $\tau = \tau_U$, and study the limit $\tau_U \to \infty$. However, we found that reaching high enough values of the UV cutoff is numerically challenging, and because of this we took a different approach, namely to make use of the explicit UV expansions of the fluctuations, selecting the subdominant modes. As noted in section 3.2.3, the two approaches agree in the limit $\tau_U \to +\infty$.

3.3.1. Tensor modes

In terms of the radial coordinate y, the equation of motion for the spin-2 fluctuations Eq. (3.22) becomes

$$\left[\partial_y^2 + \frac{v(y-2)-6y}{2(v-2)\left(y^2-1\right)}\partial_y + \frac{HPv}{4(v-2)(y-1)^2(y+1)}m^2\right]\mathfrak{e}^\mu{}_\nu = 0. \tag{3.32}$$

As promised, the dependence on Q_k, Q_c, q_c enters only as a multiplicative factor in the term containing m^2 (through H and P).

In order to understand the boundary conditions in the UV, we expand the general solution to Eq. (3.22) in the UV as

$$\begin{aligned}
\mathfrak{e}^\mu{}_\nu(\tau) &= \tilde{c}^\mu{}_\nu\, \tilde{\mathfrak{e}}^{(UV)}(\tau) + c^\mu{}_\nu\, \mathfrak{e}^{(UV)}(\tau),\\
\tilde{\mathfrak{e}}^{(UV)}(\tau) &= 1 - \frac{2\beta\left(b_0^2-1\right)m^2e^{-3\tau/2}}{45\gamma^2} + \frac{4\left(2-7b_0^2\right)m^2e^{-2\tau}}{45\gamma^2}\\
&\quad - \frac{8\left(21b_0^2-1\right)m^2e^{-5\tau/2}\tau}{315\beta\gamma^2} + O(e^{-3\tau}),\\
\mathfrak{e}^{(UV)}(\tau) &= e^{-5\tau/2} + \frac{20e^{-3\tau}}{3\beta} + \frac{240e^{-7\tau/2}}{7\beta^2} + O(e^{-4\tau}),
\end{aligned} \tag{3.33}$$

where $\tilde{c}^\mu{}_\nu$ and $c^\mu{}_\nu$ are constants associated with the dominant and subdominant modes, respectively. Imposing the boundary condition Eq. (3.28) at finite cutoff $\tau = \tau_U$ leads to

$$\tilde{c}^\mu{}_\nu = \frac{75\gamma^2e^{-\tau_U}}{2\beta\left(b_0^2-1\right)m^2}c^\mu{}_\nu + O(e^{-3\tau_U/2}), \tag{3.34}$$

and hence in the limit of $\tau_U \to \infty$, the subdominant modes are automatically selected. In the numerical computation, we thus impose directly

$$\mathfrak{e}^\mu{}_\nu(\tau_U) = c^\mu{}_\nu\, \mathfrak{e}^{(UV)}(\tau_U) \tag{3.35}$$

as the boundary condition in the UV. Conversely, in the IR we impose Eq. (3.28) at $\tau = \tau_I$. Next, we evolve Eq. (3.22) from the IR and UV, and match the solutions (and their derivatives) at an intermediate value of $\tau = (\tau_I + \tau_U)/2$. The values of m^2 for which the solutions can be matched give us the spectrum. As a final step, we make sure that the spectrum converges as $\tau_I \to -\infty$ and $\tau_U \to +\infty$.

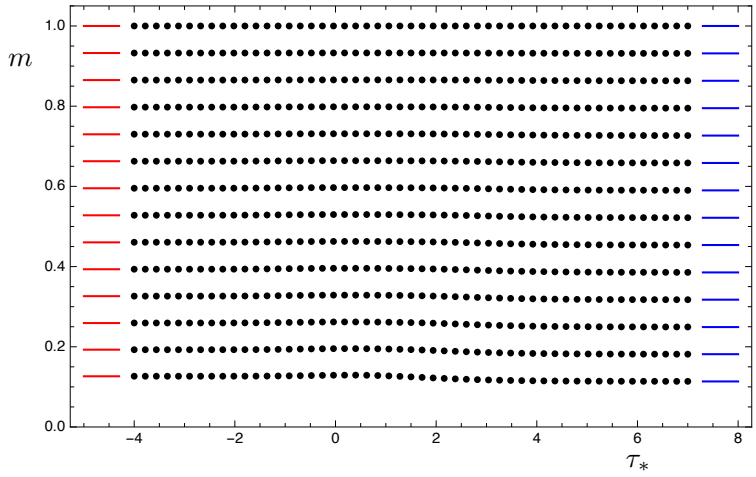

Figure 3.2.: Mass spectrum m of spin-2 states as a function of τ_* normalized to the heaviest state included in the plot, compared to the spin-2 spectrum of $\mathbb{B}_8^{\rm OP}$ (red, left) and $\mathbb{B}_8^{\rm conf}$ (blue, right).

The resulting spectrum as a function of τ_* is shown in Figure 3.2. For the numerics, we used $\tau_I = \min(-2, \tau_* - 6)$, $\tau_U = \max(5, \tau_* + 7)$. We have checked that these IR (UV) cutoffs are sufficiently low (high) for the spectrum to have converged to the physical result. As can be seen, there is a mass gap above which a tower of states appears. We have chosen to normalize the plot in such a way that the spacing of the heaviest modes remains the same as τ_* is varied in order to reflect the fact that the UV physics is the same for all the solutions. Conversely, the lowest lying states, which are sensitive to IR physics, show a slight dependence on τ_*, becoming lighter as it is increased. In the limits of $\tau_* \to \pm\infty$, the spectra corresponding to the $\mathbb{B}_8^{\rm OP}$ and $\mathbb{B}_8^{\rm conf}$ backgrounds are recovered.

In order to gain further intuition, let us rewrite Eq. (3.22) so that it takes the Schrödinger form. After a change of radial coordinate $\mathrm{d}\rho = e^A \mathrm{d}\tilde{z}$ and a rescaling $\mathfrak{e}^\mu{}_\nu = e^{-A} e^\mu{}_\nu$, we obtain

$$\left(\partial_{\tilde{z}}^2 - \mathcal{V}_s(\tilde{z}) + m^2\right) e^\mu{}_\nu = 0, \qquad \mathcal{V}_s(\tilde{z}) = (\partial_{\tilde{z}} A)^2 + \partial_{\tilde{z}}^2 A. \tag{3.36}$$

In Figure 3.3, we plot the potential $\mathcal{V}_s$ as a function of $\tilde{z}$ for a few different backgrounds,

compared to the result obtained for the $\mathbb{B}_8^{\rm conf}$ and $\mathbb{B}_8^{\rm OP}$. Note that to make this comparison in the $\tau_* \to \pm\infty$ limits, one has to take care to rescale $\mathcal{V}_s$ and $\tilde{z}$ by multiplying by $\alpha \equiv e^{2\tau_*}$ to the appropriate power (effectively choosing the units in which to measure).[5] As can be seen, the resulting potentials are box-like, leading to a gapped and discrete spectrum.

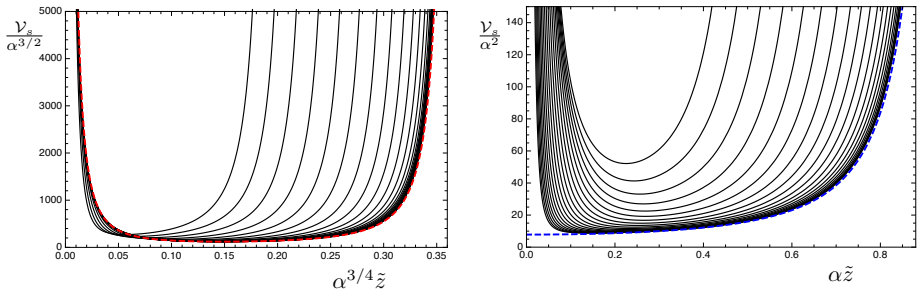

Figure 3.3.: The Schrödinger potential for a few different values of τ_* compared with the result for $\mathbb{B}_8^{\rm OP}$ (red) and $\mathbb{B}_8^{\rm conf}$ (blue).

3.3.2. Scalar modes

The scalar fluctuations satisfy the linearized equation of motion given in Eq. (3.29). The general solution can be expanded in the UV as

$$\mathfrak{a}^a(\tau) = \tilde{c}_i\, \tilde{\mathfrak{a}}_i^{(UV)a}(\tau) + c_i\, \mathfrak{a}_i^{(UV)a}(\tau)\,. \tag{3.37}$$

Here, $\tilde{c}_i$ and c_i are constants ($i = 1, \cdots, 6$) associated with six dominant modes $\tilde{\mathfrak{a}}_i^{(UV)}(\tau)$ and six subdominant modes $\mathfrak{a}_i^{(UV)}(\tau)$. Out of the dominant modes, there is one that starts at order z^{-5}, one at order z^{-4}, two at order z^0, and two at order z, while the six subdominant modes start at orders z^3, z^4, z^5, z^6, z^8, and z^{10}, respectively. In order to select the subdominant modes, we hence impose the UV boundary condition

$$\mathfrak{a}^a(\tau_U) = c_i\, \mathfrak{a}_i^{(UV)a}(\tau_U)\,. \tag{3.38}$$

After incorporating the boundary conditions — Eq. (3.27) in the IR and Eq. (3.38) in the UV — we evolve Eq. (3.29) from both sides and match at an intermediate value

[5] See also Section 7 of [1].

of τ. In order to perform this matching, we use the midpoint determinant method [36]. More precisely, we form the 12×12 matrix

$$\mathcal{M}(\tau; m^2) = \begin{pmatrix} \mathfrak{a}^{(IR)}(\tau) & \mathfrak{a}^{(UV)}(\tau) \\ \partial_\tau \mathfrak{a}^{(IR)}(\tau) & \partial_\tau \mathfrak{a}^{(UV)}(\tau) \end{pmatrix}, \tag{3.39}$$

where $\mathfrak{a}^{(IR)}$ ($\mathfrak{a}^{(UV)}$) is a 6×6 matrix obtained by putting next to each other the column vectors corresponding to six linearly independent solutions that satisfy the boundary conditions in the IR (UV). The spectrum is given by those values of m^2 for which $\det \mathcal{M}(\tau; m^2) = 0$, in which case there exists a solution which can be written both as a linear combination of the solutions evolved from the IR and the UV. For the purpose of the numerics, we chose to evaluate $\det \mathcal{M}$ at an intermediate value of $\tau = (\tau_I + \tau_U)/2$. Finally, we make sure that the spectrum converges in the limits $\tau_I \to -\infty$ and $\tau_U \to \infty$.

Figure 3.4 shows the scalar spectrum as a function of τ_*. The normalization is the same as that for the spin-2 spectrum in Figure 3.2, and we have also used the same values of the IR and UV cutoffs, namely $\tau_I = \min(-2, \tau_* - 6)$ and $\tau_U = \max(5, \tau_* + 7)$. For large values of τ_*, the spectrum approaches that of the $\mathbb{B}_8^{\text{conf}}$ background. It is interesting that the heavier states in this limit seem to come in groups of six. This may be due to the fact that these states are mostly sensitive to the UV D2-brane geometry, which is simpler than the full solution. Conversely, for small values of τ_*, the spectrum approaches the one corresponding to the $\mathbb{B}_8^{\text{OP}}$ solution. In this case, the theory flows close to the OP fixed point, and hence the $\mathbb{B}_8^{\text{OP}}$ background is valid as an effective theory up to high energy scales. In this limit we observe that certain low-lying states become approximately degenerate. Presumably, this is due to an enhancement of symmetry that takes place in the IR of these flows. Indeed, the S^3 of the internal geometry is not squashed in the $\mathbb{B}_8^{\text{OP}}$ solution, which leads to an approximate $SO(4)$ symmetry enhancement in the IR of flows that pass very close to the OP fixed point. This same symmetry is the one that allows for a consistent truncation of the sigma model from six to four scalars that admits the $\mathbb{B}_8^{\text{OP}}$ background as a solution. This truncation is described in Section 7.2 of [51], when the internal manifold is taken to be the seven-sphere. Finally, we note that despite the fact that the theory can be made to flow arbitrarily close to the IR fixed point of OP as $\tau_* \to -\infty$, there is never a parametrically light state in the spectrum. We will explore this issue further in the following sections.

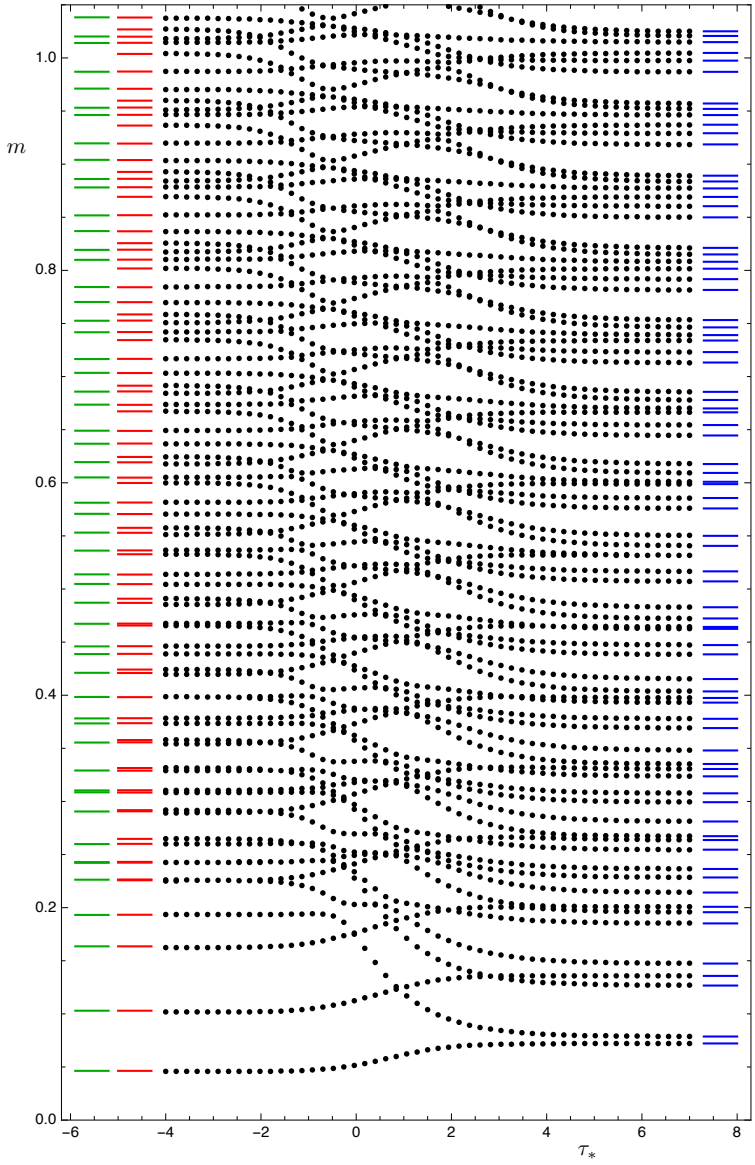

Figure 3.4.: Mass spectrum m of spin-0 states as a function of τ_* with the same normalization as for Figure 3.2. Also shown is the spin-0 spectrum of $\mathbb{B}_8^{\mathrm{OP}}$ (from left: in green for four scalars, in red for six scalars) and $\mathbb{B}_8^{\mathrm{conf}}$ (blue, right).

3.3.3. Hard-wall cutoff in the IR

In this section, we perform a numerical study of the scalar spectrum as a function of the IR cutoff τ_I, focusing in particular on when a light state is present and which dynamics is responsible for lifting its mass. A similar study investigating cutoff effects was carried out in [52], where it was argued that gauge-gravity duality can be used to facilitate the interpretation of lattice data.

Figure 3.5 shows the dependence of the scalar spectrum as a function of τ_I for a few different backgrounds. Consider first the top-left panel, for which $\tau_* = -4$, hence describing a flow that comes close to the OP fixed point. As τ_I is varied, there are three different behaviours.

- For small values of τ_I, the spectrum coincides with the physical spectrum obtained in the limit $\tau_I \to -\infty$.
- As τ_I is increased such that the IR cutoff is within the region close to AdS, there is a state whose mass decreases and becomes light.
- Increasing τ_I further such that the IR cutoff is located within the far-UV region of the background, corresponding to the D2-branes, the mass of the light state again is lifted. However, it is still parametrically light compared to the mass of the second lightest state.

There are a number of examples in the literature analogous to the second case. In these examples an RG flow that passes near an IR fixed point is modelled by the introduction of a hard-wall in an AdS geometry, which typically leads to the presence of a light state in the spectrum [47, 39]. As can be seen in our model, when τ_* is increased, the effect becomes less pronounced. Indeed, in the bottom-right panel for which $\tau_* = 3$, describing a flow that is close to the $\mathbb{B}_8^{\text{conf}}$ background, the intermediate region with a light state disappears altogether.

It may seem puzzling that in the third case, when τ_I is located in the far-UV region of the background, there is also a parametrically light state. This is due to the fact that in this region the four-dimensional metric exhibits hyperscaling violation with coefficient $\theta = -1/3$, as demonstrated by Eq. (3.20). Since AdS corresponds to $\theta = 0$, we expect that for small $|\theta|$ there will be a light dilaton which becomes exactly massless in the limit $\theta \to 0$. In appendix A, we study a simple toy model consisting of a single scalar field with a potential chosen in such a way that there exist hyperscaling violating solutions

(see also [53]). Performing a perturbative analysis of the spin-0 spectrum, we find that there is a light state whose mass m_0 is given, to leading order in θ, by

$$\frac{m_0}{m_1} = \frac{1}{\pi}\sqrt{\frac{-3\theta}{2}}\,, \tag{3.40}$$

where m_1 is the mass of the lightest spin-2 state. This estimate agrees well with the numerical result for the relevant case $\theta = -1/3$ (see Figure A.1 of appendix A). As can be seen in Figure 3.5, for large τ_I, the mass of the lightest spin-0 state approaches the value captured by this toy model (the dashed blue line).

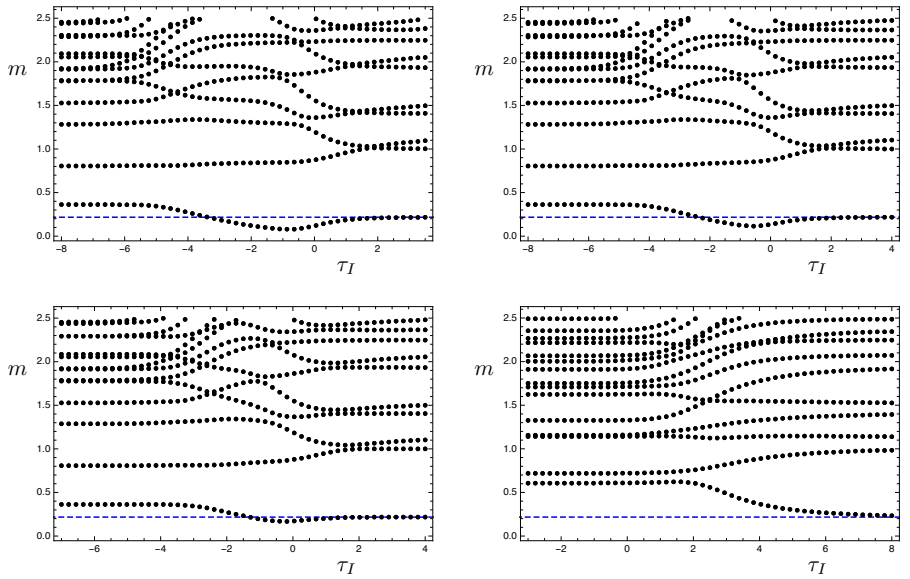

Figure 3.5.: Mass spectrum m of spin-0 states as a function of the IR cutoff τ_I, for a few backgrounds with different values of τ_*. The top-left panel has $\tau_* = -4$, the top-right panel has $\tau_* = -3$, the bottom-left panel has $\tau_* = -2$, and the bottom-right panel has $\tau_* = 3$. The dashed blue line corresponds to the mass of the lightest state in the hyperscaling violating toy model of appendix A. All the plots are normalized to the mass of the lightest spin-2 state.

3.4. Conclusions and Discussion

We performed a numerical study of the spectrum of spin-0 and spin-2 glueballs in a one-parameter family of three-dimensional theories by making use of their dual supergravity descriptions. Working within a consistent truncation to a sigma model coupled to four-dimensional gravity allowed us to utilize the gauge-invariant formalism to treat the scalar and tensor fluctuations in the bulk. As the parameter τ_* is varied, the spectrum interpolates between the two limiting cases corresponding to the confining solution $\mathbb{B}_8^{\text{conf}}$ (for large τ_*) and the solution given by $\mathbb{B}_8^{\text{OP}}$ (for small τ_*).

The OP fixed point possesses an exact moduli space [19], and small-τ_* flows exhibit quasi-conformal behaviour. Nevertheless, we did not find a light pseudo-dilaton in the physical spectrum. This can be understood as follows. The geometry of small-τ_* RG flows consists of three parts. The first part takes the theory from the UV corresponding to the D2-branes down to the vicinity of the OP fixed point, following closely the solution $\mathbb{B}_8^{\infty}$. The second part consists of a region where the geometry is approximately AdS, and the dual theory remains close to the OP fixed point. From the point of view of this fixed point, how long it stays close is determined by the size of an irrelevant operator. The smaller τ_* is, the smaller this irrelevant operator is. The third and final part describes the flow from the vicinity of the OP fixed point to the deep IR where the theory develops a mass gap. For small τ_*, this final part of the RG flow is very well captured by the $\mathbb{B}_8^{\text{OP}}$ solution. The key point is that, as mentioned in the last paragraph of Sec. 3.2.2, the RG flow described by the $\mathbb{B}_8^{\text{OP}}$ solution is triggered by both sources and VEVs of comparable sizes. In other words, the magnitudes of the explicit and the spontaneous breakings of scale invariance are similar. It would be interesting to investigate whether more general flows exist that start at the OP fixed point and for which the ratio between the spontaneous and the explicit breakings of scale invariance can be made arbitrarily large.

The above interpretation is further supported by the study of the spectrum as a function of the location of a hard-wall IR cutoff. As long as this IR cutoff remains inside the AdS region corresponding to the OP fixed point, there is a light state (for small τ_*) in the scalar spectrum. However, when the IR cutoff is taken to be close to the end-of-space, this state ceases to be light, hence showing that it is the physics of the deep IR that lifts its mass.

4. Two-dimensional gauge theories with unquenched flavour

4.1. Introduction

The gauge theory living on a stack of D-branes in flat space, as reviewed in section 1.2, contains exclusively fields transforming in the adjoint representation. Substituting the flat transverse space by more complicated geometries diversifies the possible gauge theory duals, for instance changing the gauge group to a quiver and including new degrees of freedom transforming in more complicated representations. Examples of this phenomenon are the models studied in the previous chapters, conjectured to be dual to a two-sites quiver with fields transforming in the bifundamental representation.

One of the main purposes of the holographic program is to learn about the properties of gauge theories at strong coupling, most notably QCD. Even if an exact gravitational dual of QCD seems out of reach, it is desirable that the holographic model studied shares as many properties as possible with it. In particular, quarks are an essential piece in our understanding of the strong interaction. These transform in the fundamental representation of the gauge group, so the simplest D-brane constructions discussed above do not contain degrees of freedom that could be interpreted as such. To remedy this situation, new stacks of branes with their respective modes need to be included [54].

The simplest constructions involve intersecting stacks of Dp and D$(p+4)$-branes. The strings attached between both sets transform in the fundamental representation of the group, so they can act as the quarks (or electrons in lower dimensions) of the gauge theory. Unfortunately solutions describing brane intersections of this type are difficult to find due to the Partial Differential Equations involved.[1] A possible way out is to treat the additional stack of N_f D$(p+4)$-branes in the probe approximation, that is, to ignore their effect in the underlying geometry generated by the N_c colour Dp-branes. In the

[1] A notable exception is the solution in [55]. This is however very difficult to generalise in terms of temperature, chemical potentials etc.

gauge theory dual this would mean ignoring the quantum effects involving the quarks, since we are keeping N_f finite in the large-N limit. This is the quenched approximation, in which $N_f/N_c \to 0$.

Even if we were not interested in the physics not captured by this approximation, in some circumstances this simplification is not even consistent, as emphasized for instance in [56, 23]. We should therefore consider the full backreacted system, so that in the gauge dual the flavour degrees of freedom are unquenched. This corresponds to the Veneziano limit, in which the ratio N_f/N_c is kept finite.

To circumvent technical difficulties, in many studies the flavour branes are distributed or smeared along some of the directions transverse to the colour branes. This approach, reviewed in detail in [57], retains at least part of the symmetries already present in the geometry, reducing the Partial to Ordinary Differential Equations. In this way, unquenched flavour was incorporated to four-dimensional gauge theories in [58] as a D3/D7 system. Similarly, flavoured three-dimensional gauge theories were constructed in [23] in the form of a D2/D6 arrangement. In this chapter, we will find the gravity duals to two-dimensional gauge theories in the presence of flavour by solving the smeared D1/D5 intersection.

In all these constructions, the geometric properties of the internal geometry play an important role. Among other things they control the amount of supersymmetry preserved by the solution. The flavoured backgrounds found in [58] and [23] preserve minimal supersymmetry in their respective dimensions. For the D1/D5 system the internal geometries are seven-dimensional so, as we will see, we have at our disposal several types on manifolds respecting different amounts of supersymmetries, giving rise to a rich set of solutions.

Gauge theories in dimensions lower than four are superrenormalizable and asymptotically free, so their UV can be studied perturbatively. On the other hand, these models are generically strongly coupled in the IR and frequently the endpoint of the RG flow is a conformal field theory. This was the case for the three-dimensional gauge theories in [23] at it is also the case here. Thus, the solutions we construct describe RG flows from a (super)Yang–Mills gauge theory in the UV to a fixed point in the IR, triggered by the inclusion of fundamental degrees of freedom.

The IR fixed points can of course be detached from the rest of the flow and studied independently. On the gravity side these points correspond to AdS geometries, so as a byproduct of our analysis we have found infinite new families of AdS_3 solutions in type IIB supergravity in the presence of D5-brane sources, supported exclusively by three-form flux.

4.2. Internal geometries

There are several possibilities for the space transverse to the D1-branes depending on the amount of supersymmetry that one aims to preserve. This is analogous to the situation for the space transverse to M2-branes (see [59]) in eleven-dimensional supergravity and is due ultimately to various types of seven-dimensional geometries admitting the Killing spinors that are mandatory for supersymmetry. The possible internal geometries, together with the supersymmetry they preserve and their corresponding cones (acting as transverse spaces) with their holonomy is reflected in the following table:

Geometry	Supersymmetry	Cone	Holonomy
Round sphere	$(8,8)$	$\mathbb{R}^8$	$\mathbb{I}$
Tri-Sasakian	$(0,3)$	hyperKähler	Sp(2)
Sasaki–Einstein	$(0,2)$	Calabi–Yau	SU(4)
Weak-G_2	$(0,1)$	Spin(7)	Spin(7)

Table 4.1.: Possible internal geometries and some of their properties.

Placing a stack of D1-branes at the tip of these cones and taking the decoupling limit as in [12] one obtains a two-dimensional gauge dual preserving the corresponding amount of supersymmetry. The gauge coupling in two dimensions has dimensions of energy, so these gauge theories are superrenormalizable and asymptotycally free. Perturbative methods apply in the far UV. The D1-brane solution is a faithful gravity dual in the energy interval $\sqrt{\lambda}N_c^{-5/6} \ll U \ll \sqrt{\lambda}$. Below this range the dilaton grows large and we need the S-dual description in terms of F1-strings. All this was explained in more detail in section 1.6.

We present in this section some details of the internal geometries involved in our construction. We begin with a study of tri-Sasakian manifolds, the most prominent example being S^7, since as we will explain the weak-G_2 and Sasaki–Einstein cases can be recovered as special limits of the former.

4.2.1. Tri-Sasakian manifold

Consider a seven-dimensional Riemannian manifold admitting a tri-Sasakian structure [60]. This means that we can write the metric as an SO(3) fibration over a four-dimensional quaternionic Kähler base,

$$\mathrm{d}s_7^2 = \mathrm{d}s_4^2(\mathrm{QK}) + \sum_{i=1}^{3} \eta^i \otimes \eta^i \,. \tag{4.1}$$

The vielbeins η^i parametrising the fiber can be seen as globally-defined one-forms satisfying the differential conditions

$$\mathrm{d}\eta^i = 2J^i - \epsilon^{ijk}\eta^j \wedge \eta^k, \qquad\qquad \mathrm{d}J^i = 2\epsilon^{ijk}J^j \wedge \eta^k. \tag{4.2}$$

Here, J^i is a triplet of globally defined two-forms such that $g^{-1}J^i$ is a triplet of almost complex structures on the quaternionic Kähler base.

For our purposes, the crucial property of a seven-dimensional tri-Sasakian manifold is that it admits three Killing spinors solving the equation

$$\nabla_X \psi = \frac{1}{2} X \cdot \psi, \tag{4.3}$$

where the $1/2$ factor comes from normalizing the metric in such a way that the scalar curvature is $R = 42$, and $X \cdot \psi$ is a Clifford product. These spinors can be used to build ten-dimensional spinors in type IIB supergravity and find supersymmetric solutions.

Let us characterise them in more detail. We introduce vielbeins $\mathrm{d}s_7^2 = \tilde{e}^A \tilde{e}^B \tilde{\eta}_{AB}$ on the tri-Sasakian manifold and split them according to the base and fiber

$$\begin{aligned} \tilde{e}^a &= \hat{e}^a, \qquad (a = 1,2,3,4) \\ \tilde{e}^i &= \eta^i, \qquad (i = 5,6,7) \end{aligned} \tag{4.4}$$

where $\hat{e}^a$ are vielbeins on the quaternionic Kähler. The associated spin connection is

$$\tilde{\omega}_{abc} = \hat{\omega}_{abc}, \qquad\qquad \tilde{\omega}_{aib} = \tilde{\omega}_{iab} = -J^i_{ab}, \qquad\qquad \tilde{\omega}_{ijk} = -\epsilon_{ijk}. \tag{4.5}$$

Using this, one finds that Killing spinors ψ on a tri-Sasakian manifold satisfy

$$\tilde{\partial}_a \psi + \frac{1}{4}\hat{\omega}_{abc}\tilde{\gamma}^{bc}\psi = \frac{i}{2}\tilde{\gamma}_a\psi + \frac{1}{2}J^i_{ab}\tilde{\gamma}^{ib}\psi, \tag{4.6a}$$

$$\tilde{\partial}_i \psi = \frac{i}{2}\tilde{\gamma}_i\psi + \frac{1}{4}J^i_{ab}\tilde{\gamma}^{ab}\psi + \frac{1}{4}\epsilon_{ijk}\tilde{\gamma}^{jk}\psi, \tag{4.6b}$$

where $\tilde{\gamma}^A$ are the gamma matrices of the seven-dimensional Clifford algebra.

4.2.2. Sasaki-Einstein manifold

A $(2n+1)$-dimensional manifold is Sasaki-Einstein if it is endowed with a single Sasakian structure (instead of three, in contrast with the tri-Sasakian case). As a consequence, it can be written as a U(1) fibration over a $2n$-dimensional Kähler-Einstein base. In particular, for seven dimensions

$$\mathrm{d}s_7^2 = \mathrm{d}s_6^2(\mathrm{KE}) + \eta^2, \tag{4.7}$$

where

$$\mathrm{d}\eta = 2J \tag{4.8}$$

corresponds to the Kähler form in the Kähler-Einstein base. A Sasaki-Einstein manifold possesses additionally a globally defined holomorphic three-form Ω satisfying

$$\mathrm{d}\Omega = 4i\eta \wedge \Omega. \tag{4.9}$$

The volume form of the manifold can be written as

$$\Omega_7 = \frac{1}{3!}\eta \wedge J \wedge J \wedge J = \frac{i}{8}\eta \wedge \Omega \wedge \bar{\Omega}. \tag{4.10}$$

We can build a Sasaki-Einsten manifold from a tri-Sasakian one by focusing on a single Sasakian structure from the triplet it has. This can be achieved with a suitable selection of the globally defined forms. A possible choice is

$$\eta = -\eta_1, \tag{4.11}$$

$$J = -J_1 + \eta_2 \wedge \eta_3, \tag{4.12}$$

$$\Omega = J_2 \wedge (\eta_2 + i\eta_3) - J_3 \wedge (\eta_3 - i\eta_2). \tag{4.13}$$

The desired properties (4.8) and (4.9) then follow straightforwardly from (4.2). Let us stress that not every seven-dimensional Sasaki–Einstein manifold descends form a tri-Sasakian parent through this construction.

4.2.3. Weak-G_2 manifold

It is known that every tri-Sasaki admits a metric that does not have tri-Sasakian structure but weak-G_2. That metric is

$$\mathrm{d}s_7^2 = \frac{9}{5}\mathrm{d}s_4^2(\mathrm{QK}) + \frac{9}{25}\sum_{i=1}^{3}\eta^i \otimes \eta^i. \tag{4.14}$$

The main difference with respect to (4.1) is the squashing factor of 1/5 between the fibre and the base, while the overall factor is adjusted so that the scalar curvature is $R = 42$.

A seven-dimensional manifold with G_2 structure is distinguished by the existence of a globally defined three-form, called the associative form, that (at least locally) can be written as

$$\varphi_3 = -e^{125} - e^{345} - e^{136} + e^{246} - e^{147} - e^{237} + e^{567}. \tag{4.15}$$

This form defines a calibration. Its Hodge dual $\star_7 \varphi_3$, called the coassociative form, also provides a calibration. If both are closed then the manifold has G_2 holonomy. The failure in closing defines the torsion classes and weak-G_2 is selected by the requirement

$$\mathrm{d}\varphi_3 = 4 \star_7 \varphi_3 \equiv 4\tilde{\varphi}_4. \tag{4.16}$$

When the weak-G_2 structure is inherited from the tri-Sasakian one, the associative form can be written as

$$\varphi_3 = \frac{27}{25}\left(J^1 \wedge \eta^1 + J^2 \wedge \eta^2 + J^3 \wedge \eta^3\right) + \frac{27}{125}\eta^1 \wedge \eta^2 \wedge \eta^3, \tag{4.17}$$

so that the crucial property (4.16) again follows from (4.2).

The eight-dimensional cone over a weak-G_2 manifold,

$$\mathrm{d}s_8^2 = \mathrm{d}r^2 + r^2 \mathrm{d}s_7^2(\mathrm{W}G_2), \tag{4.18}$$

has Spin(7) holonomy. These kind of manifolds possess a calibration four-form called Cayley form, that is closed and selfdual. It can be built from the associative form in the weak-G_2 base as

$$\Psi_4 = r^3 \mathrm{d}r \wedge \varphi_3 + r^4 \tilde{\varphi}_4. \tag{4.19}$$

Every weak-G_2 manifold admits a single Killing spinor (instead of three, as the tri-Sasaki). When descending from a tri-Sasaki as detailed, the Killing spinor equation becomes

$$\tilde{\partial}_a \psi + \frac{1}{4}\hat{\omega}_{abc}\tilde{\gamma}^{bc}\psi = \frac{i}{2}\tilde{\gamma}_a\psi + \frac{1}{6}J^i_{ab}\tilde{\gamma}^{ib}\psi, \tag{4.20a}$$

$$\tilde{\partial}_i \psi = \frac{i}{2}\tilde{\gamma}_i\psi + \frac{1}{12}J^i_{ab}\tilde{\gamma}^{ab}\psi + \frac{5}{12}\epsilon_{ijk}\tilde{\gamma}^{jk}\psi, \tag{4.20b}$$

with the same notation as above. Again, we should mention explicitly that not every weak-G_2 is the result of squashing a tri-Sasakian metric.

4.3. D1-branes on a tri-Sasakian manifold

Let us now consider a generic tri-Sasakian manifold as the internal space for a D1-brane ansatz. The SO(3) fibration allows us to introduce different squashing modes. In string frame, we take the following ansatz for the metric[2]

$$\mathrm{d}s_{10}^2 = h^{-1/2}\mathrm{d}x_{1,1}^2 + h^{1/2}\left(\mathrm{d}r^2 + e^{2g}\mathrm{d}s_4^2(\mathrm{QK}) + \sum_{i=1}^{3} e^{2f_i}\eta^i \otimes \eta^i\right). \tag{4.21}$$

The solution is also endowed with a Ramond-Ramond three-form supporting the metric

$$F_3 = Q_c \star \Omega_7, \tag{4.22}$$

being Ω_7 the volume form of the internal manifold. The constant Q_c is the Page charge associated to the D1-branes. It is therefore quantised and related to the number of branes N_c as

$$Q_c = \frac{(2\pi\ell_s)^6 g_s}{V_7} N_c, \tag{4.23}$$

with $V_7 = \int \Omega_7$ the volume of the internal manifold. The parameter N_c is also expected to give the rank of the gauge group in the field theory dual.

To obtain supersymmetric solutions we must force the variations of the fermions in type IIB supergravity, that is, dilatino and gravitino, to vanish. In our conventions (see appendix B) these variations read

$$\delta\lambda = \frac{i}{2}\Gamma^A\partial_A\Phi\epsilon^c - \frac{1}{4}e^{\Phi}\not{F}_3\epsilon, \tag{4.24a}$$

$$\delta\Psi_A = \nabla_A\epsilon + \frac{i}{8}e^{\Phi}\not{F}_3\Gamma_A\epsilon^c, \tag{4.24b}$$

where the slash notation means contracting all indices with gamma matrices. The ten-dimensional gamma matrices Γ^A are built from the seven-dimensional ones as

$$\begin{aligned} \Gamma^\mu &= \gamma^\mu \otimes \mathbb{1}_8 \otimes \sigma^1, && (\mu = 0,1,2) \\ \Gamma^a &= \mathbb{1}_2 \otimes \tilde{\gamma}^a \otimes \sigma^2, && (a = 3,4,5,6) \\ \Gamma^i &= \mathbb{1}_2 \otimes \tilde{\gamma}^i \otimes \sigma^2. && (i = 7,8,9) \end{aligned} \tag{4.25}$$

[2]From the six possible squashings respecting the structure, $S_{ij}\eta^i \otimes \eta^j$ with $S_{ij} = S_{(ij)}$, we have chosen to keep just the diagonal part for simplicity. Including off-diagonal terms is straightforward and has interesting geometric consequences, for instance the construction of new Spin(7) manifolds. See [61] for the case of the seven-sphere.

Here γ^μ verify a three-dimensional Clifford algebra and σ^I are the Pauli matrices. A ten-dimensional chiral spinor ϵ can be built from the chiral Killing spinors ψ on the tri-Sasaki as

$$\epsilon = \xi \otimes \psi \otimes (1,0), \tag{4.26}$$

where ξ is a three-dimensional spinor in the external directions. In order to determine the covariant derivative of ϵ we need to compute the spin connection. Introducing the vielbeins

$$E^\alpha = h^{-1/4}\mathrm{d}x^\alpha, \qquad E^2 = h^{1/4}\mathrm{d}r, \qquad E^a = h^{1/4}e^g\tilde{e}^a, \qquad E^i = h^{1/4}e^{f_i}\tilde{e}^i \tag{4.27}$$

the spin connection is

$$\begin{aligned}
\omega_{\alpha 2} &= -h^{-1/4}\frac{h'}{4h}\eta_{\alpha\beta}E^\beta,\\
\omega_{a2} &= -h^{-1/4}\left(\frac{h'}{4h}+g'\right)\delta_{ab}E^b,\\
\omega_{ab} &= \hat{\omega}_{ab} - h^{-1/4}e^{f_i-2g}J^i_{ab}E^i,\\
\omega_{i2} &= -h^{-1/4}\left(\frac{h'}{4h}+f_i'\right)\delta_{ij}E^j,\\
\omega_{ia} &= h^{-1/4}e^{f_i-2g}J^i_{ab}E^b,\\
\omega_{jk} &= h^{-1/4}\epsilon_{ijk}\left(e^{f_i-f_j-f_k} - e^{f_j-f_k-f_i} - e^{f_k-f_i-f_j}\right)E^i.
\end{aligned} \tag{4.28}$$

with $\alpha = 0, 1$ and the rest as in (4.25). Taking the variation of the dilatino and one of the components of the gravitino along the D1-brane we find that they vanish if the following differential equations hold

$$\Phi' = \frac{h'}{2h}, \tag{4.29}$$

$$h' = -Q_c e^{-f_1-f_2-f_3-4g}, \tag{4.30}$$

together with the projector

$$\Gamma^{01}\epsilon = i\epsilon^c, \tag{4.31}$$

characteristic of the D1-brane. Notice that we can integrate equation (4.29), giving

$$e^\Phi = h^{1/2}, \tag{4.32}$$

where we fixed $g_s = 1$. Using these results in the base and fiber components of the gravitino together with the Killing spinor conditions (4.6), we find the following equations

$$g' = e^{-2g}\left(\alpha_1 e^{f_1} + \alpha_2 e^{f_2} + \alpha_3 e^{f_3}\right) - e^{-g}(\alpha_1\alpha_2\alpha_3 + \alpha_1 + \alpha_2 + \alpha_3), \tag{4.33}$$

$$f_1' = -2\alpha_1 e^{f_1-2g} + \alpha_1\alpha_2\alpha_3\left(e^{f_1-f_2-f_3} - e^{f_2-f_3-f_1} - e^{f_3-f_1-f_2}\right) + 2\alpha_1 e^{-f_1}, \tag{4.34}$$

$$f_2' = -2\alpha_2 e^{f_2-2g} + \alpha_1\alpha_2\alpha_3\left(-e^{f_1-f_2-f_3} + e^{f_2-f_3-f_1} - e^{f_3-f_1-f_2}\right) + 2\alpha_2 e^{-f_2}, \tag{4.35}$$

$$f_3' = -2\alpha_3 e^{f_3-2g} + \alpha_1\alpha_2\alpha_3\left(-e^{f_1-f_2-f_3} - e^{f_2-f_3-f_1} + e^{f_3-f_1-f_2}\right) + 2\alpha_3 e^{-f_3}, \tag{4.36}$$

where we have imposed the projectors

$$\Gamma^{2734}\epsilon = \alpha_1\epsilon, \qquad \Gamma^{2835}\epsilon = \alpha_2\epsilon, \qquad \Gamma^{2936}\epsilon = \alpha_3\epsilon, \qquad \Gamma^{3456}\epsilon = -\epsilon. \tag{4.37}$$

The constants must satisfy $\alpha_i^2 = 1$ for consistency. After plugging these equations in the second order equations of motion coming from type IIB supergravity, we find that they are solved if

$$\alpha_1\alpha_2\alpha_3 + \alpha_1 + \alpha_2 + \alpha_3 = 0. \tag{4.38}$$

A possible choice is $\alpha_1 = \alpha_2 = -\alpha_3 = 1$, to which we will stick in the following. This yields the final BPS equations

$$g' = e^{-2g}\left(e^{f_1} + e^{f_2} - e^{f_3}\right), \tag{4.39}$$

$$f_1' = -2e^{f_1-2g} - \left(e^{f_1-f_2-f_3} - e^{f_2-f_3-f_1} - e^{f_3-f_1-f_2}\right) + 2e^{-f_1}, \tag{4.40}$$

$$f_2' = -2e^{f_2-2g} - \left(-e^{f_1-f_2-f_3} + e^{f_2-f_3-f_1} - e^{f_3-f_1-f_2}\right) + 2e^{-f_2}, \tag{4.41}$$

$$f_3' = 2e^{f_3-2g} - \left(-e^{f_1-f_2-f_3} - e^{f_2-f_3-f_1} + e^{f_3-f_1-f_2}\right) - 2e^{-f_3}, \tag{4.42}$$

supplemented by the projectors (4.31) and (4.37). These five projectors reduce the amount of preserved supercharges to $32/2^5 = 1$ for each spinor of the form (4.26). Since there are three chiral Killing spinors ψ on the tri-Sasakian manifold the resulting supersymmetry is the expected $(0, 3)$ stated in Table 4.1.

A particular solution to these equations is

$$e^g = e^{f_1} = e^{f_2} = e^{f_3} = r, \qquad\qquad h = \frac{Q_c}{r^6} \tag{4.43}$$

corresponding to the decoupling limit of the D1-brane on a hyperKähler cone. When the tri-Sasaki is taken to be the seven-sphere, this solution describes D1-branes in flat space and supersymmetry is enhanced to $(8, 8)$.

Before discussing how the Sasaki–Einstein and weak-G_2 cases can be recovered from these results, let us incorporate flavour into the system.

4.4. $\mathcal{N} = (0, 3)$ theories with flavour

The procedure to add flavour to our theories involves a new set of branes, in this case a stack of N_f D5-branes. These share the gauge directions with the D1-branes, extending in the radial coordinate and wrapping three directions of the internal manifold. We will take into account the backreaction of these flavour branes into the geometry, corresponding to the Veneziano limit of the gauge theory dual. Moreover, the branes will be smeared along some of the internal directions so that the distribution preserves (part of) the original symmetries of the background. In this way the resulting problem involves Ordinary instead of Partial Differential Equations.

The presence of the brane sources is described through the DBI plus Wess-Zumino (WZ) action (we work in string frame)

$$S_{\text{sources}} = -T_{\text{D5}} \int e^{-\Phi}(\mathcal{K} - C_6) \wedge \Xi, \tag{4.44}$$

where C_6 is the gauge potential dual to C_2 according to $F_7 = - \star F_3$, $\mathcal{K}$ is a suitable calibration form and Ξ is the smearing form describing the continuous distribution of branes. The only efect of the WZ piece, that describes the magnetic coupling of C_2 to the D5-branes, is to modify the Bianchi

$$\mathrm{d}F_3 = H \wedge F_1 + 2\kappa^2 T_{\text{D5}} \Xi. \tag{4.45}$$

In addition the DBI term modifies the dilaton and Einstein's equations. The whole problem then reduces to find the correct smearing and calibration forms. For that we can exploit the results in the previous section.

First of all, we can write the Ramond-Ramond three-form sourced by the D5 branes as

$$F_3^{\text{f}} = Q_1 J^1 \wedge \eta^1 + Q_2 J^2 \wedge \eta^2 + Q_3 J^3 \wedge \eta^3 + Q_\eta \, \eta^1 \wedge \eta^2 \wedge \eta^3, \tag{4.46}$$

where the superindex 'f' stands for *flavour*. This is the most general three-form that can be constructed from the available globally defined forms and compatible with the symmetries of the metric.[3] The constants Q_i and Q_η are Page charges associated to the D5-branes and should be quantised, counting the number of flavours in the gauge theory dual. Furthermore, we rename the three-form sourced by the D3-branes to

$$F_3^{\text{c}} = Q_c \star \Omega_7, \tag{4.47}$$

[3] Had we allowed for non-diagonal squashing, additional terms would have appeared.

indicating that this piece comes from *colour* branes. Then the whole system consists of the metric (4.21), the dilaton Φ and the three-form $F_3 = F_3^{\rm c} + F_3^{\rm f}$. The smearing form is then dictated by the violation of the Bianchi identity for $F_3^{\rm f}$,

$$2\kappa^2 T_{\rm D5}\Xi = \sum_{I=1}^{3} Q_I J^I \wedge J^I + (-Q_1 + Q_2 + Q_3 + Q_\eta) J_1 \wedge \eta^2 \wedge \eta^3 + \\ + (Q_1 - Q_2 + Q_3 + Q_\eta) J_2 \wedge \eta^3 \wedge \eta^1 + (Q_1 + Q_2 - Q_3 + Q_\eta) J_3 \wedge \eta^1 \wedge \eta^2 . \tag{4.48}$$

On the other hand, the calibration form can be constructed from the supersymmetry spinors as

$$\mathcal{K} = \frac{1}{6!} \epsilon^\dagger \Gamma_{A_1 \cdots A_6} \epsilon E^{A_1} \wedge \cdots \wedge E^{A_6}, \qquad (A_i = 0, \ldots, 9) \tag{4.49}$$

Using the projectors it is simple to identify which of the components are non-vanishing. The calibration form must satisfy the calibration condition

$$\mathrm{d}(e^{-\Phi}\mathcal{K}) = - \star F_3^{\rm f}. \tag{4.50}$$

Incorporating the new flavour piece in F_3 into the fermionic variations we can deduce a new set of BPS equations

$$\begin{aligned}
\Lambda' &= e^{\Lambda}\left[-2e^{-2g}\left(Q_1 e^{-f_1} + Q_2 e^{-f_2} - Q_3 e^{-f_3}\right) + Q_\eta e^{-f_1-f_2-f_3}\right], \qquad (4.51)\\
h' &= e^{\Lambda}\left\{-Q_c e^{-f_1-f_2-f_3-4g} + h\left[2e^{-2g}\left(Q_1 e^{-f_1} + Q_2 e^{-f_2} - Q_3 e^{-f_3}\right) - Q_\eta e^{-f_1-f_2-f_3}\right]\right\},\\
g' &= e^{-2g}\left(e^{f_1} + e^{f_2} - e^{f_3}\right) - \frac{e^{\Lambda}}{2}\left(Q_1 e^{-f_1-2g} + Q_2 e^{-f_2-2g} - Q_3 e^{-f_3-2g} - Q_\eta e^{-f_1-f_2-f_3}\right),\\
f_1' &= 2e^{-f_1} - e^{\Lambda-2g}\left(Q_2 e^{-f_2} - Q_3 e^{-f_3}\right) - 2e^{f_1-2g} + \left(-e^{f_1-f_2-f_3} + e^{f_2-f_3-f_1} + e^{f_3-f_1-f_2}\right),\\
f_2' &= 2e^{-f_2} - e^{\Lambda-2g}\left(Q_1 e^{-f_1} - Q_3 e^{-f_3}\right) - 2e^{f_2-2g} + \left(e^{f_1-f_2-f_3} - e^{f_2-f_3-f_1} + e^{f_3-f_1-f_2}\right),\\
f_3' &= -2e^{-f_3} - e^{\Lambda-2g}\left(Q_1 e^{-f_1} + Q_2 e^{-f_2}\right) + 2e^{f_3-2g} - \left(e^{f_1-f_2-f_3} + e^{f_2-f_3-f_1} - e^{f_3-f_1-f_2}\right),
\end{aligned}$$

where $e^{\Phi} = h^{1/2} e^{\Lambda}$. The projectors coincide with those in the absence of flavour, equations (4.31) and (4.37). Using them, it is possible to deduce the calibration form and write it in terms of the globally defined forms

$$\mathcal{K} = -E^{01} \wedge \Phi_4, \tag{4.52}$$

where

$$\begin{aligned}\Phi_4 = &\frac{1}{2}\alpha_1\alpha_2\alpha_3 e^{4g} J^1 \wedge J^1 + e^{f_1+f_2+f_3}\mathrm{d}r \wedge \eta^1 \wedge \eta^2 \wedge \eta^3 + \\ &+ \frac{1}{2}\epsilon_{ijk}\left(\alpha_j\alpha_k e^{f_i+2g}\mathrm{d}r \wedge J^i \wedge \eta^i + \alpha_i e^{f_j+f_k+2g} J^i \wedge \eta^j \wedge \eta^k\right).\end{aligned} \tag{4.53}$$

This intimidating set of equations has a particular truncation in which the system is integrable. Fixing $f_1 = f_2 = f_3 = g$, which requires the charges to be related as $Q_1 = Q_2 = -Q_3 = -Q_\eta$, we get the equations

$$\Lambda' = 7Q_\eta e^{\Lambda-3g}, \tag{4.54}$$

$$g' = e^{-3g}(e^{2g} + 2Q_\eta e^{\Lambda}), \tag{4.55}$$

$$h' = -e^{\Lambda-7g}(Q_c + 7Q_\eta e^{4g} h). \tag{4.56}$$

The system can be analytically solved in a new radial coordinate ρ defined as

$$-Q_\eta e^{3g}\frac{\mathrm{d}f}{\mathrm{d}r} \equiv \frac{\mathrm{d}f}{\mathrm{d}\rho}, \tag{4.57}$$

the solution being

$$e^{\Lambda} = \frac{1}{7\rho + c_1}, \tag{4.58}$$

$$e^{2g} = \frac{3Q_\eta}{2\left[(7\rho + c_1) - c_2(7\rho + c_1)^{4/7}\right]}, \tag{4.59}$$

$$h = \frac{Q_c}{9Q_\eta^3}(7\rho + c_1)\left[9c_3 + 4c_2^2(7\rho + c_1)^{1/7} - 2c_2(7\rho + c_1)^{4/7} + \frac{4}{7}(7\rho + c_1)\right]. \tag{4.60}$$

The three arbitrary constants can be fixed by imposing D1-brane UV asymptotics, in the decoupling limit, at $\rho \to 0$ ($r \to \infty$)

$$c_1 = 1, \qquad c_2 = 1, \qquad c_3 = -\frac{2}{7}. \tag{4.61}$$

On the other end of the radial direction, corresponding to the infrared of this flow ($\rho \to \infty$, $r \to 0$), we recover an AdS solution

$$e^{\Lambda} = \frac{1}{7\rho}, \qquad e^{2g} = \frac{3Q_\eta}{14\rho}, \qquad h = \frac{28Q_c}{9Q_\eta^3}\rho^2, \qquad e^{\Phi} = \left(\frac{Q_c}{Q_\eta^3}\right)^{1/2}\frac{2}{3\sqrt{7}}. \tag{4.62}$$

Thus, this gravitational background describes, in the dual field theory, an RG flow from a Yang–Mills type gauge theory in the UV to an IR fixed point, triggered by the inclusion of fundamental degrees of freedom.

4.5. Theories with less supersymmetry

As explained, it is possible to reduce the amount of preserved supersymmetry by changing the internal manifold. In this section we will examine the cases of Sasaki-Einstein manifolds, that gives $\mathcal{N} = (0,2)$ supersymmetry, and weak-G_2 manifolds, preserving the minimal $\mathcal{N} = (0,1)$.

4.5.1. $\mathcal{N} = (0,2)$ theories and Sasaki-Einstein manifolds

As explained in section 4.2.2, a Sasaki-Einstein manifold admits three globally defined forms η, J and Ω. Starting from our system describing D1-branes with a tri-Sasakian internal manifold, we can build the structure by means of the identifications (4.11). This allows us to deduce the desired results as a suitable limit of the equations already obtained for the tri-Sasakian case. An appropriate ansatz for the metric is now

$$\mathrm{d}s_{10}^2 = h^{-1/2}\mathrm{d}x_{1,1}^2 + h^{1/2}\left[\mathrm{d}r^2 + e^{2g}\mathrm{d}s_6^2(\mathrm{KE}) + e^{2f}\eta\otimes\eta\right] \tag{4.63}$$

which we can recover from (4.21) by setting $f_2 = f_3 = g$ and $f_1 = f$. Moreover, the three-form sourcing the flavour branes has only one piece compatible with the current Sasaki–Einstein structure, which is

$$F_3^{\mathrm{f}} = -Q_f J\wedge\eta. \tag{4.64}$$

We can restrict the ansatz for the tri-Sasakian case (4.46) by setting $Q_2 = Q_3 = 0$ and $Q_\eta = -Q_1 = -Q_f$. Then the smearing form (4.48) becomes

$$2\kappa^2 T_{\mathrm{D5}}\Xi = -Q_f J\wedge J. \tag{4.65}$$

Similarly, the calibration form reads

$$\mathcal{K} = -E^{01}\wedge\left(\frac{1}{2}e^{4g}J\wedge J + \eta\wedge J\right). \tag{4.66}$$

The BPS equations can be derived from (4.51) by doing the aforementioned identifications, yielding

$$h' = -Q_c e^{\Lambda-f-6g} + 3Q_f h e^{\Lambda-f-2g}, \tag{4.67}$$

$$\Lambda' = -3Q_f e^{\Lambda-f-2g}, \tag{4.68}$$

$$g' = e^{f-2g} - Q_f e^{\Lambda-f-2g}, \tag{4.69}$$

$$f' = 4e^{-f} - 3e^{f-2g}. \tag{4.70}$$

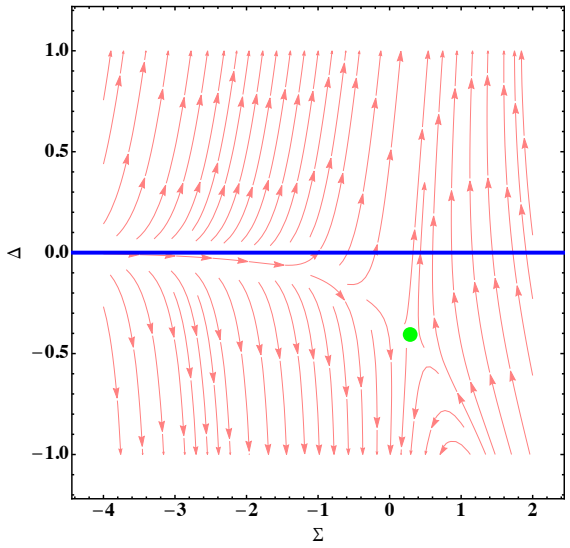

Figure 4.1.: RG flows in the system (4.67), in terms of the combinations $\Sigma = \Lambda - 2g$ and $\Delta = 2f - 2g$. The D1-brane corresponds to the horizontal line at $\Delta = 0$ while the AdS solution is located at the green dot. The desired flows starts from $\Delta = 0$ at $\Sigma \to -\infty$ and ends at the fixed point.

The projectors are the same, (4.31) and (4.37), but now the internal Killing spinors at our disposal are restricted to two, so the supersymmetry preserved is just $(0, 2)$. Notice that even if these equations were derived as a limiting case of those in section 4.4, they are valid for arbitrary seven-dimensional Sasaki-Einstein manifolds, including those that cannot be obtained from a tri-Sasakian structure.

The simplest solution to these equations is an AdS geometry given by

$$e^g = \sqrt{6}r, \qquad e^f = 2r, \qquad e^\Lambda = \frac{8r^2}{Q_f}, \qquad h = \frac{Q_c}{108 Q_f\, r^4}. \tag{4.71}$$

This fixed point can act as the IR of an RG flow that starts from the D1-brane, exactly as in the analytic solution described in the previous section, as seen in figure 4.1. The gauge theory in the UV of this flow can be taken to be one of the quivers considered in [62], modified with new couplings to fundamental matter that drive the flow towards an IR conformal field theory.

4.5.2. $\mathcal{N} = (0,1)$ theories and weak-G_2 manifolds

Weak-G_2 manifolds can be obtained by squashing a tri-Sasakian structure. This restricts the supersymmetry to $\mathcal{N} = (0,1)$ and modifies the equations characterising Killing spinors from (4.6) to (4.20). It is a simple exercise to track the consequence of this in the fermionic variations, resulting in the replacement of (4.33) by

$$g' = e^{-2g}(\alpha_1 e^{f_1} + \alpha_2 e^{f_2} + \alpha_3 e^{f_3}) + e^{-g}\left(\frac{\alpha_1+\alpha_2+\alpha_3}{3} - \alpha_1\alpha_2\alpha_3\right) \tag{4.72}$$

and

$$\begin{aligned} f_1' = &-2\alpha_1 e^{f_1-2g} + \alpha_1\alpha_2\alpha_3\left(e^{f_1-f_2-f_3} - e^{f_2-f_3-f_1} - e^{f_3-f_1-f_2}\right) + \\ &+ \frac{2}{5}(\alpha 1 + 4\alpha_1\alpha_2\alpha_3) \end{aligned} \tag{4.73}$$

and cyclic permutations. Condition (4.38) for the projectors is now

$$\frac{1}{3}(\alpha_1+\alpha_2+\alpha_3) - \alpha_1\alpha_2\alpha_3 = 0, \tag{4.74}$$

which is solved by $\alpha_1 = \alpha_2 = \alpha_3 = \pm 1$. The sign can be reabsorbed in the radial coordinate, so we will chose without loss of generality $+1$.

The simplest solution to this system is the D1-brane over a weak-G_2 manifold (which can be taken to be for instance the squashed seven-sphere), with metric functions

$$e^g = \frac{3r}{\sqrt{5}}, \qquad e^{f_1} = e^{f_2} = e^{f_3} = \frac{3r}{5}r, \qquad h = \frac{3125 Q_c}{13122\, r^6}. \tag{4.75}$$

Remarkably, if instead we set

$$e^{f_1} = a_1, \qquad e^{f_2} = a_2, \qquad e^{f_3} = a_3, \qquad e^g = 2b, \tag{4.76}$$

we recover the equations labelled (8) in [63] describing Spin(7) eight-dimensional manifolds, generalized to arbitrary weak-G_2 manifolds as principal orbits. Indeed, the BPS equations can be also obtained by imposing Ricci-flatness of the metric

$$\mathrm{d}s_8^2 = \mathrm{d}r^2 + e^{2g}\mathrm{d}s_4^2(\mathrm{QK}) + \sum_{i=1}^{3} e^{2f_i}\eta^i \otimes \eta^i \tag{4.77}$$

together with closure and selfduality of the suitable Cayley form. This ensures that the eight-dimensional manifold has Spin(7) holonomy.

Suppose that the weak-G_2 manifold is taken to be the (squashed) seven-sphere. There is a particular truncation to these equations, setting for instance $f_1 = f_2$, which describes the seven-dimensional manifold as a S^3 fibered over a S^4, where the S^3 is in turn seen as a S^1 fibered over a S^2. These are the metrics that we use in chapter 2, described by equations (2.28). This result can be recovered from the system we are considering via the redefinitions

$$\mathrm{d}\bar{r} = -(2Q_k)^{-1}e^{f_3}\mathrm{d}r, \quad e^{2g} = 4e^{2\bar{f}-\Lambda}, \quad e^{2f_1} = e^{2f_2} = 4e^{2\bar{g}-\Lambda}, \quad e^{2f_3} = 4Q_k^2 e^{\Lambda}, \tag{4.78}$$

with $Q_k < 0$, where $\bar{r}$, Λ, $\bar{f}$ and $\bar{g}$ here are to be identified with the radial coordinates and functions there.

The equations in the presence of flavour can be found by repeating the process of section 4.4 while using the new projectors (4.74). The resulting equations are

$$\begin{aligned}
\Lambda' &= e^{\Lambda}\left[2e^{-2g}\left(Q_1e^{-f_1} + Q_2e^{-f_2} + Q_3e^{-f_3}\right) + Q_\eta e^{-f_1-f_2-f_3}\right], \qquad (4.79)\\
h' &= e^{\Lambda}\left\{-Q_c e^{-f_1-f_2-f_3-4g} - h\left[2e^{-2g}\left(Q_1e^{-f_1} + Q_2e^{-f_2} + Q_3e^{-f_3}\right) + Q_\eta e^{-f_1-f_2-f_3}\right]\right\},\\
g' &= e^{-2g}\left(e^{f_1} + e^{f_2} + e^{f_3}\right) - \frac{e^{\Lambda}}{2}\left(Q_1e^{-f_1-2g} + Q_2e^{-f_2-2g} + Q_3e^{-f_3-2g} + Q_\eta e^{-f_1-f_2-f_3}\right),\\
f_1' &= 2e^{-f_1} + e^{\Lambda-2g}\left(Q_2e^{-f_2} + Q_3e^{-f_3}\right) - 2e^{f_1-2g} + \left(e^{f_1-f_2-f_3} - e^{f_2-f_3-f_1} - e^{f_3-f_1-f_2}\right),\\
f_2' &= 2e^{-f_2} + e^{\Lambda-2g}\left(Q_1e^{-f_1} + Q_3e^{-f_3}\right) - 2e^{f_2-2g} + \left(-e^{f_1-f_2-f_3} + e^{f_2-f_3-f_1} - e^{f_3-f_1-f_2}\right),\\
f_3' &= 2e^{-f_3} + e^{\Lambda-2g}\left(Q_1e^{-f_1} + Q_2e^{-f_2}\right) + 2e^{f_3-2g} + \left(-e^{f_1-f_2-f_3} - e^{f_2-f_3-f_1} + e^{f_3-f_1-f_2}\right).
\end{aligned}$$

Notice that this system corresponds to manifolds that descend from a parent tri-Sasakian structure and thus inherit all the possible squashings. However, generically a weak-G_2 manifold is not necessarily given as a fiber over a base, so it would not admit any squashing. Therefore, a generic weak-G_2 manifold would verify equations in which such squashings are suppressed. This is achieved by truncating the modes and charges as

$$e^{f_1} = e^{f_2} = e^{f_3} = \frac{1}{\sqrt{5}}e^{g}, \qquad Q_1 = Q_2 = Q_3 = 5Q_\eta, \tag{4.80}$$

reducing the equations to

$$h' = -5\sqrt{5}Q_c\, e^{\Lambda-7g} - 7\sqrt{5}Q_1 h\, e^{\Lambda-3g}, \tag{4.81a}$$

$$\Lambda' = 7\sqrt{5}Q_1 e^{\Lambda-3g}, \tag{4.81b}$$

$$g' = \frac{3}{\sqrt{5}}e^{-g} + 2\sqrt{5}Q_1 e^{\Lambda-3g}. \tag{4.81c}$$

This has the advantage of the system being integrable. Defining a new radial coordinate

$$-\left(Q_1\sqrt{5}\right)^{-1} e^{3g}\frac{\mathrm{d}f}{\mathrm{d}r} \equiv \frac{\mathrm{d}f}{\mathrm{d}\rho}, \tag{4.82}$$

the general solution is

$$e^{\Lambda} = \frac{1}{7\rho + c_1}, \tag{4.83a}$$

$$e^{2g} = \frac{5Q_1}{2\left[(7\rho + c_1) - c_2(7\rho + c_1)^{4/7}\right]}, \tag{4.83b}$$

$$h = \frac{Q_c}{5Q_1^3}(7\rho + c_1)\left[5c_3 + 4c_2^2(7\rho + c_1)^{1/7} - 2c_2(7\rho + c_1)^{4/7} + \frac{4}{7}(7\rho + c_1)\right]. \tag{4.83c}$$

D1-brane asymptotics (4.75) in the UV ($r \to \infty, \rho \to 0$) fixes the integration constants to

$$c_1 = 1, \qquad c_2 = 2, \qquad c_3 = -\frac{18}{35}. \tag{4.84}$$

In the infrared this solution reaches an AdS geometry

$$e^{\Lambda} = \frac{1}{7\rho}, \qquad e^{2g} = \frac{5Q_1}{14\rho}, \qquad h = \frac{28Q_c}{5Q_1^3}\rho^2, \qquad e^{\Phi} = \left(\frac{Q_c}{Q_1^3}\right)^{1/2}\frac{2}{\sqrt{35}}, \tag{4.85}$$

and the physics is equivalent to the solutions discussed in previous sections, with the particularity that the preserved supersymmetry is (0, 1).

4.6. Conclusions

In this chapter we have studied a system of N_c D1-branes with N_f D5-branes sharing the gauge directions in a space whose transverse manifold has special holonomy. The reason for that was to build holographic duals to theories with less than maximal supersymmetry containing flavoured degrees of freedom.

The D1-branes act as colour branes defining the gauge group of the theory in the ultraviolet. In absence of flavour the gauge theory is just an SU(N_c) super Yang-Mills. The amount of supersymmetry of the theory depends on the holonomy of the eight-dimensional transverse manifold, which is also related to the number of Killing spinors admitted by the seven-dimensional internal space.

In particular we have studied three kinds of internal spaces, these are tri-Sasaki, Sasaki-Einstein and weak-G_2. They admit three, two and one Killing spinors respectively. The resulting super Yang-Mills theories preserve $\mathcal{N} = (0,3)$, $\mathcal{N} = (0,2)$ and $\mathcal{N} = (0,1)$.

The inclusion of flavoured degrees of freedom is done by considering additional N_f D5-branes sharing the gauge directions with the D1-branes. In order to avoid Partial Differential Equations we smear the D5-branes along the transverse directions. This allows us to include the backreaction of the branes, corresponding to the Veneziano limit of the gauge theory. In the case of the tri-Sasaki space there are several cycles around which branes can be wrapped, For this reason there are several Page charges (Q_1, Q_2, Q_3 and Q_η) associated to the number of branes around each cycle.

The presence of the D5-branes excites new modes corresponding to relevant deformations of the gauge theory, controlled by the number of these branes. For each of the three cases studied, there is a particular flow whose infrared fate is an AdS_3 solution, dual to a two-dimensional Conformal Field Theory.

5. Summary

The AdS/CFT correspondence is a conjecture that establishes an equivalence between a gravitational theory in a hyperbolic space and a gauge quantum field theory living on the boundary of the former. This duality, also known as holography, is a great tool to study strongly coupled quantum field theories in situations in which the usual perturbative techniques are not useful.

The duality is formulated in the framework of (super)string theory and its original motivation comes from the study of some solitonic objects existing in the theory, the D-branes. We can understand the D-branes as hypersurfaces where boundary conditions to open strings can be imposed. Upon quantisation this gives a gauge quantum field theory living on the brane. On the other hand, we can consider the gravitational effect of the brane on the initially flat spacetime. The low energy limit (taking as characteristic energy scale the inverse of the string length) of this effect is a supergravity solution called black brane. The fact that both theories, gauge and gravity, are different descriptions of the same physical reality, a set of D-branes, is the motivation to postulate that they are equivalent or dual.

The first realisation of this duality was developed by studying D3-branes, that is, branes with three spatial dimensions and one temporal dimension. The theory living on these branes is a supersymmetric gauge theory with conformal symmetry, also known as conformal field theory or CFT. On the other hand, the gravitational effect of the branes deforms the spacetime to have an anti-de Sitter metric, or AdS. Thus the name of the correspondence. But this duality is not only about conformal theories and AdS spaces. For instance, if we consider D-branes with different dimensions, we get different field theories (not conformal) dual to different supergravity solutions (not AdS). Moreover, if instead of placing the branes in flat space we consider another background spacetime the properties of the dual field theory also change. This allows us to construct supergravity solutions dual to field theories with different properties such as confinement, baryonic charge or finite temperature.

In particular, the presence of confinement in a field theory is typically manifested in the holographic dual by the existence of a cycle in the spacetime manifold that ends regularly before reaching the horizon. In the string theory picture, a quark-antiquark

pair (quark meaning particle in the fundamental representation) is represented by strings attached to the boundary. If the geometry ends smoothly, there is no surface where we can impose boundary conditions for the strings and they must end at the boundary. This gives a potential that scales linearly with the distance between quarks, typical of confined systems.

In chapter 2 of this thesis we show, however, a counterexample to this. There a one-parameter family of supergravity solutions is described, obtained as a deformation of a D2-branes system. These solutions are dual to a family of field theories in 2 + 1 dimensions. All the backgrounds in this family present a geometry that ends smoothly. But, except in a particular case, there is no confinement. The reason for this is that the string theory description of these solution is not valid and they are only regular solutions in the context of M-theory. In this description quarks are represented by membranes wrapped around a circle that can end smoothly in a cigar-like tip. This allows a disconnected configuration. Consequently, in the field theory there exists a mass gap due to the end of the geometry at a finite value of the radial coordinate, but there is no confinement.

This unexpected lack of confinement is not the only remarkable feature of this family of solutions. One of the dual theories has a renormalization group (RG) flow that ends in a fixed point, that is, a conformal theory. Varying slightly the parameter that labels the solutions we end in solutions dual to theories whose RG flow passes near the fixed point, thus exhibiting a quasiconformal behaviour. All these theories also flow to the gapped phase at lower energies.

The existence of a quasiconformal regime in a RG flow implies that there is an approximated conformal symmetry. When the flow leaves the quasiconformal region this approximated symmetry is broken and this breaking can be either spontaneous or explicit. By the Goldstone's theorem, when a symmetry is spontaneously broken a massless scalar Goldstone boson must appear for each of the generators of the symmetry. If the symmetry is not exact, the Goldstone boson is not massless but light. In the case of the conformal symmetry, the Goldsonte boson associated to its spontaneous breaking is a dilaton, a light pseudo-dilaton for the approximated symmetry.

In chapter 3 we compute the spectra of spin-0 and spin-2 states. The result is that we did not find such pseudo-dilaton. The reason for this is that the spontaneous breaking of the symmetry is of the same order than the explicit breaking, Nevertheless, it is possible to simulate a spontaneous breaking of the conformal symmetry by putting a hard-wall cut-off in the infrared. By tuning the energy scale at which we impose the cut-off we can explore different energy regions of the flow, finding the quasiconformal

behaviour in the appropriate solutions.

Finally, in chapter 4 we consider a new system, consisting in D1-branes in a space that has as transverse manifold a space with special holonomy. This implies that the maximal supersymmetry corresponding to the D1-branes in flat space is partially broken and reduces to a number of supercharges that depends on the particular holonomy of the space considered. The internal manifolds that we study are tri-Sasaki, Sasaki-Einstein and weak-G_2, that reduce supersymmetry from $\mathcal{N} = (8, 8)$ to $\mathcal{N} = (0, 3)$, $(0, 2)$ and $(0, 1)$ respectively. Furthermore, we introduce D5-branes sharing the gauge directions with the D1-branes, which in the gauge theory translates into the presence of matter in the fundamental representation. For this reason they are called flavour branes. In these flavoured supersymmetric theories we have found renormalization group flows that connect the brane-like ultraviolet with a fixed point. Also, we have been able to connect the equations describing the weak-G_2 manifold with the equations describing the internal space of the family of solutions in chapter 2.

6. Resumen en castellano

La correspondencia AdS/CFT es una conjetura que establece una equivalencia entre una teoría gravitacional en un espacio hiperbólico y una teoría cuántica de campos gauge que vive en la frontera de la primera. Esta dualidad, también conocida como holografía, es una gran herramienta que nos permite estudiar las teorías cuánticas de campos con acoplamiento fuerte cuando las técnicas de cálculo perturbativas habituales en teorías de campos no son viables.

La dualidad se formula en el marco de la teoría de (super)cuerdas y su motivación original viene del estudio de unos objetos solitónicos presentes en ella llamados D-branas. Podemos entender las D-branas como una hipersuperficie sobre la que las cuerdas abiertas tienen condiciones de contorno, lo que al cuantizar da lugar a una teoría cuántica de campos gauge. Pero, por otro lado, podemos considerar el efecto gravitatorio que tienen en el espaciotiempo. En el límite de bajas energías (en comparación con la energía característica de la teoría de cuerdas dada por la longitud de la cuerda) este efecto es una solución de supergravedad conocida como brana negra. El hecho de que, por un lado, la teoría de campos gauge, y por el otro, la teoría de gravedad, sean dos descripciones de una misma realidad física (un conjunto de D-branas) nos hace postular que sean dos teorías equivalentes o duales.

La primera realización de esta dualidad se desarrolló estudiando D3-branas (branas de tres dimensiones espaciales y una temporal). La teoría contenida en estas branas es una teoría gauge supersimétrica con simetría conforme, también llamada teoría de campos conforme, o CFT por sus siglas en ingles. Por otro lado, el efecto gravitatorio de las branas hace que el espaciotiempo tenga una métrica anti-de Sitter, o AdS. Esto es lo que da nombre a la correspondencia. Sin embargo, ésta no se limita a la equivalencia de teorías conformes y espacios AdS. Por ejemplo, al considerar branas de otras dimensiones obtenemos diferentes teorías de campos duales (sin invariancia conforme) y otros espacios distintos. Además, el hecho de poner las branas en un espacio que no sea el espacio plano también modifica la teoría dual. Esto nos permite construir soluciones de supergravedad duales a teorías con diferentes propiedades como pueden ser la presencia de confinamiento, carga bariónica o temperatura finita.

En particular, la presencia de confinamiento en una teoría de campos típicamente

viene indicada en el dual holográfico por la existencia de un ciclo en la variedad del espaciotiempo que se cierra de manera regular (matemáticamente hablando) antes de llegar al horizonte del mismo. Desde el punto de vista de la teoría de cuerdas, esto es porque un par quark-antiquark (donde quark significa partícula en la representación fundamental) viene dado por cuerdas que terminan en la frontera. El hecho de que la geometría termine de forma regular implica que no existe una superficie donde imponer condiciones de contorno a las cuerdas, lo que significa que solo pueden estar unidas a la frontera. Entonces, los pares quark-antiquark tienen una energía potencial de separación que escala linealmente con la distancia de separación, que es típico de los sistemas confinantes.

En el capítulo 2 de esta tesis exponemos, sin embargo, un contraejemplo a esto. En él describimos una familia uniparamétrica de soluciones de supergravedad, obtenidas al modificar un sistema de D2-branas, que son duales a una familia de teorías de campos en $2 + 1$ dimensiones. Todas las soluciones de esta familia presentan una geometría que termina de forma suave. Sin embargo, salvo para un caso particular, no existe confinamiento. La razón de que esto ocurra es que la descripción en términos de teoría de cuerdas no es válida porque las soluciones no son regulares, sino que han de ser descritas en el contexto de la teoría M. En esta descripción los quarks están representados por una membrana enrollada en un círculo, que puede acabar en una forma de punta de cigarro sin necesidad de tener que definir condiciones de contorno, lo que permite la configuración desconectada. Por tanto, en la teoría de campos existe un salto o "gap" de masa (es decir, una energía mínima accesible por las partículas finita) sin la existencia de confinamiento.

Esta inesperada falta de confinamiento no es la única característica notable de esta familia de soluciones. Una de las teorías duales tiene un flujo de grupo de renormalización que pasa por un punto fijo, es decir, una teoría conforme. Al variar ligeramente el parámetro que caracteriza las soluciones obtenemos soluciones duales a teorías cuyo flujo de renormalización pasa cerca del punto fijo, exhibiendo un comportamiento cuasiconforme. Tanto estas teorías como la que pasa exactamente por el punto fijo, fluyen a más bajas energías a la fase con "gap".

El hecho de que exista un flujo que saque la teoría de un punto fijo implica la rotura de la simetría conforme. Esta rotura puede ser explícita o espontánea. Si la rotura es espontánea debería existir un bosón de Goldstone sin masa asociado a la simetría que, en el caso de la simetría conforme, es el dilatón. En las teorías que tienen comportamiento cuasiconforme la simetría es aproximada y el bosón no necesariamente ha de tener masa exactamente nula, lo que llamamos un pseudo-bosón Goldstone o, en

este caso particular, pseudo-dilatón. En el capítulo 3 calculamos el espectro de estados de spin 0 y spin 2. El resultado es que no existe tal pseudo-dilatón ligero. Esto es debido a que la rotura espontánea de la simetría es del mismo orden que la rotura explícita. No obstante, es posible simular una rotura espontánea introduciendo un cut-off the tipo hard-wall en el infrarrojo. Aplicando este cut-off a diferentes escalas de energía podemos explorar las diferentes regiones del grupo de normalización, encontrando así la región cuasiconforme en las soluciones pertinentes.

Por último, en el capítulo 4 consideramos un nuevo sistema, consistente en D1-branas en las que el espacio tiene como variedad transversa espacios de holonomía especial. Esto implica que la supersimetría maximal correspondiente a la solución de D1-branas en espacio plano se rompe parcialmente y se reduce a un número de supercargas que depende de la holonomía del espacio que estemos considerando. Las variedades internas estudiadas son tri-Sasaki, Sasaki-Einstein y weak-G_2, que hacen que la supersimetría pase de ser $\mathcal{N} = (8, 8)$ (espacio plano) a $(0, 3)$, $(0, 2)$ y $(0, 1)$ respectivamente. Además introducimos D5-branas, lo que en la teoría dual significa incluir materia en la representación fundamental. Por ello se llaman también branas de sabor. En estas teorías supersimétricas con sabor hemos conseguido encontrar flujos de renormalización que pasan por un punto fijo, o una solución AdS en el dual gravitatorio. Además hemos podido relacionar las ecuaciones que describen la métrica weak-G_2 con las ecuaciones que describen la variedad interna de las soluciones de D2-branas en el capítulo 2.

Appendices

A. Hyperscaling violating toy model

Consider a $(d+1)$-dimensional model consisting of a single scalar field χ coupled to gravity with the action

$$S = \int \mathrm{d}\rho\, \mathrm{d}^d x\, \sqrt{-g}\left(\frac{R}{4} - \frac{1}{2}\partial_M\chi\partial^M\chi - \mathcal{V}(\chi)\right), \tag{A.1}$$

where

$$\begin{aligned} \mathrm{d}s^2 &= e^{2\delta\chi(\rho)}\mathrm{d}\rho^2 + e^{2A(\rho)}\mathrm{d}x^2_{1,d-1}\,, \\ \mathcal{V}(\chi) &= -\frac{(d-\theta)(d-\theta-1)}{4}e^{-2\delta\chi}\,, \end{aligned} \tag{A.2}$$

and we have defined

$$\theta = \frac{(d-1)^2\delta^2}{(d-1)\delta^2 - 2}\,. \tag{A.3}$$

The model admits solutions

$$\begin{aligned} \chi &= \frac{\delta}{2}(d-\theta-1)\rho\,, \\ A &= \frac{d-\theta-1}{d-1}\rho\,. \end{aligned} \tag{A.4}$$

Under a scale transformation $x \to \lambda x$, $\rho \to \rho - \log\lambda$, the metric transforms as

$$\mathrm{d}s^2 \to \lambda^{\frac{2\theta}{d-1}}\mathrm{d}s^2\,. \tag{A.5}$$

This shows that the solutions are hyperscaling violating with hyperscaling violation coefficient θ.

For θ close to 0, the background metric is close to AdS, and because of this there should be a light state in the spectrum. In order to understand how its mass depends on θ, we now perform a perturbative analysis. The equation of motion and boundary

condition for the spin-0 fluctuation are given by

$$\partial_\rho^2 \mathfrak{a} + (d-\theta)\partial_\rho \mathfrak{a} + e^{-2\rho} m^2 \mathfrak{a} = 0\,,$$
$$\frac{e^{2\rho}}{d-1}\frac{\theta}{m^2}\partial_\rho \mathfrak{a}|_{\rho_{I,U}} = \mathfrak{a}|_{\rho_{I,U}}\,. \tag{A.6}$$

Consider the expansion (perturbative in θ)

$$\mathfrak{a} = \mathfrak{a}_0 + \theta\,\mathfrak{a}_2 + O(\theta^2)\,,$$
$$m^2 = \theta\,\tilde{m}^2 + O(\theta^2)\,. \tag{A.7}$$

At leading order in θ, the general solution of the equation of motion in eq. (A.6) is given by

$$\mathfrak{a}_0 = c_1 + c_2 e^{-d\rho}\,, \tag{A.8}$$

where c_1 and c_2 are constants. After imposing the boundary conditions in the IR (UV), and solving for $\tilde{m}^2$, we obtain that the mass m_0 of the lightest spin-0 state is given by

$$m_0^2 = \frac{d\,\theta}{d-1}\frac{e^{d\rho_U} - e^{2\rho_U}}{e^{d\rho_U}-1}\,, \tag{A.9}$$

where we have fixed $\rho_I = 0$ without loss of generality. Finally, as long as $d > 2$, the limit of $\rho_U \to \infty$ leads to

$$m_0^2 = \frac{d\,\theta}{1-d}\,. \tag{A.10}$$

The spin-2 fluctuations satisfy the same equation of motion as the spin-0 fluctuations

$$\partial_\rho^2 \mathfrak{e}^\mu{}_\nu + (d-\theta)\partial_\rho \mathfrak{e}^\mu{}_\nu + e^{-2\rho} m^2 \mathfrak{e}^\mu{}_\nu = 0\,, \tag{A.11}$$

the general solution of which is given by

$$\mathfrak{e}^\mu{}_\nu = e^{\frac{(\theta-d)\rho}{2}} m^{d/2}\left(c^\mu{}_\nu J_{\frac{d-\theta}{2}}(e^{-\rho}m) + d^\mu{}_\nu J_{\frac{\theta-d}{2}}(e^{-\rho}m)\right)\,, \tag{A.12}$$

where $c^\mu{}_\nu$ and $d^\mu{}_\nu$ are constants. After imposing the boundary condition

$$\partial_\rho \mathfrak{e}^\mu{}_\nu|_{\rho_{I,U}} = 0\,, \tag{A.13}$$

and taking the limit $\rho_U \to \infty$, one can show that for $\theta < d-2$, the spin-2 states have masses given by the positive roots of the equation

$$J_{\frac{d-\theta-2}{2}}(m) = 0\,. \tag{A.14}$$

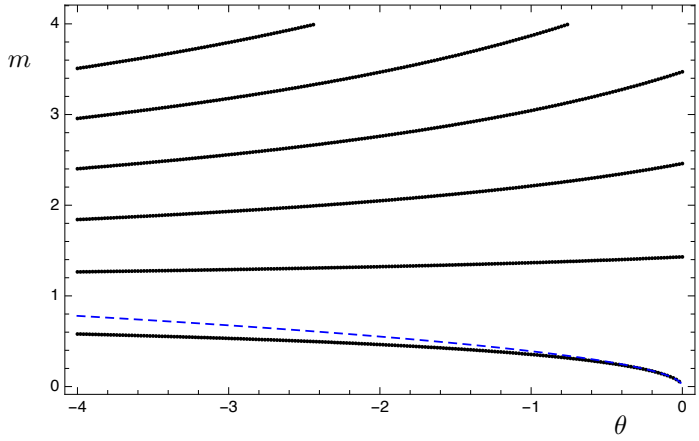

Figure A.1.: Mass spectrum of spin-0 states normalized to the mass of the lightest spin-2 state for the hyperscaling violating toy model with $d = 3$, $\rho_I = 0$, $\rho_U = 50$. The dashed blue line is the perturbative result to leading order in θ given in Eq. (A.15).

For $d = 3$, one obtains that to leading order in θ, the ratio between the masses of the lightest spin-0 and spin-2 states is given by

$$\frac{m_0}{m_1} = \frac{1}{\pi}\sqrt{\frac{-3\theta}{2}} \tag{A.15}$$

In Figure A.1, we show the spin-0 spectrum for $d = 3$ as a function of θ compared to the perturbative result.

B. Conventions for the supersymmetric analysis

We will use conventions analogous to those in [64] but adapted to a 3 + 7 splitting instead of 5 + 5. The ten-dimensional gamma matrices satisfy

$$\{\Gamma^A, \Gamma^B\} = 2\eta^{AB} \tag{B.1}$$

with a mostly plus signature. The chirality projector is then taken to be

$$\Gamma^{(11)} = \Gamma^0\Gamma^1\cdots\Gamma^9. \tag{B.2}$$

We decompose Cliff(1,9) into

$$\begin{aligned}\Gamma^\mu &= \gamma^\mu \otimes \mathbb{1}_8 \otimes \sigma^1,\\ \Gamma^m &= \mathbb{1}_2 \otimes \tilde{\gamma}^m \otimes \sigma^2,\end{aligned} \tag{B.3}$$

where μ and m are respectively external and internal flat indices. The corresponding gamma matrices thus verify

$$\{\gamma^\mu, \gamma^\nu\} = 2\eta^{\mu\nu}, \qquad\qquad \{\tilde{\gamma}^m, \tilde{\gamma}^n\} = 2\delta^{mn}. \tag{B.4}$$

The chiral matrices can be taken to be $-\mathbb{1}_2$ for the external part and $i\mathbb{1}_8$ for the internal one, in such a way that

$$\Gamma^{11} = \mathbb{1}_2 \otimes \mathbb{1}_8 \otimes \sigma^3. \tag{B.5}$$

A ten-dimensional Majorana–Weyl spinor $\hat{\epsilon}$ can the be decomposed into

$$\hat{\epsilon} \;=\; \psi \otimes \chi \otimes \theta\,, \tag{B.6}$$

with ψ and χ spinors living in the external and internal spaces respectively. The chirality condition is

$$\Gamma^{11}\hat{\epsilon} = \hat{\epsilon}, \tag{B.7}$$

while charge conjugation is done with the help of D-intertwiners verifying

$$\left(\Gamma^A\right)^* = D^{-1}\Gamma^A D\,, \qquad\qquad DD^* = 1\,. \tag{B.8}$$

Thus, for a ten-dimensional spinor $\hat{\epsilon}$ we have

$$\hat{\epsilon}^c \equiv D\hat{\epsilon}^*. \tag{B.9}$$

Now, type IIB supersymmetry is parametrized by two Majorana-Weyl spinors ϵ_i, each with 16 real components, and we take

$$\epsilon_i = \psi \otimes \chi_i \otimes \theta + \psi^c \otimes \chi_i^c \otimes \theta\,. \tag{B.10}$$

Finally, we complexify to

$$\epsilon \equiv \epsilon_1 + i\epsilon_2 \equiv \psi \otimes \xi_1 \otimes \theta + \psi^c \otimes \xi_2^c \otimes \theta\,, \tag{B.11}$$

with the combinations $\xi_1 = \chi_1 + i\chi_2$ and $\xi_2^c = \chi_1^c + i\chi_2^c$. In this way

$$\epsilon^c = \psi \otimes \xi_2 \otimes \theta + \psi^c \otimes \xi_1^c \otimes \theta\,. \tag{B.12}$$

In terms of these spinors, the supersymmetric variations read as in (4.24).

Bibliography

[1] A. F. Faedo, D. Mateos, D. Pravos, and J. G. Subils, "Mass Gap without Confinement," *JHEP*, vol. 06, p. 153, 2017.

[2] D. Elander, A. F. Faedo, D. Mateos, D. Pravos, and J. G. Subils, "Mass spectrum of gapped, non-confining theories with multi-scale dynamics," *JHEP*, vol. 05, p. 175, 2019.

[3] A. F. Faedo, B. Fraser, and D. Pravos, "Two dimensional theories with unquenched flavour." To appear.

[4] J. M. Maldacena, "The Large N limit of superconformal field theories and supergravity," *Int. J. Theor. Phys.*, vol. 38, pp. 1113–1133, 1999. [Adv. Theor. Math. Phys.2,231(1998)].

[5] S. S. Gubser, I. R. Klebanov, and A. M. Polyakov, "Gauge theory correlators from noncritical string theory," *Phys. Lett.*, vol. B428, pp. 105–114, 1998.

[6] E. Witten, "Anti-de Sitter space and holography," *Adv. Theor. Math. Phys.*, vol. 2, pp. 253–291, 1998.

[7] J. Polchinski, *String Theory*, vol. 1 of *Cambridge Monographs on Mathematical Physics*. Cambridge University Press, 1998.

[8] B. Zwiebach, *A First Course in String Theory*. Cambridge University Press, 2 ed., 2009.

[9] D. Mateos, "String Theory and Quantum Chromodynamics," *Class. Quant. Grav.*, vol. 24, pp. S713–S740, 2007.

[10] A. V. Ramallo, "Introduction to the AdS/CFT correspondence," *Springer Proc. Phys.*, vol. 161, pp. 411–474, 2015.

[11] G. 't Hooft, "A Planar Diagram Theory for Strong Interactions," *Nucl. Phys.*, vol. B72, p. 461, 1974. [,337(1973)].

[12] N. Itzhaki, J. M. Maldacena, J. Sonnenschein, and S. Yankielowicz, "Supergravity and the large N limit of theories with sixteen supercharges," *Phys. Rev.*, vol. D58, p. 046004, 1998.

[13] M. Cvetic, G. W. Gibbons, H. Lu, and C. N. Pope, "New cohomogeneity one metrics with Spin(7) holonomy," *J. Geom. Phys.*, vol. 49, pp. 350–365, 2004.

[14] A. Loewy and Y. Oz, "Branes in special holonomy backgrounds," *Phys. Lett.*, vol. B537, pp. 147–154, 2002.

[15] A. Hashimoto, S. Hirano, and P. Ouyang, "Branes and fluxes in special holonomy manifolds and cascading field theories," *JHEP*, vol. 06, p. 101, 2011.

[16] I. R. Klebanov and M. J. Strassler, "Supergravity and a confining gauge theory: Duality cascades and chi SB resolution of naked singularities," *JHEP*, vol. 08, p. 052, 2000.

[17] O. Aharony, O. Bergman, D. L. Jafferis, and J. Maldacena, "N=6 superconformal Chern-Simons-matter theories, M2-branes and their gravity duals," *JHEP*, vol. 10, p. 091, 2008.

[18] M. Cvetic, G. W. Gibbons, H. Lu, and C. N. Pope, "New complete noncompact Spin(7) manifolds," *Nucl. Phys.*, vol. B620, pp. 29–54, 2002.

[19] H. Ooguri and C.-S. Park, "Superconformal Chern-Simons Theories and the Squashed Seven Sphere," *JHEP*, vol. 11, p. 082, 2008.

[20] R. L. Bryant and S. M. Salamon, "On the construction of some complete metrics with exceptional holonomy," *Duke Math. J.*, vol. 58, pp. 829–850, 06 1989.

[21] G. W. Gibbons, D. N. Page, and C. N. Pope, "Einstein metrics on s^3,$\mathbb{R}^3$ and $\mathbb{R}^4$ bundles," *Communications in Mathematical Physics*, vol. 127, pp. 529–553, Feb 1990.

[22] E. Conde and A. V. Ramallo, "On the gravity dual of Chern-Simons-matter theories with unquenched flavor," *JHEP*, vol. 07, p. 099, 2011.

[23] A. F. Faedo, D. Mateos, and J. Tarrio, "Three-dimensional super Yang-Mills with unquenched flavor," *JHEP*, vol. 07, p. 056, 2015.

[24] M. Cvetic, H. Lu, and C. N. Pope, "Brane resolution through transgression," *Nucl. Phys.*, vol. B600, pp. 103–132, 2001.

[25] M. Cvetic, G. W. Gibbons, H. Lu, and C. N. Pope, "Supersymmetric nonsingular fractional D-2 branes and NS NS 2 branes," *Nucl. Phys.*, vol. B606, pp. 18–44, 2001.

[26] D. Marolf, "Chern-Simons terms and the three notions of charge," in *Quantization, gauge theory, and strings. Proceedings, International Conference dedicated to the memory of Professor Efim Fradkin, Moscow, Russia, June 5-10, 2000. Vol. 1+2*, pp. 312–320, 2000.

[27] O. Aharony, A. Hashimoto, S. Hirano, and P. Ouyang, "D-brane Charges in Gravitational Duals of 2+1 Dimensional Gauge Theories and Duality Cascades," *JHEP*, vol. 01, p. 072, 2010.

[28] E. Witten, "Supersymmetric index of three-dimensional gauge theory," pp. 156–184, 1999.

[29] J. M. Maldacena and H. S. Nastase, "The Supergravity dual of a theory with dynamical supersymmetry breaking," *JHEP*, vol. 09, p. 024, 2001.

[30] A. Butti, M. Grana, R. Minasian, M. Petrini, and A. Zaffaroni, "The Baryonic branch of Klebanov-Strassler solution: A supersymmetric family of SU(3) structure backgrounds," *JHEP*, vol. 03, p. 069, 2005.

[31] C. Nunez, I. Papadimitriou, and M. Piai, "Walking Dynamics from String Duals," *Int. J. Mod. Phys.*, vol. A25, pp. 2837–2865, 2010.

[32] D. Elander, J. Gaillard, C. Nunez, and M. Piai, "Towards multi-scale dynamics on the baryonic branch of Klebanov-Strassler," *JHEP*, vol. 07, p. 056, 2011.

[33] D. Elander, A. F. Faedo, C. Hoyos, D. Mateos, and M. Piai, "Multiscale confining dynamics from holographic RG flows," *JHEP*, vol. 05, p. 003, 2014.

[34] V. Gorbenko, S. Rychkov, and B. Zan, "Walking, Weak first-order transitions, and Complex CFTs," *JHEP*, vol. 10, p. 108, 2018.

[35] M. Bianchi, M. Prisco, and W. Mueck, "New results on holographic three point functions," *JHEP*, vol. 11, p. 052, 2003.

[36] M. Berg, M. Haack, and W. Mueck, "Bulk dynamics in confining gauge theories," *Nucl. Phys.*, vol. B736, pp. 82–132, 2006.

[37] M. Berg, M. Haack, and W. Mueck, "Glueballs vs. Gluinoballs: Fluctuation Spectra in Non-AdS/Non-CFT," *Nucl. Phys.*, vol. B789, pp. 1–44, 2008.

[38] D. Elander, "Glueball Spectra of SQCD-like Theories," *JHEP*, vol. 03, p. 114, 2010.

[39] D. Elander and M. Piai, "Light scalars from a compact fifth dimension," *JHEP*, vol. 01, p. 026, 2011.

[40] J. M. Maldacena and C. Nunez, "Towards the large N limit of pure N=1 superYang-Mills," *Phys. Rev. Lett.*, vol. 86, pp. 588–591, 2001.

[41] A. H. Chamseddine and M. S. Volkov, "NonAbelian BPS monopoles in N=4 gauged supergravity," *Phys. Rev. Lett.*, vol. 79, pp. 3343–3346, 1997.

[42] D. Elander, C. Nunez, and M. Piai, "A Light scalar from walking solutions in gauge-string duality," *Phys. Lett.*, vol. B686, pp. 64–67, 2010.

[43] D. Elander and M. Piai, "On the glueball spectrum of walking backgrounds from wrapped-D5 gravity duals," *Nucl. Phys.*, vol. B871, pp. 164–180, 2013.

[44] D. Elander, "Light scalar from deformations of the Klebanov-Strassler background," *Phys. Rev.*, vol. D91, no. 12, p. 126012, 2015.

[45] D. Elander and M. Piai, "Calculable mass hierarchies and a light dilaton from gravity duals," *Phys. Lett.*, vol. B772, pp. 110–114, 2017.

[46] D. Elander and M. Piai, "Glueballs on the Baryonic Branch of Klebanov-Strassler: dimensional deconstruction and a light scalar particle," *JHEP*, vol. 06, p. 003, 2017.

[47] S. P. Kumar, D. Mateos, A. Paredes, and M. Piai, "Towards holographic walking from N=4 super Yang-Mills," *JHEP*, vol. 05, p. 008, 2011.

[48] L. Anguelova, "Electroweak Symmetry Breaking from Gauge/Gravity Duality," *Nucl. Phys.*, vol. B843, pp. 429–454, 2011.

[49] L. Anguelova, P. Suranyi, and L. C. R. Wijewardhana, "Holographic Walking Technicolor from D-branes," *Nucl. Phys.*, vol. B852, pp. 39–60, 2011.

[50] D. Cassani and A.-K. Kashani-Poor, "Exploiting N=2 in consistent coset reductions of type IIA," *Nucl. Phys.*, vol. B817, pp. 25–57, 2009.

[51] D. Cassani and P. Koerber, "Tri-Sasakian consistent reduction," *JHEP*, vol. 01, p. 086, 2012.

[52] A. Athenodorou, E. Bennett, G. Bergner, D. Elander, C. J. D. Lin, B. Lucini, and M. Piai, "Large mass hierarchies from strongly-coupled dynamics," *JHEP*, vol. 06, p. 114, 2016.

[53] D. Elander, R. Lawrance, and M. Piai, "Hyperscaling violation and Electroweak Symmetry Breaking," *Nucl. Phys.*, vol. B897, pp. 583–611, 2015.

[54] A. Karch and E. Katz, "Adding flavor to AdS / CFT," *JHEP*, vol. 06, p. 043, 2002.

[55] S. A. Cherkis and A. Hashimoto, "Supergravity solution of intersecting branes and AdS/CFT with flavor," *JHEP*, vol. 11, p. 036, 2002.

[56] S. A. Hartnoll, J. Polchinski, E. Silverstein, and D. Tong, "Towards strange metallic holography," *JHEP*, vol. 04, p. 120, 2010.

[57] C. Nunez, A. Paredes, and A. V. Ramallo, "Unquenched Flavor in the Gauge/Gravity Correspondence," *Adv. High Energy Phys.*, vol. 2010, p. 196714, 2010.

[58] F. Benini, F. Canoura, S. Cremonesi, C. Nunez, and A. V. Ramallo, "Unquenched flavors in the Klebanov-Witten model," *JHEP*, vol. 02, p. 090, 2007.

[59] B. S. Acharya, J. M. Figueroa-O'Farrill, C. M. Hull, and B. J. Spence, "Branes at conical singularities and holography," *Adv. Theor. Math. Phys.*, vol. 2, pp. 1249–1286, 1999.

[60] C. P. Boyer and K. Galicki, "3 - Sasakian manifolds," *Surveys Diff. Geom.*, vol. 7, pp. 123–184, 1999.

[61] Z. W. Chong, "General metrics of G(2) and spin(7) holonomy," 2004.

[62] S. Franco, D. Ghim, S. Lee, R.-K. Seong, and D. Yokoyama, "2d (0,2) Quiver Gauge Theories and D-Branes," *JHEP*, vol. 09, p. 072, 2015.

[63] M. Cvetic, G. W. Gibbons, H. Lu, and C. N. Pope, "Cohomogeneity one manifolds of Spin(7) and G(2) holonomy," *Phys. Rev.*, vol. D65, p. 106004, 2002.

[64] J. P. Gauntlett, D. Martelli, J. Sparks, and D. Waldram, "Supersymmetric AdS(5) solutions of type IIB supergravity," *Class. Quant. Grav.*, vol. 23, pp. 4693–4718, 2006.